



NTNU – Trondheim
Norwegian University of
Science and Technology

Characterization of Sulfated Alginate Hybrid Gels for Tissue Engineering

Ragnhild Aaen

Chemical Engineering and Biotechnology

Submission date: Januar 2015

Supervisor: Gudmund Skjåk-Bræk, IBT

Co-supervisor: Øystein Arlov, IBT

Norwegian University of Science and Technology
Department of Biotechnology

Preface

The work described in this project was carried out at the Norwegian Biopolymer laboratory, Department of Biotechnology at the Norwegian University of Science and Technology (NTNU), and at the Department of Cancer Research and Molecular Medicine, NTNU.

I would like to thank my supervisors Professor Gudmund Sják-Bræk, for giving me the chance to work with this master project and for helping me understand osmotic swelling, and Ph.D. student Øystein Arlov, for all assistance in my experiments and for always being available for discussions of the results. I would also like to thank Professor Berit Løkensgard Strand for help and guidance on the swelling and distribution experiments, and Ph.D. student Marianne Øksnes Dalheim for ideas on bead experiments. A great thanks goes to Senior Engineers Ann-Sissel Teialeret Ulset, Wenche Iren Strand and Gerd Inger Sætrom for running the SEC-MALLS analysis, helping me whenever I have questions and for creating a welcoming and open working environment. Lastly, I would like to thank Ron for all his love and support.

NTNU, Trondheim

Ragnhild Aaen

Abstract

Tissue engineering is a field aiming to replace damaged tissue while reducing the great need of organ donors the world is facing today. Alginates are linear co-polymers consisting of the two monosaccharides β -D-mannuronic acid (M), and its 5-epimer α -L-guluronic acid (G). They can form hydrogels, and are candidates for use in tissue engineering scaffolds. Alginate is readily available at a low cost, and its hydrogels meet requirements of scaffolds such as mechanical strength and good biocompatibility, but lack the ability to interact with cells and proteins. The aims of this study was to investigate properties of alginate/alginate-sulfate mixtures for tissue engineering applications. This included the gel strength, osmotic stability in physiological solutions, distribution in gels, and interactions with the growth factor FGF. Mixing of formamide and HClSO_3 with alginate LF200S yielded, as shown by ICP-MS, sulfated alginate with degrees of sulfation (DS) depending on the concentration of HClSO_3 , volume of reaction mixture and the solubility of the alginate. Use of SEC-MALLS revealed some depolymerization of the alginate during the sulfation process, and showed that sulfation of alginate increases its susceptibility to acid hydrolysis at 95°C and pH 5.6. Use of alginate/alginate-sulfate mixtures was shown by swelling studies to have a higher osmotic stability in a physiological solution than pure alginate-sulfate beads when comparing total sulfate content. Increased content of sulfate in the beads generally led to decreased stability. Some hybrid beads containing low proportions of alginate-sulfate showed a higher stability than beads made from pure alginate. Increased proportions of alginate-sulfate in mixtures led to decreasing gel strengths, as shown by a longitudinal compression test. The Young's modulus of the gels ranged from 310 kPa (135 kPa when corrected for syneresis) to 26 kPa (16 kPa), placing them in the same range as several tissues. Interactions between FGF and alginate-sulfate in solution increased in strength for an increasing DS or a higher proportion of alginate-sulfate in mixtures. Gel disks made from mixtures all released FGF gradually into the surrounding medium. Gels containing alginate-sulfate still retained some FGF after 12 days, in contrast to the pure alginate gels. The mechanical strength, ability to interact with FGF, osmotic stability and tunable distribution make alginate/alginate-sulfate mixtures possible candidates for tissue engineering applications.

Sammendrag

Feltet "tissue engineering" tar sikte på å erstatte skadd vev, og samtidig redusere det store behovet for organdonorer verden står overfor i dag. Alginater er lineære polymerer bestående av monosakkaridene β -D-mannuronsyre (M) og dens 5-epimer α -L-guluronsyre (G). Alginater kan danne hydrogeler, og er kandidater for bruk som stillasverk i "tissue engineering". Alginat er lett tilgjengelig til en lav pris, med hydrogeler som innfrir stillasverk-egenskaper som mekanisk styrke og god biokompabilitet, men mangler evnen til samhandling med proteiner og celler. Målet for denne studien var å undersøke egenskaper ved alginat/alginatsulfat-blandinger for bruk innen "tissue engineering". Dette omfatter gelstyrke, osmotisk stabilitet i fysiologiske løsninger, fordeling i geler, og interaksjon med vekstfaktoren FGF. Alginat LF200S ble, som bekreftet av ICP-MS, sulfatert ved bruk av formamid og HClSO_3 . Den resulterende sulfateringsgraden var avhengig av konsentrasjon av HClSO_3 , reaksjonsvolum og alginatets løselighet. Bruk av SEC-MALLS viste at sulfateringsprosessen førte til en delvis depolymerisering av alginatet. Videre ble det vist at sulfatering av alginatet medførte en høyere sårbarhet for syrehydrolyse ved 95°C og pH 5.6. Bruk av alginat/alginatsulfat-blandinger hadde, målt ved bruk av svellestudier, høyere osmotisk stabilitet i en fysiologisk løsning enn rene alginatsulfat-kuler ved sammenlikning av totalt sulfatinnhold. Økt innhold av sulfat i kulene gav generelt lavere stabilitet, skjønt noen hybridgeler med lavt innhold av alginatsulfat viste en høyere stabilitet enn kuler laget av rent alginat. En lavere gelstyrke ble, ved bruk av en kompresjonstest, vist ved økt innhold av alginatsulfat i gelene. Youngs modulus for gelene strakte seg fra 310 kPa (135 kPa ved korreksjon for synerese) til 26 kPa (16 kPa), hvilket plasserer dem i samme område som flere vevstyper. Interaksjon mellom FGF og alginatsulfat i løsning økte i omfang ved økende sulfateringsgrad eller for økende andel alginatsulfat i blandinger. Gelskiver laget av blandinger gav alle en gradvis frigjøring av FGF til omkringliggende medium. Etter 12 dager var det fortsatt noe FGF tilstede i gelskiver som inneholdt alginat-sulfat, i motsetning til i de rene alginatskivene. Den mekaniske styrken, evnen til å binde til FGF, den osmotiske stabiliteten og justerbare fordelingen gjør blandinger av alginat og alginatsulfat til mulige kandidater for bruk innen "tissue engineering".

Symbols and Abbreviations

$\frac{dn}{dc}$	The specific refractive increment
D_{av}	Average diameter
% S	The weight % of sulfur in the alginate sample
A_2	The second virial coefficient
aFGF	Acidic FGF
AP	Alkaline Phosphatase
APA	Alginate-PLL-Alginate
ATTP	Activated Partial Thrombosis Time
bFGF	Basic FGF
BSA	Bovine Serum Albumin
DS	Degree of sulfation
E	The Young's modulus
ECMs	Extracellular Matrices
EDC	N-(3-Dimethylaminopropyl)-N'-ethylcarbodiimide hydrochloride
EDTA	Ethylenediaminetetraacetic acid
F_{GG}	The fraction of G-monosaccharides in the polysaccharide followed by a G-residue in the polymer chain

F_G	The fraction of G-monomers in an alginate polymer chain
FCS	Fetal calf serum
FGFRs	FGF Receptors
FGFs	Fibroblast growth factors
G	α -L-guluronic acid
GAG	Glycosaminoglycan
GDL	D-glucono- δ -lactone
GlcN	D-glucosamine
HEPES	4-(2-hydroxyethyl)-1-piperazineethanesulfonic acid
HR-ICP-MS	High-resolution inductively coupled plasma mass spectrometry
HRP	Horseradish Peroxidase
LSCM	Laser Scanning Confocal Microscopy
M	β -D-mannuronic acid
MES	2-(N-morpholino)ethanesulfonic acid
MQ-water	Filtrated and deionized water with a resistivity of $18.2 M\Omega \times cm$ at $25^\circ C$
PBS	Phosphate Buffered Saline
PLL	Poly-L-Lysine
PMT	Photomultiplier Tube
ppm	Parts per million
ppt	Parts per trillion
RGD	Arginine glycine aspartic acid

SEC-MALLS	Size exclusion chromatography coupled with multiangle laser light scattering
Sulfo-NHS	N-Hydroxysulfosuccinimide sodium salt

Table of Contents

Preface	i
Abstract	iii
Sammendrag	v
Symbols and Abbreviations	ix
Table of Contents	ix
List of Figures	xvii
List of Tables	xxii
1 Introduction	1
1.1 Alginate	1
1.1.1 Alginate Chemistry and Structure	1
1.1.2 Alginate Gelling Properties	4
1.1.3 Sulfated Alginate as a Heparin-Analogue	6
1.2 Tissue Engineering	9
1.2.1 Properties of Scaffolds for Use in Tissue Engineering	9
1.2.2 Alginate Hydrogels as Scaffolds	10
1.2.3 Alginate Gel Beads	12
1.3 Fibroblast Growth Factors (FGFs)	13
1.4 The Young's Modulus	14
1.5 Laser Scanning Confocal Microscopy	15
1.6 Structural Characterization	16
1.6.1 HR-ICP-MS	16
1.6.2 SEC-MALLS	17
1.7 Characterization of Biological Properties	19
1.7.1 Flow Cytometry	19
1.7.2 ELISA	20
1.8 The aims of the study	21

2	Materials and Methods	23
2.1	Materials	23
2.2	Sulfation of Alginate	24
2.3	Elemental Analysis and the Degree of Sulfation	25
2.4	Acid Hydrolysis of Alginate and SEC-MALLS Analysis	26
2.5	Preparation of Alginate Gel Beads for Swelling Experiments	27
2.6	Measuring the Swelling of Alginate Gel Beads	28
2.7	Content of Ca^{2+} in swelling gel beads	29
2.8	Preparation of Alginate Gel Cylinders	30
2.9	Gel Strength Measurements	32
2.10	Fluorescence labelling of Alginate-Sulfate	32
2.11	Preparation and Distribution Studies of Alginate/Alginate- Sulfate Gel Beads	33
2.12	Interactions Between Alginate-Sulfate in Solution and FGF	34
2.13	Release of FGF-basic from Alginate/Alginate-Sulfate Gels	36
3	Results	39
3.1	Sulfation of Alginate	39
3.2	Molecular Weight	40
3.2.1	Acid Hydrolysis	40
3.2.2	Sulfated Samples	43
3.3	Swelling of Alginate Gel Beads	44
3.3.1	Beads from Sulfated Alginate	45
3.3.2	Beads from Alginate/Alginate-Sulfate Mixtures Gelled with CaCl_2	46
3.3.3	Beads from Alginate/Alginate-Sulfate Mixtures Gelled with BaCl_2	51
3.3.4	The Content of Ca^{2+} in Swelling Beads	53
3.4	The Young's Modulus	55
3.5	Distribution of Sulfated Alginate in Gel Beads	59
3.6	Interactions between FGF and Alginate/ Alginate-Sulfate	62
3.6.1	Alginate/Alginate-Sulfate in Solution	62
3.6.2	Release of FGF from Alginate/Alginate-Sulfate Gel Disks	64
4	Discussion	67
5	Future Directions	75

6	Conclusions	77
	Appendices	I
A	Risk Assessment	III
B	Calculation of the Degree of Sulfation from Elemental Analysis Data	XI
C	The Young's Modulus of Gels Made from Sulfated Alginate of Varying DS	XV
D	Calculating the Pseudo First Order Rate Constant of Acid Hydrolysis	XVII
E	Data From the Swelling of Alginate Beads in NaCl	XXI
	E.1 Sulfated Alginate Samples	XXI
	E.2 Alginate/Alginate-Sulfate Mixtures, CaCl ₂	XXIII
	E.3 Beads from Alginate/Alginate-Sulfate Mixtures Gelled with BaCl ₂	XXX
F	Data from the Longitudinal Compression Test of Gels	XXXIX
G	Calculations of the Young's Modulus	XLVII
H	The Young's Modulus of Alginate/Alginate-Sulfate Gels	XLIX
I	Standard for FGF Using ELISA and Results from Gel Disk Measurements	LI



List of Figures

1.1.1	The structure of β -D-mannuronic acid (M) and α -L-guluronic acid (G).	1
1.1.2	Conformation of G and M residues in an alginate chain . .	2
1.1.3	The "egg-box" model of gel formation	5
1.1.4	The major repeating structural unit of heparin	7
2.6.1	Method for measuring alginate bead diameter	29
2.8.1	Method for making alginate gel cylinders	31
2.13.1	Distribution of gel disks in well plates for studying the release of FGF.	36
3.2.1	The inverse of the weight average molecular weight as a function of the time of acid hydrolysis for alginate and alginate-sulfate samples.	42
3.3.1	The number of beads made from alginate with varying DS as a function of number of treatments with 0.9 % NaCl. . .	45
3.3.2	The average increase in volume of beads made from alginate with different DS as a function of the number of treatments with 0.9 % NaCl.	46
3.3.3	The number of beads present in samples made from DS 0.90/LF200S mixtures as a function of the number of treatments with 0.9 % NaCl.	47
3.3.4	The average increase in volume of alginate beads made from DS 0.90/LF200S mixtures as a function of the number of treatments with 0.9 % NaCl.	48
3.3.5	The number of beads present in samples made from DS 0.68/LF200S mixtures as a function of the number of treatments with 0.9 % NaCl.	49

3.3.6	The average increase in volume of alginate beads made from DS 0.68/LF200S mixtures as a function of the number of treatments with 0.9 % NaCl.	50
3.3.7	The number of beads present in samples made from DS 0.90/LF200S mixtures in BaCl ₂ as a function of the number of treatments with 0.9 % NaCl.	52
3.3.8	The average increase in volume of alginate beads made from DS 0.90/LF200S mixtures in BaCl ₂ as a function of the number of treatments with 0.9 % NaCl.	53
3.3.9	The content of calcium alginate/alginate-sulfate beads after 0, 6 and 13 treatments with 0.9 % NaCl.	54
3.3.10	The content of sulfur in alginate/alginate-sulfate beads after 0, 6 and 13 treatments with 0.9 % NaCl.	55
3.4.1	The Young's modulus of DS 0.77/LF200S mixtures corrected for syneresis, along with hydrolysed alginate/LF200S mixtures.	57
3.4.2	The Young's modulus corrected for syneresis of DS 0.77/LF200S mixtures and gels made from pure sulfated alginate of various DS.	59
3.5.1	The distribution of alginate-sulfate in alginate/alginate-sulfate beads stored in a NaCl solution.	60
3.5.2	The distribution of alginate-sulfate in alginate/alginate-sulfate beads stored in a CaCl ₂ solution.	61
3.5.3	The distribution of alginate-sulfate in alginate/alginate-sulfate beads stored in a HEPES solution.	61
3.6.1	The median fluorescence intensity of cells with labelled FGF after treatment with alginates of different DS.	63
3.6.2	The median fluorescence intensity of cells with labelled FGF after treatment with alginate/alginate-sulfate (DS 0.80) mixtures.	63
3.6.3	The measured absorbance of samples in from solutions over gel disks containing FGF at 405 nm.	65
3.6.4	The calculated concentration of FGF in gel disks after 12 days in a HEPES medium.	66
B.1	The standard curve for the relationship between % S and the degree of sulfation (DS).	XIII

F.1	The force-distance plots for the six gels from the 10 % DS 0.77/LF200S sample.	XL
I.1	The constructed standard curve for FGF using a sandwich ELISA.	LII



List of Tables

2.2.1	Overview of the batches of sulfated alginate prepared . . .	25
2.5.1	Overview of the alginate gel beads prepared for the swelling experiments.	28
2.11.1	The solutions used for storage of alginate gel beads containing alginate-sulfate labelled with fluorescence.	34
3.1.1	Content of sulfur and degree of sulfation for samples of alginate-sulfate.	39
3.2.1	The molecular weight averages of sulfated and nonsulfated alginate samples after acid hydrolysis	41
3.2.2	The pseudo first order rate constant, k , for the random depolymerization of two samples of alginate-sulfate and for pure alginate.	43
3.2.3	Average molecular weight of LF200S, alginate-sulfates and samples subjected to acid hydrolysis.	44
3.3.1	The number of treatments with 0.9 % NaCl beads made from different samples of alginate and alginate-sulfate could tolerate before bursting.	51
3.4.1	The Young's modulus for gels from alginate DS 0.77/LF200S mixtures.	56
3.4.2	The Young's modulus of DS 0.77/LF200S mixtures corrected for syneresis, along with hydrolysed alginate/LF200S mixtures.	58
3.6.1	The approximated degree of sulfation for the mixtures of alginate-sulfate (DS 0.80) and LF200S.	64
B.1	The calculated values of % S for theoretical DS values. . .	XII

C.1	The calculated Young's modulus for samples of alginate-sulfate with varying DS.	XVI
D.1	Average M_w , and DP_w of alginate LF200S after acid hydrolysis over time.	XVIII
D.2	Average M_w , and DP_w of alginate-sulfate (DS 0.27) after acid hydrolysis over time.	XVIII
D.3	Average M_w , and DP_w of alginate-sulfate (DS 0.90) after acid hydrolysis over time.	XIX
E.1.1	The number of beads made from samples of alginate of different DS after each treatment with NaCl.	XXII
E.1.2	The average diameter of beads made from samples of alginate of different DS after each treatment with NaCl.	XXII
E.1.3	The average increase in volume of beads made from samples of alginate of different DS after each treatment with NaCl.	XXIII
E.2.1	The number of Ca-alginate beads made from alginate DS 0.90/LF200S mixtures after each treatment with NaCl.	XXIV
E.2.2	The average diameter of Ca-alginate beads made from alginate DS 0.90/LF200S mixtures after each treatment with NaCl.	XXV
E.2.3	The average increase in volume of Ca-alginate beads made from alginate DS 0.90/LF200S mixtures after each treatment with NaCl.	XXVI
E.2.4	The number of Ca-alginate beads made from alginate DS 0.68/LF200S mixtures after each treatment with NaCl.	XXVII
E.2.5	The average diameter of Ca-alginate beads made from alginate DS 0.68/LF200S mixtures after each treatment with NaCl.	XXVIII
E.2.6	The average increase in volume of Ca-alginate beads made from alginate DS 0.68/LF200S mixtures after each treatment with NaCl.	XXIX
E.3.1	The number of Ba-alginate beads made from alginate DS 0.90/LF200S mixtures after each treatment with NaCl.	XXX
E.3.2	The average diameter of Ba-alginate beads made from DS 0.90/LF200S mixtures after each treatment with NaCl.	XXXII

E.3.3	The average increase in volume of Ba-alginate beads made from DS 0.90/LF200S mixtures after each treatment with NaCl.	XXXV
F.1	The raw data for the calculation of the Young's modulus and correction for syneresis for gels made of pure alginate.	XLI
F.2	The raw data for the calculation of the Young's modulus and correction for syneresis for gels made of DS 0.77/LF200S, with 5 % alginate-sulfate.	XLI
F.3	The raw data for the calculation of the Young's modulus and correction for syneresis for gels made of DS 0.77/LF200S, with 10 % alginate-sulfate.	XLII
F.4	The raw data for the calculation of the Young's modulus and correction for syneresis for gels made of DS 0.77/LF200S, with 20 % alginate-sulfate.	XLII
F.5	The raw data for the calculation of the Young's modulus and correction for syneresis for gels made of DS 0.77/LF200S, with 40 % alginate-sulfate.	XLIII
F.6	The raw data for the calculation of the Young's modulus and correction for syneresis for gels made of DS 0.77/LF200S, with 60 % alginate-sulfate.	XLIII
F.7	The raw data for the calculation of the Young's modulus and correction for syneresis for gels made of DS 0.77/LF200S, with 80 % alginate-sulfate.	XLIV
F.8	The raw data for the calculation of the Young's modulus and correction for syneresis for gels made of pure DS 0.77 alginate-sulfate.	XLIV
F.9	The raw data for the calculation of the Young's modulus and correction for syneresis for gels made of partially hydrolysed alginate/LF200S, with 10 % partially hydrolysed alginate.	XLV
F.10	The raw data for the calculation of the Young's modulus and correction for syneresis for gels made of partially hydrolysed alginate/LF200S, with 20 % partially hydrolysed alginate.	XLV

F.11	The raw data for the calculation of the Young's modulus and correction for syneresis for gels made of partially hydrolysed alginate/LF200S, with 60 % partially hydrolysed alginate.	XLVI
G.1	The raw data for the calculation of the Young's modulus and correction for syneresis for one of the gels made of the 5 % sample of DS 0.77/LF200S.	XLVII
H.1	The weight and the corrected Young's modulus of gels made from DS 0.77/LF200S mixtures.	L
H.2	The weight and the corrected Young's modulus of gels made from hydrolysed alginate/LF200S mixtures.	L
I.1	Calculations of the concentration of FGF in gel disks after 12 days in a HEPES solution.	LIII

1. Introduction

1.1 Alginate

1.1.1 Alginate Chemistry and Structure

Alginates are linear co-biopolymers consisting of the two monosaccharides β -D-mannuronic acid (M), and its 5-epimer α -L-guluronic acid (G), coupled by 1,4-glycosidic bonds (Nelson and Cretcher, 1930; Fischer and Dörfel, 1955; Haug et al., 1974). The structure of the two monosaccharides are shown in Figure 1.1.1.

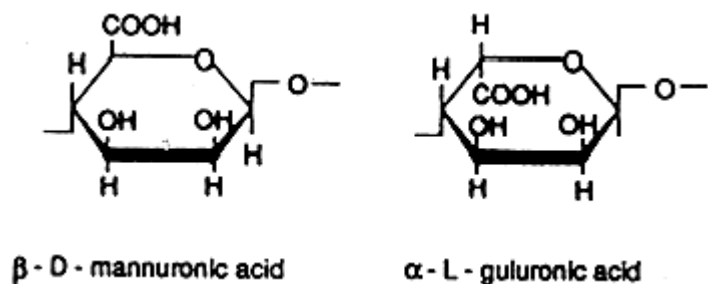


Figure 1.1.1: Adapted from Gombotz et. al (Gombotz and Wee, 2012a). The structure of β -D-mannuronic acid (M) and α -L-guluronic acid (G).

The distribution of M and G along the polysaccharide chain is non-random, and long stretches consisting of only one of the residues are found in the polysaccharides (Haug et al., 1966, 1967a). These homopolymeric stretches are called G- blocks and M- blocks, depending on which monosaccharide is present, while the alternating sequences in between are called MG- blocks

(Haug et al., 1967b). The natural synthesis of alginates begins with polymannuronic acid, followed by conversion of some monosaccharides to α -L-guluronic acid residues by mannuronan C5-epimerases. (Smidsrød and Moe, 2008). Several different epimerases exist, giving different block structures depending on the specific epimerase (Strand et al., 2003b). A selection of different epimerases have been isolated and purified, which allows for specific tailoring of the final alginate structure in laboratories (Strand et al., 2003b). Upon epimerization, the α -L-guluronic acid changes its ring conformation from the 4C_1 ring conformation of β -D-mannuronic acid to a 1C_4 ring conformation, leaving the hydroxyl groups at C1, C3 and C4 in axial positions, while the carboxyl group at C6 and the hydroxyl group at C2 are in an equatorial position (Draget et al., 1997; Smidsrød and Moe, 2008). As the glycosidic linkages are all between C1 and C4, the conformational change alters the geometry of these linkages, so they can be either di-equatorial (eq-eq), for an M-M linkage, di-axial (ax-ax), for a G-G linkage, or eq-ax /ax-eq, for an M-G/G-M linkage (Draget et al., 1997; Smidsrød and Moe, 2008). The conformation of the G monosaccharides leads to a cavity formation between two neighbouring G-residues, as shown in Figure 1.1.2 (Draget et al., 1997).

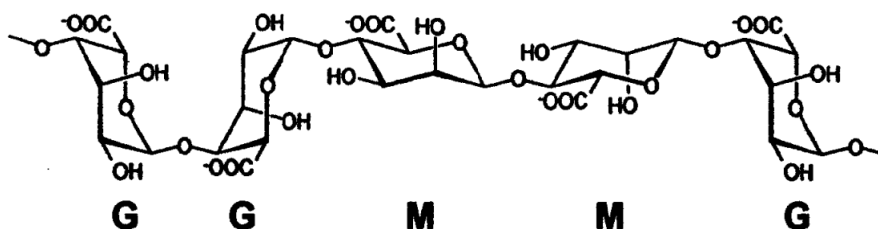


Figure 1.1.2: Figure from (Draget et al., 1997) The conformation of β -D-mannuronic and α -L-guluronic acid residues in an alginate chain, showing how neighbouring G-residues form a cavity between them because of their di-axial linkage.

The physical properties of alginates, such as viscosity, strength of gels and susceptibility to hydrolysis, are determined by the proportion between the two monosaccharide residues, and by the sequences of these, with a great variability between different alginate sources (Haug et al., 1967b). All algi-

nates are susceptible to thermal depolymerization, and the rate of thermal depolymerization has been shown to increase as the pH of the solution decreases, and causes a random depolymerization of the polymer (Holme et al., 2008; Smidsrød and Moe, 2008). The MG- blocks are more susceptible to acid hydrolysis than the homopolymeric G- and M-blocks (Haug et al., 1966). Acid hydrolysis of the polysaccharides dextran and dextran sulfate showed that for pH values above 1, the hydrolysis rate was higher for the sulfated sample, which Smidsrød *et al.* concluded was probably due to a higher proton concentration around the negatively charged polysaccharide than in the bulk solution (Smidsrød et al., 1966). For random depolymerization of a linear polymer with n monosaccharides, and $n-1 \approx n$ linkages, one can assume a pseudo first order reaction with respect to n , as shown in Equation 1.1.1 (Christensen, 2013).

$$\frac{-dn}{dt} = kn \quad (1.1.1)$$

Assuming long chains, and thus large molecular weights, Equation 1.1.2 can be used to determine the rate constant graphically when molecular weights are known, as a plot of $\frac{1}{M_w}$ against time gives a straight line with slope $\frac{k}{2M_0}$ and interception at $\frac{1}{M_{w,0}}$ (Christensen, 2013).

$$\frac{1}{M_w} = \frac{1}{M_{w,0}} + \frac{k}{2M_0}t \quad (1.1.2)$$

where M_w is the weight average molecular weight of the sample at a time t , $M_{w,0}$ is the initial weight average molecular weight of the polymers in the sample, M_0 is the molecular weight of each monosaccharide in the polymer chain, and k is the pseudo first order rate constant.

The pK_a values of the individual monosaccharides are found to be 3.65 for the G monomers, and 3.38 for the M monomers in 0.1 M NaCl, and an abrupt decrease in pH will cause precipitation of alginate from the solution (Haug, 1964; Draget et al., 1994).

Alginate acts as a structural element in brown algae such as *Laminaria Hyperborea* or *Ascophyllum nodosum* and is also produced extracellularly by some bacteria such as *Azotobacter vinelandii*, *Azotobacter choococcum* and several *Pseudomonas* species (Haug et al., 1967b; Linker and Jones, 1966; Sherbrock-Cox et al., 1984). Bacterial alginates are usually O-acetylated on

the 2- or 3- position, or both, of the M-residues, while the alginates isolated from algae are without these modifications (Linker and Jones, 1966; Gacesa, 1998).

Alginates are abundant in the nature and commercially available at low cost, making it an attractive material for use in the industry (Draget et al., 1989). Alginates from seaweeds are used commercially as stabilisers, emulsifiers and gelling agents in the food industry, in cosmetics, in textile industry and for pharmaceutical applications (Sherbrock-Cox et al., 1984; Sandford et al., 1984; Augst et al., 2006).

1.1.2 Alginate Gelling Properties

Most alkaline earth metals can cause gel formation in contact with alginate solutions (Haug and Smidsrød, 1965). The most common ions used for alginate gelation are Ba^{2+} , Ca^{2+} and Sr^{2+} , where Ba^{2+} is the ion binding strongest to alginate, and Ca^{2+} is the one with the weakest binding of these three (Haug and Smidsrød, 1965). The differences between binding strength for different ions is most notable for alginates with a high content of G-residues (Smidsrød, 1974). In addition to gelation with divalent ions, direct addition of D-glucono- δ -lactone (GDL) to sodium alginate can also produce gels, called alginic acid gels (Draget et al., 1994).

One explanation of the gelation process of alginate is the "egg-box" model, proposed by Grant *et. al* in 1973, which suggests that cavities formed between neighbouring G-residues offers binding places for divalent cations with a charge dispersion on the polymer chain optimal for ionic interaction, and a physical room fitting the size of the ions (Grant et al., 1973). An illustration of the binding of ions in the G-block cavities is shown in Figure 1.1.3.

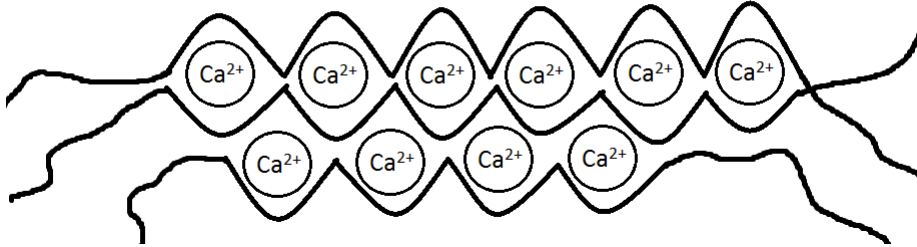


Figure 1.1.3: Adapted from Grant et. al (Grant et al., 1973). The aggregation of several alginate chains by association to divalent cations, according to the "egg-box model". Divalent cations, such as Ca^{2+} , interact with the negative charges on the alginate chain, and the G-blocks accommodate close binding between cations and polysaccharide.

Two different approaches are used to obtain calcium-alginate gels, where the application of the gel determines which approach is the most suitable (Draget et al., 1993). The diffusion method is based upon letting calcium ions diffuse into the alginate solution from an external reservoir to achieve gelation. Using this method, the gels show an inhomogeneous alginate distribution, with a gradual decrease in concentration towards the center of the gel. This effect becomes even more prominent when using a high alginate concentration or alginate of low molecular weight (Skjåk-Bræk et al., 1989). Microcapsules show much less inhomogeneity if they are gelled in the presence of non-gelling ions, or after washing with saline (Strand et al., 2003a).

While external gelation is the preferred method in alginate bead immobilization techniques, the other method, internal gelation, can be used to obtain a more homogenous gel when this is desirable (Smidsrød and Skjåk-Bræk, 1990; Draget et al., 1989). In internal gelation, use of complexed calcium or calcium-salts of a low solubility mixed into the solution, such as CaCO_3 , together with the slowly hydrolysing acid GDL, allows for a slow and controlled release of calcium into the alginate solution, causing gelation (Draget et al., 1990; Skjåk-Bræk et al., 1986). Internal gelation using these two chemicals in the alginate leads to the formation of homogeneous gels over a wide pH range, leaving the non-toxic by-products CO_2 and D-gluconic acid (Draget et al., 1989). For internal gelation inhomogeneous gels are more probable for less viscous polymer solutions, where carbonate sedimentation occurs during

the gelation process (Draget et al., 1990).

Ca-alginate gels have shown some syneresis in previous experiments, a state where water is released from the hydrogel, thus leading to an increase in the alginate concentration of the gel (Smidsrød et al., 1972; Mørch, 2008). The syneresis is greater for gels with many and long MG-blocks, high Ca^{2+} concentration and a higher molecular weight (Martinsen et al., 1989; Mørch, 2008). A high concentration of CaCO_3 during internal gelation can also contribute to an increase in the syneresis of the gels (Draget et al., 1990).

1.1.3 Sulfated Alginate as a Heparin-Analogue

Functionalization of alginate is relatively easy, with its free hydroxyl and carboxyl groups along the backbone of the polysaccharide (Yang et al., 2011). Modifications of alginate by researcher groups include oxidation, reductive amination, esterification, grafting methods, amidation and sulfation (Boonthekul et al., 2005; Andresen et al., 1977; Rastello De Boisseson et al., 2004; Polyak et al., 2004; Ronghua et al., 2003).

The sulfation of alginate makes its structure more similar to that of heparin, a linear acidic polysaccharide belonging to the glycosaminoglycan (GAG) family (Zhao et al., 2007; Shriver et al., 2012). The heparin chain consists of 1 \rightarrow 4 linked pyranosyluronic acid (uronic acid) and 2-amino- 2-deoxyglucopyranose (D-glucosamine, GlcN) repeating units (Casu, 1985). While there is at least seven different disaccharide units present in heparin, the most common disaccharide unit is a 2-O-sulfonated L-iduronic acid 1 \rightarrow 4 linked to a 6-O, N-sulfonated D-glucosamine, as shown in Figure 1.1.4 (Lindahl et al., 1979; Shriver et al., 2012). The L-iduronic acid can sometimes be replaced by its epimer D-glucuronic acid, and the sulfation pattern can also vary along the polysaccharide chain, contributing to a complex structure of these polysaccharides (Shriver et al., 2012).

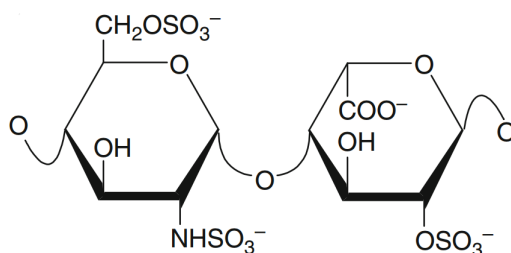


Figure 1.1.4: *The major repeating disaccharide unit of the heparin structure in its fully sulfated form. The L-iduronic acid can sometimes be replaced by its epimer D-glucuronic acid, and the sulfation pattern can also vary along the polysaccharide chain (Shriver et al., 2012).*

Heparin interacts with hundreds of different proteins, including growth factors such as fibroblast growth factor (FGF), enzymes such as thrombin, and matrix proteins such as fibronectin (Linhardt, 2003). Heparin is used extensively clinically as an anticoagulant, as it can bind to antithrombin and slow down the coagulation process (Linhardt, 2003; Lindahl et al., 1979). It is a naturally occurring polysaccharide produced mainly in mast cells found in organs such as liver, intestines and lung (Linhardt, 2003) Heparin is isolated from animal tissue, mostly porcine intestine, and goes through an extensive purification process before it can be used as a pharmaceutical product (Shriver et al., 2012). The expensive and time-consuming process to obtain heparin makes it attractive to develop heparin analogues that can be made in a more rapid and cost effective way. Tailored heparin analogues also allow for a more controlled structure, with less variability than the heparin extracted from animal tissue. Heparin analogues produced by researcher groups so far include polyglycerol sulfates, pentosan polysulfate and alginate sulfates (Türk et al., 2004; de Prost, 1986; Ronghua et al., 2003; Zhao et al., 2007).

Sulfation of alginate have been obtained by two different approaches. One of the approaches includes a conversion of a sodium salt to a tertiary amine salt followed by O-sulfation with carbodiimide and sulfuric acid (Freeman et al., 2008). This approach was found to cause some depolymerization of the samples during the sulfation process (Freeman et al., 2008). Ronghua *et al.* used another approached, where formamide and chlorosulfonic acid were added to alginate followed by heating to 60 °C for 4 h to obtain alginate sulfate with 1.4 sulfate groups per uronic acid on average (Ronghua et al.,

2003). The maximum degree of substitution, or degree of sulfation (DS) theoretically possible is 2, corresponding to sulfate substitution on both the available hydroxyl groups on each residue in the polysaccharide chain (Arlov et al., 2014). Using the Ronghua method, Arlov *et al.* reported maximum values for DS of 1.15 for poly-G alginate and 0.9 for poly-M alginate. They also observed an increase in DS for increasing concentrations of $HClSO_3$ in the reaction mixture up to 4 % (v/v) $HClSO_3$, where the DS value reached a plateau, possibly due to a decrease in the alginate solubility as the acidity of the solution increases (Arlov et al., 2014). The sulfation process for this method is probably random, shown by a greater heterogeneity in sulfation patterns for samples of moderate degrees of sulfation of 0.4-0.5 than for samples close to saturation (Arlov et al., 2014).

Alginate sulfate has shown some anticoagulant activity by prolonging the activated partial thrombosis time (ATTP) to almost the same degree as heparin (Ronghua et al., 2003). Heparin binding proteins have also been shown to bind to both heparin and alginate sulfate, but not to alginate (Freeman et al., 2008). Mixtures of alginate and alginate-sulfate were able to produce beads that caused a slower release of basic FGF (bFGF) into the surrounding medium compared to pure alginate beads (Freeman et al., 2008). Scaffolds containing mixtures of alginate and alginate-sulfate with bound bFGF implanted in rats increased the angiogenetic activity and led to a higher maturity of the formed vessels compared to the pure alginate scaffolds (Freeman et al., 2008). Alginate sulfate has also been immobilized onto polysulfone ultrafiltration membranes to give selective binding of low-density lipoprotein (LDL) in blood. High levels of LDL, a major cholesterol transporter in the blood, is associated with an increased risk of atherosclerosis and heart attacks, and LDL adsorbents are used to reduce this risk (Wang et al., 2014). The immobilized alginate sulfate had a good blood compatibility, and LDL could be desorbed by addition of NaCl, making therapeutical reuse of the membranes possible (Wang et al., 2014). The bicompatibility and the ability to interact with proteins makes sulfated alginate a possible candidate for use in tissue engineering.

1.2 Tissue Engineering

1.2.1 Properties of Scaffolds for Use in Tissue Engineering

The number of patients in need of an organ transplantation far exceeds the number of available donors, resulting in the death of patients as they wait for a suitable donor. This has brought forward the field of tissue engineering, where the idea is that new and functional tissue can be fabricated using living cells associated with a scaffold guiding tissue development (Lanza et al., 2011). These scaffolds must be biocompatible, accommodate cell adhesion, proliferation and vascularization, be able to organize cells into three dimensional structures, provide a mechanical support for the growing tissue and ensure that nutrients and metabolites are free to diffuse to and from the cells (Rowley et al., 1999a; Bose et al., 2012). The extracellular matrix (ECM) associated with cells in the body affects both cell growth and differentiation as well as tissue strength and structure, and scaffolds imitating the ECM should be able to interact with cells in a similar manner (Shoichet et al., 1996).

The ideal mechanical strength of the scaffold should match the desired tissue, and as the Young's modulus of tissues ranges from less than 1 kPa for liver, via 25 kPa for skeletal muscle cells and 100 kPa for cardiac cells, and up to as high as 20 GPa for bone, the mechanical requirements of scaffolds vary greatly (Bose et al., 2012; Ashman et al., 1984; Yoon and Katz, 1976; Chen et al., 1996; Mathur et al., 2001). The scaffolds can be made using materials that are permanent or biodegradable, natural, synthetic or hybrids (Lanza et al., 2011). Biodegradable materials must have a controlled degradation rate, matching the development of the newly formed tissue, giving room for this as it grows (Bose et al., 2012).

The scaffold permeability is essential for the distribution of cells throughout the whole scaffold, and for the flow of nutrients and oxygen (Melchels et al., 2010). Not only the pore size, but also the size of the interconnection channels is important for a good cell distribution, as cells seldom enter interconnections smaller than 5-10 times the size of a single cell (Melchels et al., 2010). Porous scaffolds involving both micro- ($< 20\mu\text{m}$) and macro ($> 100\mu\text{m}$) porosities is an advantage to cell growth (Bose et al., 2012). As a

high porosity compromises the mechanical strength, this can be a challenge when making scaffolds with the requirement for a high mechanical strength (Bose et al., 2012). Carefully engineered surfaces and pore sizes of scaffolds can also help guide the alignment of cells such as muscle cells, where the cell orientation is important for the function of the tissue (Guillemette et al., 2010; Engelmayr et al., 2008).

Cells can be seeded in the scaffold before implantation, or they can be recruited *in vivo* (Lanza et al., 2011). Co-seeding of different cell types *in vitro* can increase the levels of vascular endothelial growth factor expression in the construct and promote formation and stabilization of the endothelial vessels after implantation (Levenberg et al., 2005). As tissues are often composed of more than one single cell type, the scaffold must be able to accommodate and guide the development of several cell types at the same time (Lanza et al., 2011). Biomolecules such as growth factors and differentiation factors can be incorporated into the scaffold to help the vascularization, cell differentiation and growth in and around the graft, and to guide the development of the desired tissue (Lanza et al., 2011; Bose et al., 2012).

1.2.2 Alginate Hydrogels as Scaffolds

Hydrogels are hydrophilic three-dimensional polymeric networks containing more than 30 % water, and are attractive materials in the field of tissue engineering as they have physical properties similar to many tissues (Pepas et al., 2000; Drury and Mooney, 2003). Alginate is one of the natural polymers used to create hydrogels for use in tissue engineering. Alginate hydrogels have been used as injectable cell delivery vehicle, as wound dressing, dental impression, immobilization matrix, as a synthetic extracellular matrix (ECM) and for transplantation of chondrocytes, hepatocytes and islets of Langerhans (Lee and Mooney, 2001; Drury and Mooney, 2003; Augst et al., 2006; Rowley et al., 1999a).

Alginate is an attractive material for applications like the ones mentioned because of its biocompatibility, the possibility of gelation under mild conditions, allowing for incorporation of proteins or live cells and because it is readily available and relatively easy to modify (Rokstad et al., 2011; Drury and Mooney, 2003; Augst et al., 2006; Mørch, 2008). The porosity of the alginate gels can be regulated by changing concentrations and G/M-ratio in

the gels (Gombotz and Wee, 2012b). The porosity of gels can be monitored by use of electron microscopy, diffusion studies with proteins of different molecular weights, or by packing of gels in a column and recording the exclusion volumes for macromolecular standards (Gombotz and Wee, 2012b). Alginate hydrogels can be moulded into complex geometries to make suitable scaffolds (Kuo and Ma, 2001). Unfortunately, alginate also has some weaknesses for tissue engineering applications, the most important ones being the poorly regulated degradation rate, and the lack of cell adherence (Rowley et al., 1999a; Augst et al., 2006; Rowley et al., 1999b). Alginate gels also experience a rapid drop in mechanical strength initially in physiological solutions, but composites, e.g polymers and ceramics can be used to maintain the strength if a high mechanical strength is required for a longer period of time (Bose et al., 2012; LeRoux et al., 1999).

For applications such as release of incorporated biomolecules or in functional tissue regeneration, a controlled degradation rate is essential to the function of the hydrogel (Drury and Mooney, 2003; Augst et al., 2006). Ionically crosslinked alginate gels experience a slow and uncontrolled degradation *in vivo* as the crosslinking ions leak out of the hydrogel and the gelation junctions are disrupted (Augst et al., 2006). Methods used for improving the control over the degradation rate of ionically crosslinked alginate hydrogels includes producing methacrylated photocrosslinked gels, also allowing for control of swelling behavior and the elastic modulus, and the mixing of high- and low molecular weight partially oxidized alginates (Jeon et al., 2009; Kong et al., 2004). Alginates can also be crosslinked covalently by use of carbodi-imide chemistry to control the stability of the gel (Rowley et al., 1999b).

The hydrophilic surface of alginate hydrogels does not encourage cell adhesion of either eukaryotic or prokaryotic cells, and lack the ability of interaction with proteins (Smetana Jr, 1993; Rowley et al., 1999b). Cell anchorage is critical for the survival for many cell types, and is also involved in cell migration, proliferation, differentiation and apoptosis (Rowley et al., 1999b). A way to improve the ability of alginate to interact biologically is by coupling cellular adhesion molecules such as laminin, fibronectin or collagen to the alginate (Augst et al., 2006). Short amino acid sequences found in the ECM, such as fibronectin-derived peptide arginin-glycine-aspartic acid (RGD), or derivatives of such sequences, are often used for obtaining biological activity (Augst et al., 2006). Myoblasts have been shown to adhere to, proliferate and

fuse in contact with RGD-modified alginate gels, and a co-transplantation of osteoblasts and chondrocytes in alginate-RGD gels led to self-organization into growth plate-like structures (Augst et al., 2006; Rowley et al., 1999b).

1.2.3 Alginate Gel Beads

The mild conditions for alginate gel formation makes it possible to entrap living microbial or mammalian cells inside alginate gels by mixing them into the alginate solution prior to gelation (Martinsen et al., 1989). The inhomogeneity obtained by use of external gelation is often a preferred structure in microcapsules due to low porosity and high stability (Strand et al., 2003a). One application of alginate microcapsules is as immune barriers for cell transplantation, where the alginate bead protects the entrapped cells from the host immune system (Mørch et al., 2006). This method for cell transplants does however involve problems such as early graft rejection due to overgrowth by fibroblasts, as well as chemical and mechanical instability of the capsules (Moe et al., 1993).

In order to stabilize the microcapsules against osmotic swelling, the alginate beads are often coated with a polycation, such as poly-L-lysine (PLL) (Orive et al., 2006). As PLL is known to activate immune responses in blood, a final coat of alginate is often applied, giving alginate-PLL-alginate (APA) microcapsules. (Orive et al., 2006). However, this extra coating does not fully mask the immunogenic activity of PLL, and is not an optimal system (Rokstad et al., 2011; Orive et al., 2006). Coating with poly(ethylene glycol)-grafted PLL or use of hydroxyethyl methacrylate-grafted alginate are methods to improve the biocompatibility of the microcapsules without loss of stability (Shoichet et al., 1996).

The sensitivity of Ca^{2+} -gels towards chelating agents such as phosphate and citrate, as well as nongelling ions such as Na^+ and Mg^{2+} is one reason for gel instability. In a physiological solution the ion replacement in the gel will lead to osmotic swelling of the beads or microcapsules, where the pore size increases and the gel is eventually destabilized and prone to rupture (Thu et al., 1996). The non-condensed ions in the alginate network, such as Na^+ and Ca^{2+} , are held back from diffusing out into a solution with a lower chemical potential by the negative charges of the alginate backbone. This causes an osmotic pressure inside the gel and an inflow of water (Moe, 1993). In a

stable gel the osmotic pressure will be balanced by the elastic and retracting reaction of the gel network and the volume will stay constant (Moe, 1993). In a NaCl solution, the sodium ions can replace Ca^{2+} or Ba^{2+} ions in the gel structure, causing the release of these ions into the medium, giving a reduction in the gel strength (Martinsen et al., 1989). A high crosslinking ratio and few hydrophilic groups are some factors that will give a hydrogel with less swelling (Peppas et al., 2000).

1.3 Fibroblast Growth Factors (FGFs)

Fibroblast growth factors (FGFs) are part of a large family of polypeptide growth factors, where the first isolated members were acidic FGF (aFGF) and basic FGF (bFGF) (Gospodarowicz, 1975; Johnson et al., 1990). FGFs are found in a wide range of organisms, from nematodes to humans (Ornitz and Itoh, 2001). They are involved in the regulation of cell proliferation, migration, morphogenesis, angiogenesis and differentiation during embryonic development, and act as homeostatic factors and contribute to tissue repair in adult organisms (Linhardt, 2003; Ornitz and Itoh, 2001). Whereas most FGFs are readily secreted from the cell, some members of the family are only existing intracellularly (Ornitz and Itoh, 2001). The role of FGF on cell development depends on the microenvironment, where both mechanical and chemical factors influence the effect of FGF on cells (Ingber and Folkman, 1989).

An important part of the biology of FGFs is their ability to interact with heparin or heparan sulfate proteoglycan (Ornitz and Itoh, 2001). These interactions protect FGF from acidic, thermal and proteolytic degradation. (Ornitz and Itoh, 2001; Gospodarowicz and Cheng, 1986). Binding to heparin or heparan sulfate has also been shown to increase the diffusion radius of bFGF in agarose and fibrin gels, and on a cellular monolayer, increasing the range of action of one single protein (Flaumenhaft et al., 1990).

The FGFs bind to cell surface receptors called FGF receptors (FGFRs) (Linhardt, 2003). These receptors include both transmembrane tyrosine kinase receptors and extracellular receptors and are also heparin binding proteins (Linhardt, 2003; Johnson et al., 1990). Heparin is thought to promote the formation of a stable FGF:FGFR:heparin ternary complex, and to stabilize

the interaction with a second similar complex, so that a receptor dimerization followed by signal transduction can occur (Schlessinger et al., 2000).

1.4 The Young's Modulus

The Young's modulus, or the elastic modulus, E , is a measure of the gel's resistance towards compression, and can be calculated from the initial tangent of a force-deformation curve obtained from a longitudinal compression test (Draget et al., 1993). The calculation also requires knowledge of the initial height of the gel, and of the cross-sectional area of the gel surface, as shown in Equation 1.4.1 (Draget et al., 1994).

$$E = \frac{F}{\Delta l} \times \frac{l}{A} \quad (1.4.1)$$

where E is given in N/m^2 (Pa), $\frac{F}{\Delta l}$ is the initial slope of the force-distance plot, where the gel with initial length l , is compressed a distance Δl , and A is the initial cross-sectional area of the gel.

Alginate gel strength is correlated to the content of G residues in the polymer, the length of the G-blocks, the alginate concentration and molecular weight, and the choice of divalent cation for gelation (Draget et al., 1990; Mørch et al., 2012; Smidsrød et al., 1972). MG-sequences can also contribute to an increase in gel strength, due to the formation of mixed junctions between G-blocks and MG-blocks (Mørch, 2008). An increasing pore size in alginate hydrogels is correlated to a decrease in the gel strength (Shoichet et al., 1996).

While use of Ba^{2+} as gelling agent can improve the mechanical strength of alginate gels, its use alone is not suited for biological applications, as barium in its soluble state is toxic to humans, leading to conditions such as extra-cellular hypokalemia, renal failure and cardiac arrest (Dart, 2004). However, some experiments have been conducted where both 1 mM BaCl_2 and 50 mM CaCl_2 were used together in the gelling bath to form gel beads for use in microencapsulation (Mørch et al., 2012). These beads had a higher junction formation and gave stiffer gels than pure CaCl_2 gels, and when implanted in mice, the concentration of barium in the blood did not exceed the estimated

tolerance set by WHO at 0.02 mg barium/kg body weight per day (Mørch et al., 2012). Use of low concentrations of barium may thus be possible for gels in biological applications to improve the stability and strength of the gels.

A linear relationship has been observed between the stiffness and the square of the concentration of alginate gels (Smidsrød et al., 1972). As alginate gels often undergo syneresis, the actual alginate concentration is often higher than the initial concentration of the gel solution, and the measured gel strength should be corrected for the increase in concentration for more accurate comparison between different gels (Martinsen et al., 1989). Assuming the weight of the alginate gel before and after syneresis is known, the corrected gel strength can be calculated as shown in Equation 1.4.2 (Martinsen et al., 1989).

$$E_{corrected} = E_{measured} \times \left(\frac{w_t}{w_0}\right)^2 \quad (1.4.2)$$

1.5 Laser Scanning Confocal Microscopy

Laser scanning confocal microscopy (LSCM) is widely used by researchers and for medical applications, and can offer several advantages over the conventional widefield optical microscopy (Olivier and Moine, 2013). LSCM offers the ability to control depth of field, to collect serial optical sections from thick specimen, and excludes secondary fluorescence from other planes than the one studied at the time. The result is that the images acquired by use of a confocal microscope is less blurred and reveal a significantly higher degree of structural detail than images from conventional widefield optical microscopy (Olivier and Moine, 2013).

In a laser scanning confocal microscope illumination of the sample from a laser light source, and the detection are confined to a single, diffraction-limited point in the specimen (Paddock, 2000). The laser light is focused by use of an objective lens and a raster scanning mechanism is used for scanning across the specimen, giving what is known as a point scanning of the sample (Paddock, 2000; Murphy and Davidson, 2013). Lasers for fluorophore excitation includes Argon-ion, Helium-neon, diode and diode-pumped solid state, which together provide excitation lines across the visible spectrum (Paddock,

2000). Points of light from the specimen are detected by a photomultiplier tube (PMT) detector positioned behind a pinhole and a barrier filter, and only a small fraction of background noise reaches the PMT detector (Paddock, 2000). Analog-to-digital converters changes the voltage fluctuations of the PMT detector into digital signals for image display on the computer monitor (Murphy and Davidson, 2013).

1.6 Structural Characterization

1.6.1 HR-ICP-MS

High resolution inductively coupled plasma mass spectrometry (HR-ICP-MS) is used in a wide range of research fields, including environmental, geological biomedical and nuclear research fields (Gießmann and Greb, 1994; Thomas, 2013). It is an effective method for rapid multielement determinations from down to the low range of parts per trillion (ppt) and up to the parts per million (ppm) range (Thomas, 2013).

In ICP-MS, the liquid sample is pumped into a nebulizer and converted to a fine aerosol by the use of argon gas (Thomas, 2013). In a spray chamber, the fine droplets (about 1-2 % of the sample) is separated from larger droplets and enters a plasma torch via a sample injector (Thomas, 2013). At the plasma torch, temperatures above 6000 K ensures drying, vaporization, atomization and finally ionization even of elements with high ionization potential, sending positively charged ions towards the mass spectrometer (Gießmann and Greb, 1994). The ions pass through the ion optics, where a series of electrostatic lenses focus the ion beam towards the mass separation advice, keeping photons, particulates, and neutral species from reaching the detector (Thomas, 2013).

At the mass separation device, which for HR-ICP-MS would be a magnetic sector based high resolution analyzer, only analyte ions of a particular mass-to-charge ratio are allowed to pass through to the detector, while other ions are filtered out (Gießmann and Greb, 1994). An ion detector, usually a discrete dynode detector, converts the ions into an electrical signal, which is in turn converted into analyte concentration by use of calibration ICP-MS standards (Thomas, 2013).

1.6.2 SEC-MALLS

The molecular weight of polymers is important for their physical properties, and methods for calculating the molecular weight of samples are frequently used (Smidsrød and Moe, 2008). In some samples, such as with alginate, the molecular weight of the polymer chains vary between the molecules in the sample, and the sample is said to be polydisperse. The average molecular weight of these polymers can be calculated in different ways, where the number average molecular weight, M_n , and the weight average molecular weight, M_w , are the most common ones (Smidsrød and Moe, 2008). The definitions of these averages are shown in Equation 1.6.1 and Equation 1.6.2.

$$M_n = \frac{\sum_i N_i M_i}{\sum_i N_i} \quad (1.6.1)$$

where N_i is the number of molecules with molecular weight M_i .

$$M_w = \frac{\sum_i w_i M_i}{\sum_i w_i} = \frac{\sum_i N_i M_i^2}{\sum_i N_i M_i} \quad (1.6.2)$$

where w_i is the weight of molecule number i .

The degree of polymerization, DP is defined as the number of monosaccharides per polymer chain, and can be calculated as shown in Equation 1.6.3 (Smidsrød and Moe, 2008).

$$DP = \frac{M}{M_0} \quad (1.6.3)$$

where M can be either M_n or M_w , and M_0 is the molecular weight of one single monosaccharide in the chain.

Lastly, the polydispersity index, the ratio between M_w and M_n can give information about how polydisperse the sample is. A monodisperse sample would have an index of 1, while for a randomly degraded polymer sample, the polydispersity index is usually close to 2. (Smidsrød and Moe, 2008).

Size exclusion chromatography (SEC) is by far the most convenient and popular method for determining the average molecular weight and the molecular

weight distribution of a sample (Mori and Barth, 1999). SEC optimally separates solely on the basis of hydrodynamic volume or size, and consists of a solid phase of porous particles with a known pore size packed in a column, and a mobile phase (Mori and Barth, 1999). The mobile phase must have known pH and ionic strength, as these parameters affect the elution behaviour of the sample, and should have a composition preventing adsorption of the sample to the packing material or damage to the solid phase (Barth et al., 1996).

The sample is dissolved in a solvent, usually the same solvent used as the mobile phase, and injected into the column (Mori and Barth, 1999). Sample molecules that are too large to enter the pores of the packing material follow a path around the packing material and are eluted from the column first. Smaller molecules enter the pores of the packing material and spend more time getting through the column, giving a separation based on size for the macromolecules (Mori and Barth, 1999).

Multiangle laser light scattering (MALLS) is used together with SEC to give a more accurate estimate of the average molecular weight of the sample (Podzimek, 2003). The method is based upon the ability of light to displace the electron cloud of molecules, creating oscillating dipoles which become sources of radiation that can be detected (Podzimek, 2011). The tendency of displacement of the electron cloud by light interaction varies between different molecules, and is proportional to the specific refractive increment ($\frac{dn}{dc}$) of the molecule (Podzimek, 2011). To compute average molecular weights, $\frac{dn}{dc}$ and the second virial coefficient, A_2 , which depend on the solvent-molecule interactions, must be known (Podzimek, 2003, 2011). The value of $\frac{dn}{dc}$ changes when the molecule is chemically modified, and has been shown to decrease with an increasing number of sulfate groups for the polysaccharide carrageenan (Berth et al., 2008). The $\frac{dn}{dc}$ for unmodified alginates has been determined to be 0.150 ml/g in 0.05 NaSO₄ at pH 6, and 0.154 ml/g in 0.1 M NaCl at pH 7 (Vold et al., 2006; Mackie et al., 1980).

1.7 Characterization of Biological Properties

1.7.1 Flow Cytometry

Flow cytometry is a fast and effective method using light scattering and emission from dyes or fluorochromes to determine physical and chemical properties of single cells in suspension (Shapiro, 2005; Leach et al., 2013). Some of the properties that can be determined by use of flow cytometry are cell size, nuclear complexity, cytoplasmic granularity, DNA content and protein expression (Leach et al., 2013; Gronthos et al., 2001).

In flow cytometry, the sample is inserted in a stream into the center of a second stream of fluid, called a sheath fluid (Shapiro, 2005). The two streams are under pressure, and before the cells pass the laser beam used as the illumination source, the sample stream is focused in the middle of the sheath stream, forcing the sample cells into a single file (Leach et al., 2013). The measurement region where the laser beam hits the passing cells is placed in a flat-sided quartz cuvette to minimize noise from the surroundings (Shapiro, 2005). Argon, krypton and helium-cadmium lasers are used as illumination sources to cover a wide range of wavelengths for larger systems, while smaller systems often use a single argon laser with a wavelength of 488 nm. The laser is focused by lenses before it hits the sample cells (Shapiro, 2005). The light is scattered at small angles forward and at side angles up to 90 ° by the cells according to physiological properties (Leach et al., 2013). A beam stopper stops the illuminating beam after it has traversed the cuvette, and before it can be detected at the forward scatter detector (Shapiro, 2005). A forward scatter collection lens focuses the forward scattered light towards the detector, while fluorescence and side scattered light is focused by collection optics and directed towards detectors for different wavelength by use of dichroic mirrors and optical filters (Shapiro, 2005). At the detector, the photons are converted to electrical signals, and a numerical value is generated for the pulse height, width and area and assigned to a channel number by an analogue-to-digital converter (Leach et al., 2013).

The fluorescence intensity of any captured event is recorded by the flow cytometer for the relevant channel (Leach et al., 2013). After many events have been captured, the mean fluorescence intensity can be derived, giving valuable information about the occurrence of the labelled substance in the

sample (Leach et al., 2013). When using several fluorescence labels or dyes, compensation for fluorescence emission spectral overlap should be carried out in cases when emission from one fluorochrome can cause noise at a detector intended for another fluorochrome (Shapiro, 2005).

1.7.2 ELISA

Enzyme-linked immunosorbent assay (ELISA) is a method for detecting analytes, usually antigens, by use of enzymes as reporters (Engvall and Perlmann, 1971). The capture system, the analyte and the detection system make up the assay (Butler, 2000). There are many different assay configurations, but a principle they all have in common is that the analyte must be the limiting component in the assay. One of the common configurations is a sandwich-ELISA in which a capture antibody is immobilized on a surface, usually in the wells of an ELISA plate, before the analyte is added, binding specifically to the antibody. Detergents or blocking agents in buffers prevents nonspecific binding of proteins to the solid phase (Butler, 2000). Detection antibodies are added to the system and bind to the analyte. Either the detection antibody itself or a secondary antibody is conjugated to an enzyme, catalysing a reaction that usually leads to color development when a suitable substrate solution is added to the plate wells (Butler, 2000; Engvall and Perlmann, 1971). The color development can be detected by use of a plate reader, and compared to a standard to quantify the amount of analyte in each well (Butler, 2000).

As the solid phase is rinsed with a buffer solution between every step, the only enzymes catalysing a reaction are those associated with the presence of the analyte (Engvall and Perlmann, 1971). At least 15 different enzymes have been used as signal detectors, with horseradish peroxidase (HRP), alkaline phosphatase (AP) and β -galactosidase being the most common ones. Each of these can be used with different substrates (Butler, 2000). The signals from the catalysed reaction can also be amplified by use of cascades, making it possible to detect analytes down to just a few molecules (Engvall and Perlmann, 1971).

1.8 The aims of the study

The main objective of this master thesis was to investigate the properties of alginate/alginate-sulfate mixtures with respect to its suitability as a tissue engineering material. This includes determining the effect of different mixing proportions on properties such as gel strength, stability under physiological conditions and interactions with the protein fibroblast growth factor (FGF).

The distribution of alginate-sulfate in gel microbeads made from alginate/alginate-sulfate was also studied under different conditions to investigate how the properties of alginate microcapsules for use in cell transplantation can be tuned using different storage solutions.

To make mixtures of alginate/alginate-sulfate attractive for use in tissue engineering scaffolds, the mixtures should be able to form gels of a tunable mechanical strength and to keep their initial shape in biological solutions over time. Interaction with proteins such as FGF and a controllable release of proteins from hydrogels are also desirable properties of a scaffold material.

2. Materials and Methods

A risk assessment was conducted prior to the master project to identify potential hazards associated with the work in the laboratory. The risk assessment is shown in Appendix A.

2.1 Materials

The water used to dissolve alginate under sulfation and preparation of gel cylinders and beads was Milli-Q (MQ) filtered and deionized water, that has a resistivity of $18.2\text{ M}\Omega\times\text{cm}$ at 25°C . The water was dispensed through a $0.22\text{ }\mu\text{m}$ Millipore filter. The Protanal LF200S alginate that was sulfated, Lot.no S21483 was bought from FMC Biopolymer AS, and has the properties $F_G = 0.68$, $F_{GG} = 0.57$ and $M_w = 250\text{ }000\text{ g/mol}$. Alginate Pronova UP LVG used in the gel beads for the distribution experiments together with the fluorescence labelled sulfated alginate was purchased from NovaMatrix[®], FMC BioPolymer, and have an F_G of at least 0.60.

For use in the fluorescence labelling, 2-(N-morpholino)ethanesulfonic acid (MES), N-(3-Dimethylaminopropyl)-N'-ethylcarbodiimide hydrochloride (EDC), N-Hydroxysulfosuccinimide sodium salt (Sulfo-NHS) and Fluoresceinamine were all purchased from Sigma-Aldrich AS (Oslo, Norway).

Formamide, acetone, CaCl_2 , BaCl_2 , HNO_3 , D-Mannitol, ethylenediaminetetraacetic acid disodium salt dihydrate (EDTA) and NaCl from Merck Millipore was purchased from VWR AS (Oslo, Norway). 99 % chlorosulfonic acid (HClSO_3), 4-(2-hydroxyethyl)-1-piperazineethanesulfonic acid (HEPES), and D-glucono δ -lactone (GDL) was purchased from Sigma-Aldrich AS (Oslo, Norway). The CaCO_3 use for gelling was 'Eskal 50' (average particular size

5 pm) from KSL Staubtechnik GmbH (Lauingen, Germany).

The cells used in the flow cytometry for assessing the ability of alginate to bind FGF was RPMI-8226 (American Type Culture Collection, Rockville, MD, USA). The cells were cultured in RPMI 1604 (Gibco, Paisley, UK) supplemented with L-glutamine (100 $\mu\text{g}/\text{ml}$) and gentamicin (20 $\mu\text{g}/\text{ml}$) with 20 % fetal calf serum (FCS). The cells were cultured at 37 °C in a humidified atmosphere with 5 % CO_2 , and the growth medium was replenished twice weekly. Recombinant Human FGF-basic derived from E.coli and antibodies used for labelling were produced by R&D System[®] (Minneapolis, MN, USA). The antibodies used for primary labelling were anti-FGF basic, FGF basic Affinity Purified Goat IgG and Mouse IgG₁ pure. Anti-goat IgG, phycoerythrin conjugated donkey IgG was used for secondary labelling.

For studies of the release of FGF-basic from alginate gels, recombinant human FGF-basic (146 a.a) was purchased from Peprotech[®] (New Jersey, NJ, USA), along with a Human FGF-basic ELISA Development Kit. The ELISA kit contained antigen-affinity purified rabbit anti-FGF-basic, biotinylated antigen-affinity purified rabbit anti-FGF-basic, recombinant hFGF-basic and Avidin-HRP conjugate.

2.2 Sulfation of Alginate

Alginate LF200S was subjected to sulfation by mixing with chlorosulfonic acid and formamide. The reaction mixture consisted of 2.7 % (w/v) alginate and varying amounts of HClSO_3 in formamide. There were some variations in the volumes of the different reaction mixtures, as shown in Table 2.2.1. The alginate was either in powder powder form, as produced by the manufacturer, or in a freeze-dried form. An overview of the amount of HClSO_3 , the total reaction volume, and the alginate form used for all the mixtures is given in Table 2.2.1.

The reaction mixture was placed in an oven at 60°C and left there under magnetic stirring for 2.5 hours. Acetone at approximately 4°C was added in order to precipitate the alginate. The solution was then subjected to 8 minutes of centrifugation at 4750 rpm at 10°C in a Beckman Coulter Allegra[®] X-15R centrifuge. The pellet of precipitated alginate was resuspended

in MQ-water and the pH was adjusted to 7-8 by the addition of 5 M NaOH dropwise to the solution. The fully dissolved alginate in solution was dialyzed against 35 mM NaCl, 25 mM NaCl and 3× pure MQ water to remove excess formamide and ions. After the dialysis step, the solution was freeze dried.

Table 2.2.1: **The batches of sulfated alginate prepared, with the given % (v/v) of HClSO₃, the form of the alginate used, and the volume of each reaction mixture. Batch numbers were only assigned to the samples where the same amount of HClSO₃ was used fro several sulfation batches. 2.7 % (w/v) alginate was used in every reaction mixture, where formamide and HClSO₃ constituted the liquid volume.**

% (v/v) HClSO₃	Batch Number	Freeze- dried/Powder Alginate LF200S	Rection Volume [ml]
3.5	1	Powder	60
3.5	2	Freeze-dried	120
3.5	3	Freeze-dried	120
3.5	M _w 45 kDa	Freeze-dried	6.8
2.75		Powder	60
2.25		Powder	60
1.75		Powder	60

2.3 Elemental Analysis and the Degree of Sulfation

Elemental analysis to determine the content of sulfur in the different alginate samples was performed by Syverin Lierhagen at the Institute of Chemistry, NTNU, by the use of high-resolution inductively coupled plasma mass spectrometry (HR-ICP-MS). The samples were prepared for analysis by dissolving 5 mg of alginate-sulfate in 0.1 M HNO₃.

The data from the elemental analysis were used to find the average num-

ber of sulfate groups attached to each alginate monosaccharide, the degree of sulfation, DS. A standard curve for calculations of the DS was constructed by calculating the percentage (w/w) of sulfur (% S) for samples of a range of theoretical DS values. For the calculations it was assumed that each monosaccharide in the alginate chain is associated with one water molecule, and additionally that one sodium ion is associated with each carboxyl group and one ion with each sulfate group, giving the expression for the average molecular weight of one monosaccharide shown in Equation 2.3.1.

$$M_w = C_6O_6H_5 + H_2O + (1 + DS) \times Na^+ + DS \times SO_3^- \quad (2.3.1)$$

An example of the calculation of % S from DS can be seen in Appendix B together with the constructed standard curve where % S is plotted as a function of DS. A second degree polynomial was fitted to the curve, and was used to estimate the DS for each sample from the % S obtained from the elemental analysis.

2.4 Acid Hydrolysis of Alginate and SEC-MALLS Analysis

To study the susceptibility of sulfated alginates with different DS values to acid hydrolysis, LF200S, alginate with a DS 0.27 and DS 0.90 were subjected to acid hydrolysis. In addition, two samples of alginate LF200S were submitted to a partial hydrolysis in order to obtain one sample of low molecular weight and one of the same weight average molecular weight, M_w , as the highly sulfated sample used in the gel strength measurements. This allows for an observation of the change in gel strength caused by a decrease in the molecular weight relative to the expected decrease in modulus from increasing degrees of sulfation.

The alginate was dissolved in MQ-water to a concentration of 1 mg/ml. The pH of the samples was adjusted to 5.6 by use of 1 M HCl. For the samples with different DS values the samples were distributed into small glass containers with 2 ml of sample in each container, and incubated at 95°C. One sample container from each alginate sample were removed and rapidly cooled

down to room temperature after 0, 10, 20, 30, 50, 100, 150 and 200 minutes of heating. The the sample for gel strength measurement was distributed in two bottles each containing 250 ml of the alginate solution, and incubated for 30 minutes at 95°C followed by rapid cooling and adjustment of the pH to 7.

In preparation for SEC-MALLS analysis the samples were filtered through a 0.8 μm filter and diluted with a $\text{NaNO}_3/\text{EDTA}$ solution at pH 6, giving an alginate concentration of 0.80 $\mu\text{g}/\text{ml}$. Samples from all the batches of highly sulfated alginate were also prepared for SEC-MALLS analysis. The SEC-MALLS analysis of the samples was carried out by Ann-Sissel Teialeret Ulset at the Institute of Biotechnology, NTNU. The dn/dc value was set to 0.150 ml/g for all samples, as used by Vold *et al.* (Vold *et al.*, 2006). A_2 was set to 5.0000e-0.003 $\text{ml}\times\text{mol}\times\text{g}^{-2}$.

The weight average molecular weight, M_w of each of the samples were calculated by use of the Astra 6.1.1.17 software from WTC. Two measurements were done for each sample, and the average of these two was calculated.

2.5 Preparation of Alginate Gel Beads for Swelling Experiments

Alginate gel beads were made from either sulfated alginate with varying DS, or from mixtures consisting both of alginate-sulfate (DS 0.90 or DS 0.68) and of unmodified alginate LF200S in varying proportions. A list of the gel beads produced is given in Table 2.5.1.

Table 2.5.1: Overview of the alginate gel beads prepared for the swelling experiments.

Pure Samples		
	CaCl ₂	BaCl ₂
LF200S	x	x
DS 0.27	x	
DS 0.59	x	
DS 0.79	x	
Mixtures of LF200S and sulfated alginate		
	CaCl ₂	BaCl ₂
DS 0.68	x	
DS 0.90	x	x

A 1.8 % (w/v) alginate solution was prepared by dissolving 90 mg alginate in 5 ml MQ- water. A solution for making 20 % DS 0.90 beads would then consist of 72 mg pure LF200S and 18 mg sulfated alginate with DS 0.90 mixed together with the 5 ml of MQ water. A 3 ml plastic pasteur pipette was used to drip the solution into a 150 ml bath consisting of 50 mM CaCl₂ or 50 mM BaCl₂ to give spherical gel beads. The gel beads were left in the gelation bath over night.

2.6 Measuring the Swelling of Alginate Gel Beads

The alginate gel beads were isolated from the CaCl₂ or BaCl₂ solution and transferred to 50 ml centrifuge tubes. The beads were rinsed with 3 × 10 ml of a 0.9 % (w/v) NaCl solution. After the removal of the last 10 ml of NaCl solution, 50 spherical beads were placed side by side along a ruler, as shown in Figure 2.6.1.

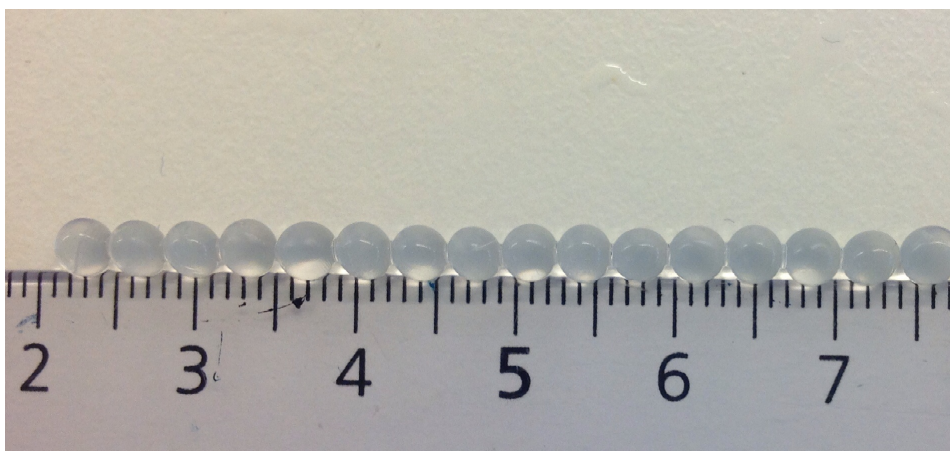


Figure 2.6.1: *Measurement of alginate bead diameter of LF200S beads before the first treatment with 0.9 % (w/v) NaCl.*

The total length of the beads along the ruler was used to calculate the average diameter and volume of the beads. The beads were then transferred back to the tube using a spatula, and subjected to a 1 hour treatment with 18 ml of the 0.9 % NaCl solution to an assumed equilibrium. After the treatment, the NaCl solution was removed, the beads were counted and the total length of the beads measured to find the average diameter and volume increase. After the diameter measurements the beads were transferred back to the tube and 18 ml of new NaCl solution was added for a new 1 hour treatment. This procedure was repeated until the beads burst from osmotic swelling. Some of the later treatments within a series of swelling measurements lasted for several hours and comparisons at this point can therefore only be made between beads measured within the same experiment.

2.7 Content of Ca^{2+} in swelling gel beads

The content of Ca^{2+} in the beads before and during swelling was measured to find out whether there is any difference between the beads in their ability to bind and retain Ca^{2+} in a 0.9 % (w/v) NaCl-solution.

1.8 % (w/v) alginate gel beads where 0, 20 and 40 % of the alginate was alginate-sulfate were made as described in the section 2.5, using 50 mM CaCl_2 in the gelation bath.

120 beads from each sample were isolated from the gelation bath and rinsed with 3×10 ml 0.9 % NaCl. 20 of the beads were placed on a tissue for a few seconds to remove excess water, and transferred to a test tube for later analysis. The remaining 100 beads from each sample were subjected to treatments with 20 ml 0.9 % (w/v) NaCl lasting for 30 minutes. The beads were counted between every treatment. 20 new beads from each sample were placed on a tissue and transferred to test tubes after 6 and 13 treatments.

The beads were dissolved in 9 mM EDTA and 0.1 M HNO₃ before an elemental analysis was performed. Elemental analysis to determine the content of calcium in the different alginate samples was performed by Syverin Lierhagen at the Institute of Chemistry, NTNU, by the use of high-resolution inductively coupled plasma mass spectrometry (HR-ICP-MS). The sulfate content of the beads was determined in the same analysis.

2.8 Preparation of Alginate Gel Cylinders

Alginate gel cylinders were prepared from a 2 % (w/v) alginate solution. The alginate used was a mixture of highly sulfated alginate (DS = 0.77) and unmodified alginate LF200S. As the sulfation process causes some depolymerization of the alginate, three batches of alginate gel cylinders consisting of mixtures of partially hydrolysed alginate and untreated alginate LF200S were also prepared to study the effect of lower molecular weights on the mechanical strength of the gel cylinders.

To prepare 18.75 ml of the 2 % alginate solution the alginate was dissolved in MQ-water before CaCO₃ in MQ-water was added to give a concentration of 15 mM CaCO₃ in the final solution. Degassing by use of a vacuum pump was done in order to reduce the formation of air bubbles in the gels. MQ-water was mixed with D-glucono δ -lactone (GDL) and immediately added to the alginate-CaCO₃ solution to 30 mM GDL under stirring. After 10 seconds of stirring, the solution was transferred to six cylindrical plastic moulds with an inner diameter of 14 mm and a height of 15 mm. About 2.5 ml solution was added to each mould, giving a convex meniscus in the moulds. The moulds were sealed at both ends by use of dialysis membranes and rubber bands, as shown in Figure 2.8.1.



Figure 2.8.1: A graphical overview of the process of making an alginate gel cylinder using cylindrical moulds capped at both ends with a dialysis membrane. The mould is sealed at one end before the alginate solution is added. The other end is sealed before the mould is placed in a gelation bath containing 50 mM BaCl_2 .

The filled moulds were transferred to a bath of 50 mM BaCl_2 and left there for 24 hours before the gel cylinders were subjected to a longitudinal compression test. The moulds were placed in the bath in the way shown in the lower right corner of Figure 2.8.1 to give an optimal diffusion of calcium into the gel. BaCl_2 was used in the gelation bath instead of CaCl_2 as the samples with the highest content of sulfated alginate were unable to form gels with the use of CaCl_2 .

2.9 Gel Strength Measurements

The alginate gel cylinders were subjected to a longitudinal deformation test by the use of a TA.XTPlus Texture Analyzer with a 5 kg load cell and a 35 mm diameter cylinder aluminium probe. The cylinders were compressed to a 12 mm distance at a compression rate of 0.10 mm/sec. A deformation-force relationship was obtained by the use of the Texture Exponent software. Six specimens were compressed for each sample. In an early linear area of the deformation [mm] -force [N] curve a linear regression was performed. The slope of the fitted line was used in the calculations of the Young's modulus, E . The average Young's modulus, the standard deviation and the coefficient of variation were calculated for each sample. An example calculation of the Young's modulus for a gel from one of the samples is shown in Appendix G.

From earlier work in my specialization project at the Department of Biotechnology, NTNU, the Young's moduli of samples containing only alginate-sulfate with different degrees of sulfation have been calculated. These results were used to compare the effect of using mixtures instead of homogeneous samples on the gel strength. The Young's modulus data from this project are given in Appendix C. The content of sulfate groups in the mixed gels was converted to an approximate value for degree of sulfation of the whole gel, in order to be able to compare the results with earlier results of gels made from sulfated alginate of various degrees of sulfation. Equation 2.9.1 was used to convert the total sulfate content of the mixed gels to an approximate DS, DS_{app} .

$$DS_{app} = 0.77 \times \frac{\% \text{ alginate} - \text{sulfate}}{100} \quad (2.9.1)$$

2.10 Fluorescence labelling of Alginate-Sulfate

Highly Sulfated Alginate with a DS of 0.83 and a molecular weight of about 45 kDa was labelled with fluorescence. This allows for a study of the distribution of alginate-sulfate in gel beads consisting of mixtures of alginate and alginate-sulfate.

0.5 g of alginate-sulfate was dissolved in 15 ml of MQ- water. A buffer consisting of 0.2 M 2-(N-morpholino)ethanesulfonic acid (MES) and 0.6 M

NaCl was prepared by dissolving 1.171 g MES and 1.052 NaCl in 30 ml of MQ-water before the pH was adjusted to 5.5. 11 ml of the buffer was added to the alginate solution. N-(3-Dimethylaminopropyl)-N'-ethylcarbodiimide hydrochloride (EDC) and N-Hydroxysulfosuccinimide sodium salt (Sulfo-NHS) was dissolved in 1 ml buffer each and added to the solution to give 9 mM of both. The mixture was left under stirring in room temperature for 45 minutes before the fluoresceinamine was added. Fluoresceinamine was dissolved in 1 ml buffer before addition to the solution, and had a final concentration of 4.5 mM. To get all the fluoresceinamine into the solution, 1 ml of buffer was used to rinse the beaker, giving the reaction mixture a total volume of 30 ml. The mixture was left under stirring in room temperature for 18 hours.

The solution was filtered through a 0.80 μm filter before it was submitted to dialysis to remove excess fluoresceinamine from the solution. After leaving the dialysis tube in one initial bucket of pure MQ-water overnight, the solution was dialysed against 0.1 M NaCl and MQ-water. The pH of the solution was adjusted to 7.4 and submitted to freeze drying.

2.11 Preparation and Distribution Studies of Alginate/Alginate-Sulfate Gel Beads

1.8 % (w/v) alginate gel beads were prepared for studies of the distribution of alginate-sulfate in alginate/alginate-sulfate beads in different solutions. The beads were made by dissolving UP LVG alginate and fluorescence labelled alginate-sulfate of DS 0.83 and a molecular weight of about 45 kDa in 0.3 M D-Mannitol. The alginate-sulfate made up 10 % (w/w) of the alginate in the solution. The solution was stirred until all the alginate was fully dissolved, and filtered through a 0.80 μm filter before it was transferred to a 20 ml syringe.

The syringe was fastened to a GrasebyTM3500 anaesthesia pump set to a flow rate of 10 ml/h. The syringe was coupled to a plastic tube leading to a needle placed inside a electrostatic bead generator. The voltage in the bead generator was set to 7 kV. A bath containing 50 mM CaCl_2 in 0.15 M D-Mannitol under magnetic stirring was placed beneath the needle, causing the falling droplets to form spherical beads as they hit the gelation bath. The

beads were left in the gelling solution for 5 minutes before they were distributed into three different solutions, as shown in Table 2.11.1. The beads were studied using laser scanning confocal microscopy (LSCM) 15 minutes after they were transferred to their solutions, and again after one and two weeks.

Table 2.11.1: **The solutions used for storage of alginate gel beads containing alginate-sulfate labelled with fluorescence.**

Solution 1: NaCl	The beads were rinsed with 3×10 ml of 0.9 % (w/v) NaCl and stored in 0.9 % (w/v) NaCl with 1 mM CaCl_2
Solution 2: CaCl_2	50 mM CaCl_2 in 0.15 M D-Mannitol
Solution 3: HEPES	20 mM HEPES solution with 154 mM NaCl, 2 mM CaCl_2 , 0.1 % BSA and 0.02% NaN_3 , pH 7.4

The alginate gel beads were studied by use of LSCM the same day they were made, and after one and two weeks after production, to study the distribution of the sulfated alginate in the beads over time. A Zeiss LSM 510 Confocal Microscope was used with an argon laser at 488 nm, and a $10\times$ Plan Apochromat/0.45 W objective to study the samples. Pictures of the beads were acquired and processed by use of the software LSM 510 Image Browser, version 4.2. All samples were studied by scanning through an equatorial slice of the sample. An intensity curve was drawn for one bead from each sample from the intensities measured throughout the center of the bead.

2.12 Interactions Between Alginate-Sulfate in Solution and FGF

The binding of mixtures of alginate and alginate-sulfate to the heparin binding protein fibroblast growth factor (FGF) was investigated by the use of flow

cytometry. The FGF used in the experiment was recombinant human FGF-basic (rhFGF-basic) isolated from *Escherichia coli*. The alginate/alginate-sulfate mixtures contained from 20 % alginate-sulfate with DS 0.90, via 40 %, 60 % and 80 % to 100 % alginate-sulfate.

Stock solutions of alginate/alginate-sulfate were prepared by dissolving 10 mg of mixed alginate and alginate-sulfate in different proportions in 1 ml of sterile water. These were further diluted in phosphate buffered saline (PBS) containing 0.1 % bovine serum albumin (BSA) to 10 $\mu\text{g}/\text{ml}$. In addition to the alginate/alginate-sulfate mixtures used in the experiment, there were also two samples of pure sulfated alginate with DS 0.27 and DS 0.59. A sample of 10 $\mu\text{g}/\text{ml}$ unsulfated alginate LF200S, an untreated sample and a sample using a different antibody were used as three different controls.

About 3.9 million myeloma RPMI cells were centrifuged and washed in PBS/0.1 % BSA, followed by stimulation with 200 μl , 4 $\mu\text{g}/\text{ml}$ FGF in PBS/0.1 % BSA for 10 minutes. After the incubation time, 800 μl of PBS/0.1 % BSA was added to the tube and the cells were centrifuged and resuspended in PBS/0.1 % BSA.

200 μl of the alginate solutions were transferred to individual flow tubes. To the tubes for the controls with untreated sample and the Mouse IgG pure sample, 200 μl PBS/0.1 % BSA was added instead, giving a total of 17 tubes. Approximately 200 000 cells were added to each tube, and incubated for 10 minutes.

FGF antibody FGF basic Affinity Purified Goat IgG was added to 16 of the sample tubes, while Mouse IgG pure was added to the last tube as an isotype control, and the samples were left on ice for 25 minutes. For secondary labelling, phycoerythrin conjugated donkey IgG was added to all the tubes and left on ice for 25 minutes. The samples were washed with PBS/0.1 % BSA and centrifuged before and after each labelling step. After the last centrifugation step, the samples were resuspended in PBS, and the flow cytometer analysis was run to detect the labelled FGF still attached to the cells. The median fluorescence intensity of cells from each sample was recorded.

2.13 Release of FGF-basic from Alginate/Alginate-Sulfate Gels

The release of FGF from gels made of mixtures between alginate and alginate-sulfate was studied using ELISA. A buffer containing 20 mM HEPES, 154 mM NaCl, 2 mM CaCl₂, 0.1 % (w/v) BSA and 0.02 % (w/v) NaN₃ was prepared for use in the experiment.

Alginate gels containing 1.5 % (w/v) alginate were made using LF200S alginate and alginate-sulfate with a DS of 0.77 in different proportions to each other. The gels also contained 18 mM CaCO₃ and 36 mM GDL for an internal gelation process. Gel solutions where 0, 20, 40, and 60 % of the total alginate content was alginate-sulfate were prepared. Gel solutions for each of the four mixtures were made by dissolving mixed alginate/alginate-sulfate in sterile water before CaCO₃ dissolved in sterile water was added. The solution was degassed by use of a vacuum pump, before FGF-basic was mixed gently into the solution to a concentration of 2 μg/ml. GDL was dissolved in sterile water and immediately added to the alginate solution. After 10 seconds of stirring, 1 ml of alginate solution was added to each of three center wells in a 4 × 6 well plate, giving a total of 12 filled wells, on two different plates, as shown in Figure 2.13.1. Only the center wells were used in order to minimize the loss of liquid from the wells by evaporation.

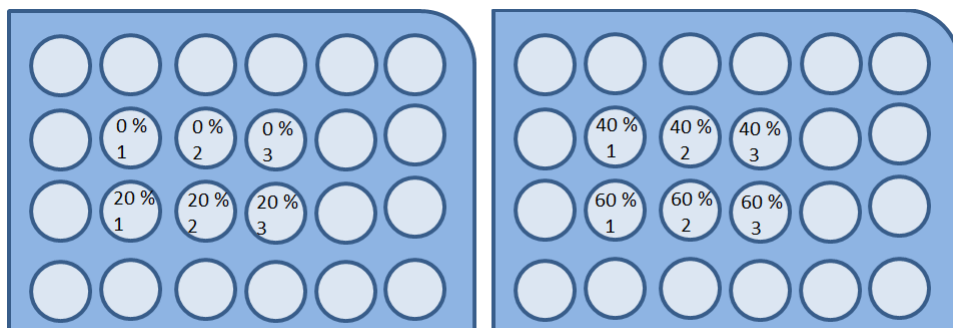


Figure 2.13.1: *The distribution of the gel disks in two 6 × 4 well plates. The percentages represents how many % (w/w) of the total alginate content is alginate-sulfate. Each of the four mixtures was distributed between three different wells.*

The plates were left for 24 hours to allow the gel solution to form gel disks in the wells. After 24 hours the plates were placed in a heating cabinet holding 37 °C and 1 ml of the HEPES solution was added to each well containing a gel disk. After 30 minutes, 500 μ l of the HEPES solution was removed from each well and transferred to separate wells on another plate for later analysis. 500 μ l of new HEPES solution was added to each well containing gel disks. The two test plates were wrapped up in parafilm to avoid evaporation, and a beaker containing water was placed in the heating cabinet to ensure a humid environment. The procedure for taking out samples and replenish the wells with new HEPES medium was repeated daily for 12 days.

A human FGF-basic ELISA development kit with a sandwich ELISA format, as well as human recombinant bFGF was bought from PeptoTech (Rocky Hill, NJ, United States). The kit contained antigen-affinity purified rabbit anti-FGF-basic, biotinylated antigen-affinity purified rabbit anti-FGF-basic, avidin-HRP conjugate and human FGF-basic standard. The gel disks were removed from the HEPES solution after 12 days. The height and diameter of each gel disk were measured before each disk was dissolved in 10.5 ml of a solution of 7 mM EDTA in sterile water. The solutions containing the dissolved gel disks were diluted in series of 1/10, 1/100 and 1/1000 of the original concentrations. The FGF standard was diluted giving a standard range of 0 to 4000 pg/ml.

The ELISA analysis was carried out for the solution removed from the wells during the first 12 days, the standard and the dilution series of dissolved gel disks as described in the protocol from the manufacturer, with the exception that samples from the 12 days were tested in duplicate and not triplicate due to the large number of samples. The absorbances were read using a plate reader set at 405 nm with 650 nm as the reference wavelength. The absorbance obtained at 650 nm was subtracted from the one read at 405 nm for the same well, giving a net absorbance for each well read.

The absorbance results obtained from the plate readings were used to calculate the remaining concentration of FGF in the 12 gel disks after 12 days. The results from the samples taken out from the wells daily were all outside of the range of the standard. As the standard curve was a second degree polynomial, and not linear, an extrapolation would not give a good estimate for the concentration in these samples. An attempt to widen the range of the

standard to include these samples was not successful. The results from the plate readings of the solutions containing dissolved gel disks were converted into FGF concentrations using the calculated standard curve.

3. Results

3.1 Sulfation of Alginate

Alginate LF200S was sulfated in several batches using formamide and chlorosulfonic acid. The resulting alginate-sulfate was subjected to elemental analysis by HR-ICP-MS to measure the content of sulfur in each sample. The sulfur content from the elemental analysis, given in $\mu\text{g S/g}$ sample, was converted to % S in the sample before Equation B.7 in Appendix B was used to calculate the degree of sulfation (DS) of the sample.

The results from the elemental analysis for all three of the sulfated LF200S alginate samples, together with the conversion to percentage sulfur in each sample and the calculated DS are all given in Table 3.1.1.

Table 3.1.1: **The content of sulfur in all the sulfated LF200S alginate samples, along with the calculated degree of sulfation (DS). The percentage (v/v) of chlorosulfonic acid used in the reaction mixture is given in the names of the samples. Freeze dried alginate, rather than alginate in powder form, was used in batch 2 and 3 with 3.5 % HClSO_3 .**

Sample	$\mu\text{g S/g}$ sample	% S in the sample	DS
1.75 % HClSO_3	33 239	3.32	0.27
2.25 % HClSO_3	66 461	6.65	0.59
2.75 % HClSO_3	84 824	8.48	0.79
3.5 % HClSO_3 batch 1	93 590	9.36	0.90

Continued on next page

Table 3.1.1 – continued from previous page

Sample	$\mu\text{g S/g}$ sample	% S in the sample	DS
3.5 % HClSO_3 batch 2	82 886	8.29	0.77
3.5 % HClSO_3 batch 3	85 632	8.56	0.80
3.5 % HClSO_3 M_w 45 kDa	88 356	8.84	0.83

As shown in Table 3.1.1 increasing the content of chlorosulfonic acid in the sulfation mixture lead to an increase in the resulting degree of sulfation for mixtures of the same reaction volume. The freeze-dried alginate used in batch 2 and 3 turned out to dissolve slower in the sulfation mixture than the alginate powder used in batch 1, and had, as can be seen in Table 3.1.1 a lower degree of sulfation than the alginate in batch 1. The alginate from batch 2 even had a lower DS than the alginate from the 2.75 % HClSO_3 sample. The 3.5 % HClSO_3 sample of molecular weight 45 kDa had a DS somewhat higher than batch 2 and 3 of samples containing 3.5 % HClSO_3 .

3.2 Molecular Weight

3.2.1 Acid Hydrolysis

Sulfated alginates with DS 0.27 and 0.90, as well as unmodified alginate LF200S were subjected to acid hydrolysis at 95°C with pH 5.6 over time to assess the susceptibility of sulfated alginate to hydrolysis. The resulting alginate samples were analysed by use of SEC-MALLS to find the molecular weight averages, with the results given in Table 3.2.1.

Table 3.2.1: The molecular weight averages of sulfated and nonsulfated alginate samples after acid hydrolysis. The hydrolysis was carried out with alginate concentrations of 1mg/ml at 95°C with a pH of 5.6 for 0 to 200 minutes.

Time [min]	Mw [kDa]		
	LF200S	DS 0.27	DS 0.90
0	284	159	161
10	229	152	139
20	204	135	131
30	196	127	109
50	157	95	92
100	114	68	67
150	93	53	50
200	81	44	44

In order to calculate the pseudo first order rate constant for the degradation of the three samples using Equation 1.1.2, $\frac{1}{M_w}$ was calculated and plotted against the time of acid hydrolysis. The plot for each sample was fitted to a linear regression line, giving the results shown in Figure 3.2.1.

The calculated values for $\frac{1}{M_w}$ for all three samples are given in Table D.1, D.2 and D.3 in Appendix D. The molecular weight for an average monosaccharide in each sample was calculated as shown in Equation D.1 and Equation D.2 in Appendix D. The average molecular weight of a monosaccharide in a chain of alginate LF200S is 198 Da, while the average weights in the samples DS 0.27 and 0.90 are 226 Da and 291 Da, respectively.

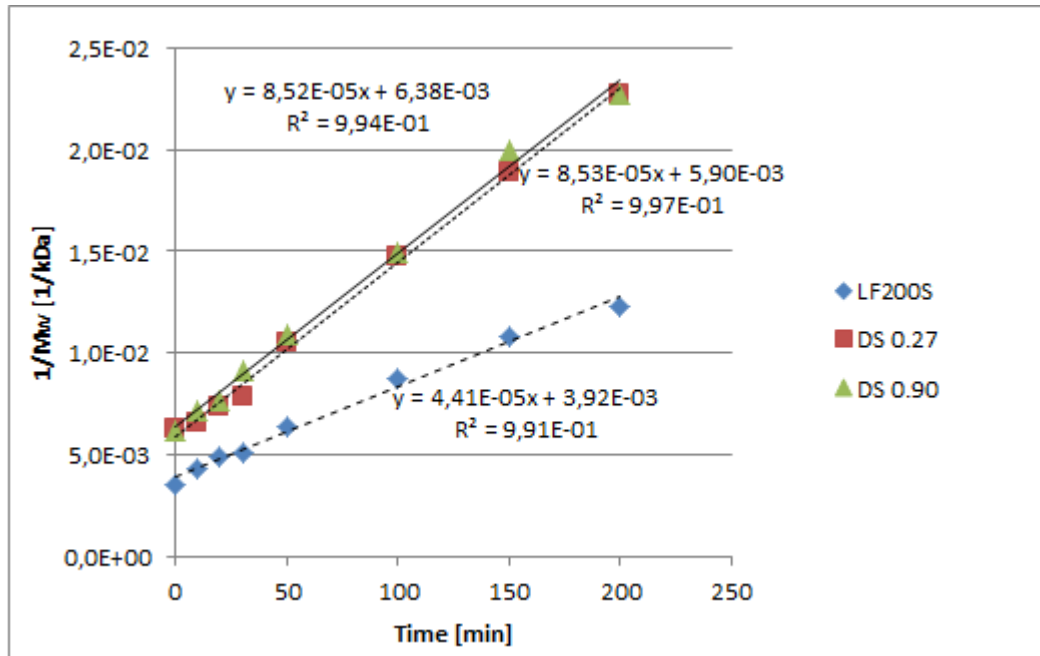


Figure 3.2.1: The inverse of the weight average molecular weight as a function of the time of acid hydrolysis for two sulfated samples with DS 0.27 and 0.90 and for unsulfated alginate LF200S. Each plot is fitted with a linear regression line, and the formulas for the regression lines are shown in the figure.

Using the slopes obtained from Figure 3.2.1 together with the values for M_0 given above, it can be seen from Equation 1.1.2 that the pseudo first order rate constant, k is given by Equation 3.2.1.

$$k = 2M_0 \times \text{the slope} \quad (3.2.1)$$

The slope and the calculated rate constant, k , for each alginate sample is given in Table 3.2.2.

Table 3.2.2: The slopes from the plots given in Figure 3.2.1 where the inverse of the weight average molecular weight was plotted as a function as a function of the time of acid hydrolysis for two sulfated samples and one unmodified sample of alginate LF200S. The table also gives the values of the pseudo first order rate constant, k , for the random depolymerization of each of the samples.

Sample	Slope [$\text{kDa}^{-1}\text{min}^{-1}$]	k [min^{-1}]
LF200S	4.41E-05	0.017
DS 0.27	8.53E-05	0.039
DS 0.90	8.52E-05	0.050

Figure 3.2.1 shows that the depolymerization data from all samples fall in a straight line, confirming a random depolymerization. The sulfated samples show steeper slopes than the unmodified alginate sample, with little difference between the two sulfated samples. From Table 3.2.2 it can be seen that the higher proportion of sulfate groups per monosaccharide in the DS 0.90 sample, gives a higher rate constant for the depolymerization for this sample than for the DS 0.27 sample.

3.2.2 Sulfated Samples

The weight average molecular weight of the sulfated samples DS 0.77, DS 0.82 and DS 0.90 were determined since the sulfation process involves high temperature and acidic conditions that can cause some reduction in molecular weight. As a control for the influence of molecular weight in alginate gel strength, alginate LF200S was subjected to acid hydrolysis for 30 minutes, to obtain a molecular weight similar to that of the sample with DS 0.77 used in the gel compression experiments. A sample was also subjected to acid hydrolysis for 150 minutes, to obtain a low molecular sample for use in the experiment on distribution of sulfated alginate in microbeads. The results from the analysis of all samples are shown in Table 3.2.3.

Table 3.2.3:]

The weight average molecular weight of unmodified alginate LF200S, for sulfated samples and for alginate samples subjected to acid hydrolysis for 30 and 150 minutes at 95°C and pH 5.6.

Sample	M_w [kDa]
LF200S	284
LF200S, 30 min	154
LF200S, 150 min	45
DS 0.90	161
DS 0.77	160
DS 0.82	175

The results in Table 3.2.3 show that the sample that was partially degraded by acid hydrolysis for 30 minutes has a weight average molecular weight just slightly below the molecular weight of the sample with a DS of 0.77 used in the gel compression experiments. The sample DS 0.82 has a somewhat higher molecular weight than the other samples produced by sulfation with 3.5 % $HClSO_3$. All the sulfated samples have molecular weights far below the molecular weight of the unmodified alginate LF200S sample.

3.3 Swelling of Alginate Gel Beads

To study the stability of alginate gel beads in solution containing physiological NaCl levels, calcium-alginate beads were prepared and kept in 18 ml 0.9 % (w/v) NaCl with a change of solution every hour. The number of beads and the average diameter for the beads of each sample were measured between every treatment.

3.3.1 Beads from Sulfated Alginate

Alginate gel beads were made by use of external gelation with 50 mM CaCl_2 for sulfated alginate samples of DS 0.27, DS 0.59, DS 0.79 and unmodified alginate LF200S.

The beads made from the sample containing alginate with a DS of 0.79 did not form proper beads in the CaCl_2 solution. The number of beads, the average diameter and the average increase in volume for each of the other samples are shown in Table E.1.1, Table E.1.2 and Table E.1.3 in Appendix E.1, while graphical presentations of the number and the relative volumetric increase of the beads are given in Figure 3.3.1 and Figure 3.3.2.

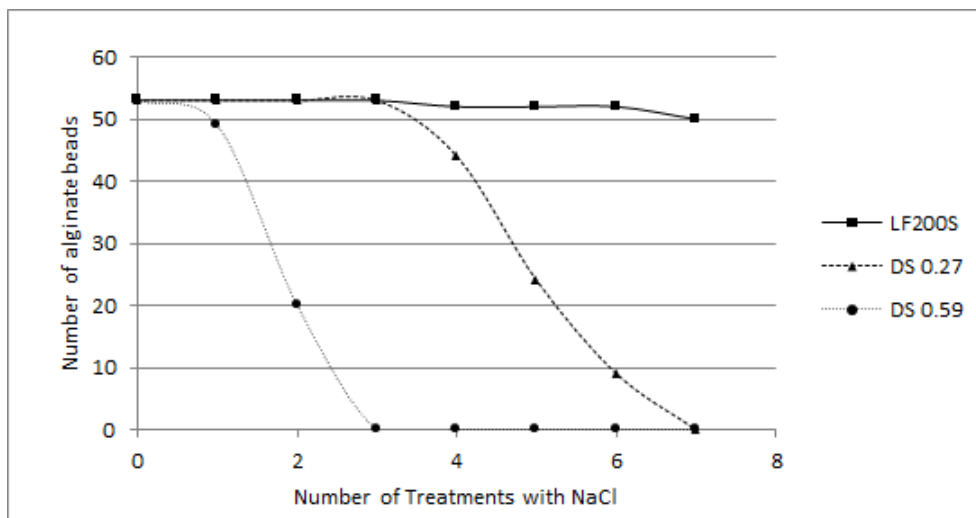


Figure 3.3.1: The number of whole alginate beads present in samples made from alginate with different DS as a function of the number of treatments with 0.9 % NaCl.

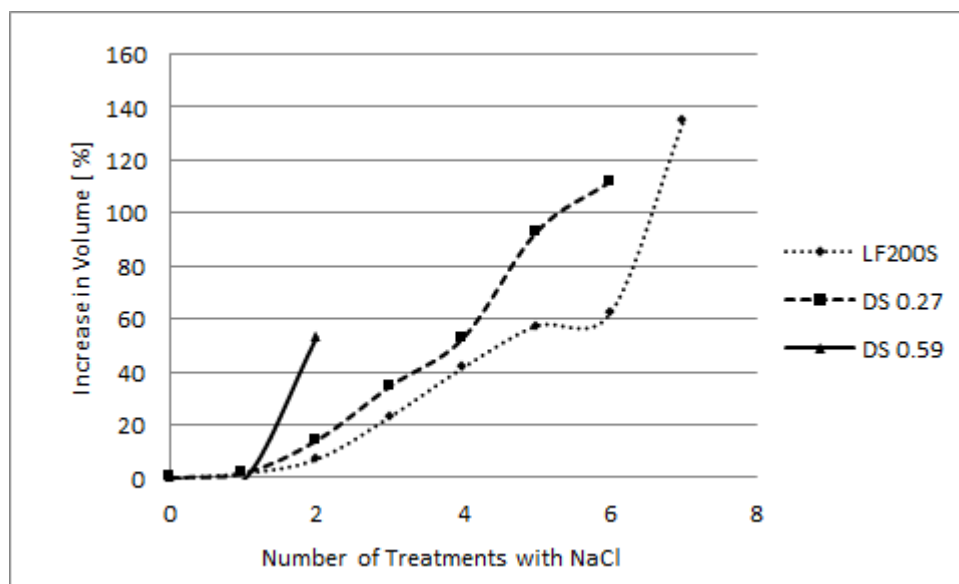


Figure 3.3.2: *The average increase in volume of alginate beads made from alginate with different DS as a function of the number of treatments with 0.9 % NaCl.*

As can be seen from Figure 3.3.1, the beads made from pure sulfated alginate are very unstable, and even the beads made from the not too highly sulfated sample with a DS of 0.27, experience a rapid drop in the number of beads, with all beads gone after seven treatments with 0.9 % NaCl.

3.3.2 Beads from Alginate/Alginate-Sulfate Mixtures Gelled with CaCl_2

Alginate beads were prepared by use of external gelation with 50 mM CaCl_2 for mixtures of alginate-sulfate with a DS of 0.68 or 0.90 with unmodified alginate Protanal LF200S. The percentages given for each sample represent the percentage of alginate-sulfate in the sample relative to the total alginate content of the beads.

Alginate/Alginate-Sulfate Mixtures using a DS 0.90 Alginate-Sulfate

The number of beads from each sample of mixtures between alginate of DS 0.90 and LF200S, counted between every measurement is shown in Table E.2.1 in Appendix E.2. The 100 % beads containing only alginate-sulfate of DS 0.90 were unable to form beads and were excluded from the experiment. The measured average diameter of the other beads and the average increase in volume are given in Table E.2.2 and Table E.2.3 in Appendix E.2. Graphical representations of the number of beads and the relative increase in volume as a function of the number of treatments with 0.9 % NaCl is given in Figure 3.3.3 and Figure 3.3.4.

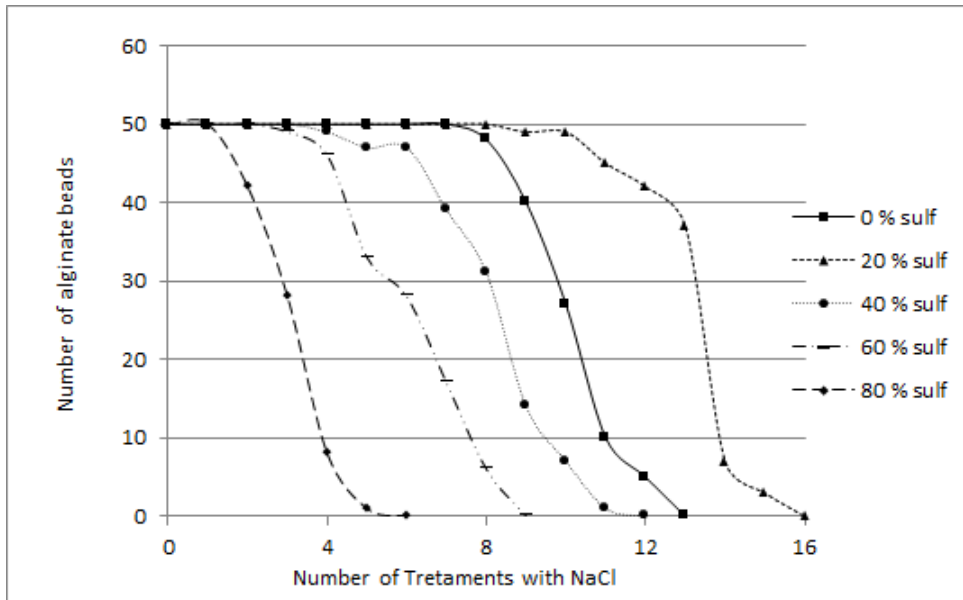


Figure 3.3.3: The number of whole alginate beads present in samples made from alginate mixtures with various proportions of alginate-sulfate with DS 0.90 and alginate LF200S as a function of the number of treatments with 0.9 % NaCl.

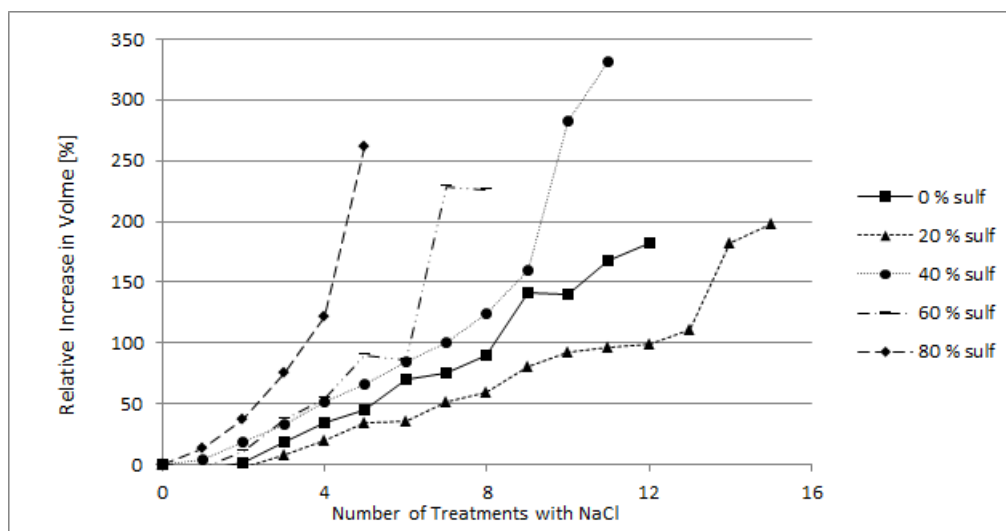


Figure 3.3.4: The average increase in volume of alginate beads made from alginate mixtures with various proportions of alginate-sulfate with DS 0.90 and alginate LF200S as a function of the number of treatments with 0.9 % NaCl.

Figure 3.3.3 and Figure 3.3.4 show that the stability of alginate gel beads from DS 0.90/LF200S mixtures decreases as the proportion of alginate-sulfate increases. The samples containing much DS 0.90 alginate relative to total alginate content experience a rapid drop in bead number, and a faster increase in the volume compared to samples containing small proportions of DS 0.90 alginate. The exception to this trend is the sample containing 20 % alginate-sulfate, which shows a greater stability both in the bead count and in the relative volume increase compared to the 0 % beads containing only LF200S.

Alginate/Alginate-Sulfate Mixtures using a DS 0.68 Alginate-Sulfate

The number of beads from each sample of mixtures between alginate of DS 0.68 and LF200S, counted between every measurement is shown in Table E.2.4 in Appendix E.2. The measured average diameter of the beads and the average increase in volume of the beads are given in Table E.2.5 and Table E.2.6. Graphical representations of the number of beads and the relative increase in volume as a function of the number of treatments with 0.9 % NaCl is given in Figure 3.3.5 and Figure 3.3.6.

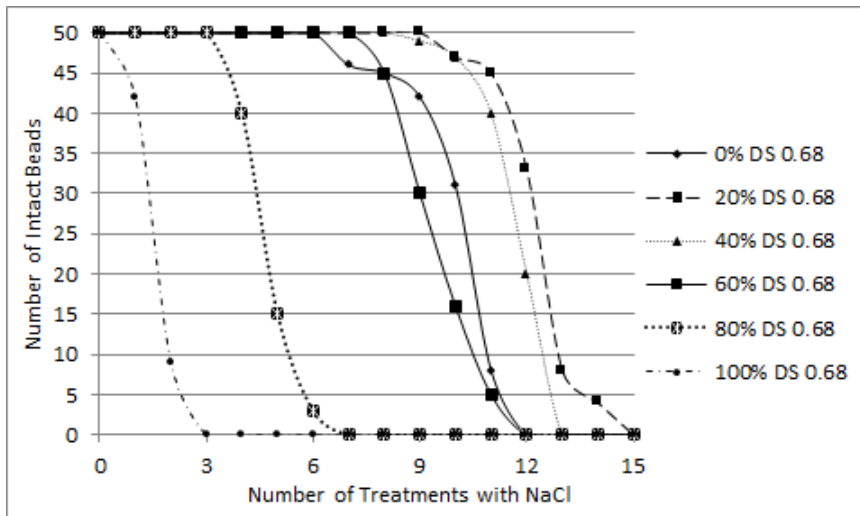


Figure 3.3.5: The number of whole alginate beads present in samples made from alginate mixtures with various proportions of alginate-sulfate with DS 0.68 and alginate LF200S as a function of the number of treatments with 0.9 % NaCl.

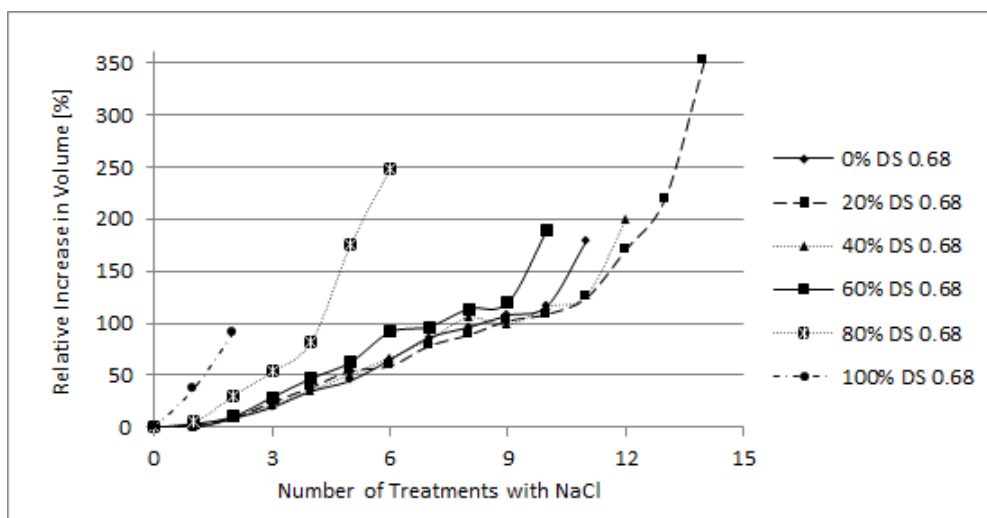


Figure 3.3.6: *The average increase in volume of alginate beads made from alginate mixtures with various proportions of alginate-sulfate with DS 0.68 and alginate LF200S as a function of the number of treatments with 0.9 % NaCl.*

Figure 3.3.5 and Figure 3.3.6 show similar results for the DS 0.68/LF200S beads as for the DS 0.90/LF200S beads, but with a less marked difference between the 0 % and the 20 % sample, as well as for the 40 % and 60 % sample. The 100 % beads of DS 0.68 did form beads in 50 mM CaCl₂, although they were fairly unstable.

The total sulfate concentration of each alginate/alginate-sulfate mixture is translated into an approximate DS value, and given in Table 3.3.1 along with the number of treatments with 0.9 % NaCl required before all beads were gone from each sample of pure alginate-sulfate and of alginate/alginate-sulfate mixtures.

Table 3.3.1: The number of treatments with 0.9 % NaCl before all beads were gone from each sample of pure alginate-sulfate and of alginate/alginate-sulfate mixtures. The total sulfate concentration of beads from alginate/alginate-sulfate mixtures are translated into an approximate (DS_{app}) for each sample.

Sample	DS_{app}	Number of Treatments
DS 0.27	0.27	7
DS 0.59	0.59	3
DS 0.79	0.79	0
0 % DS 0.90	0.00	13
20 % DS 0.90	0.18	16
40 % DS 0.90	0.36	11
60 % DS 0.90	0.54	9
80 % DS 0.90	0.72	6
100 % DS 0.90	0.90	0
0 % DS 0.68	0.00	12
20 % DS 0.68	0.14	15
40 % DS 0.68	0.27	13
60 % DS 0.68	0.41	12
80 % DS 0.68	0.54	7
100 % DS 0.68	0.68	3

3.3.3 Beads from Alginate/Alginate-Sulfate Mixtures Gelled with $BaCl_2$

To investigate whether gelation with $BaCl_2$ would give the same results with respect to the 0 % sample and the 20 % sample for the DS 0.90/LF200S beads as gelation with $CaCl_2$, the experiment was repeated using 50 mM $BaCl_2$ in the gelation bath.

The number of beads from each sample of mixtures between alginate of DS 0.90 and LF200S, counted between every measurement is shown in Table E.3.1 in Appendix E.2. The measured average diameter of the beads and the average increase in volume of the beads are given in Table E.3.2 and Ta-

ble E.3.3. Graphical representations of the number of beads and the relative increase in volume is given in Figure 3.3.7 and Figure 3.3.8.

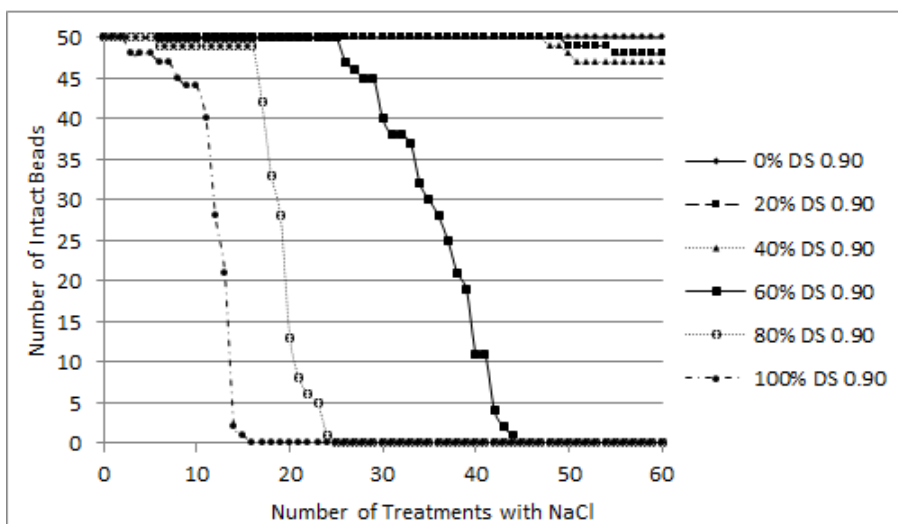


Figure 3.3.7: The number of whole alginate beads present in samples made from alginate mixtures with various proportions of alginate-sulfate with DS 0.90 and alginate LF200S as a function of the number of treatments with 0.9 % NaCl. The beads were made by external gelation with $BaCl_2$.

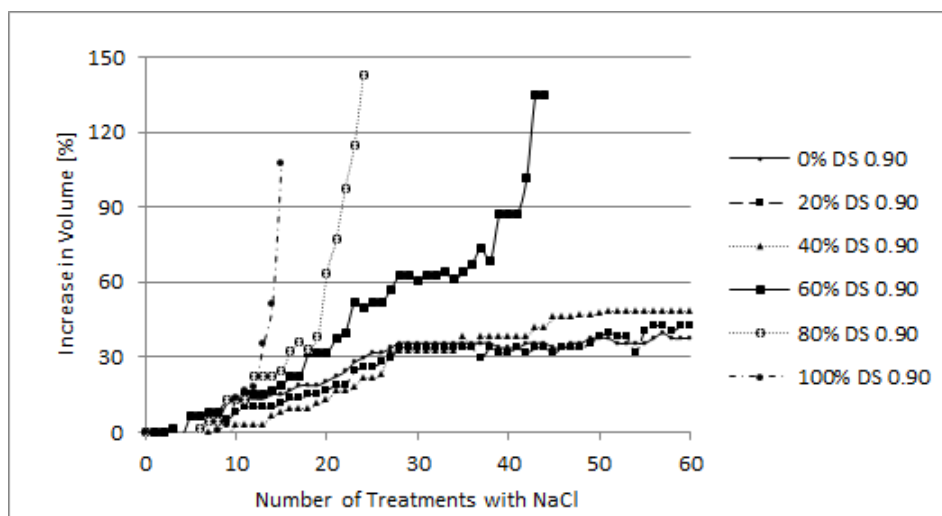


Figure 3.3.8: The average increase in volume of alginate beads made from alginate mixtures with various proportions of alginate-sulfate with DS 0.90 and alginate LF200S as a function of the number of treatments with 0.9 % NaCl. The beads were made by external gelation with $BaCl_2$.

As can be seen from Figure 3.3.7 and Figure 3.3.8 the samples where 60 % or more of the total alginate content was alginate with DS 0.90 showed the same trend as earlier, with a decreasing stability of the beads as the DS 0.90 content increases. The samples where the DS 0.90 content was 40 % or below gave beads that stabilised in number and volume after approximately 45 treatments with 0.9 % NaCl. While the 40 % sample experienced a slightly larger increase in volume than the 20 % and 0% sample, not much difference can be seen between the two later samples.

3.3.4 The Content of Ca^{2+} in Swelling Beads

The capacity of gel beads made from alginate/alginate-sulfate to bind up and retain calcium for gel beads was investigated. The hypothesis was that a higher content of calcium in the beads containing 20 % alginate DS 0.90 than in the pure LF200S beads could be the cause of the higher stability of the 20 % beads. Beads containing 0, 20 or 40 % alginate-sulfate compared to total alginate content were prepared. The beads were rinsed and treated with 0.9 % NaCl solution, and 20 beads taken out for analysis after 0, 6 and 13 treatments. The beads were dissolved, and the Ca^{2+} concentration

determined by use of HR-ICP-MS.

The resulting content of Ca^{2+} in 20 beads from each samples at different times is shown in Figure 3.3.9.

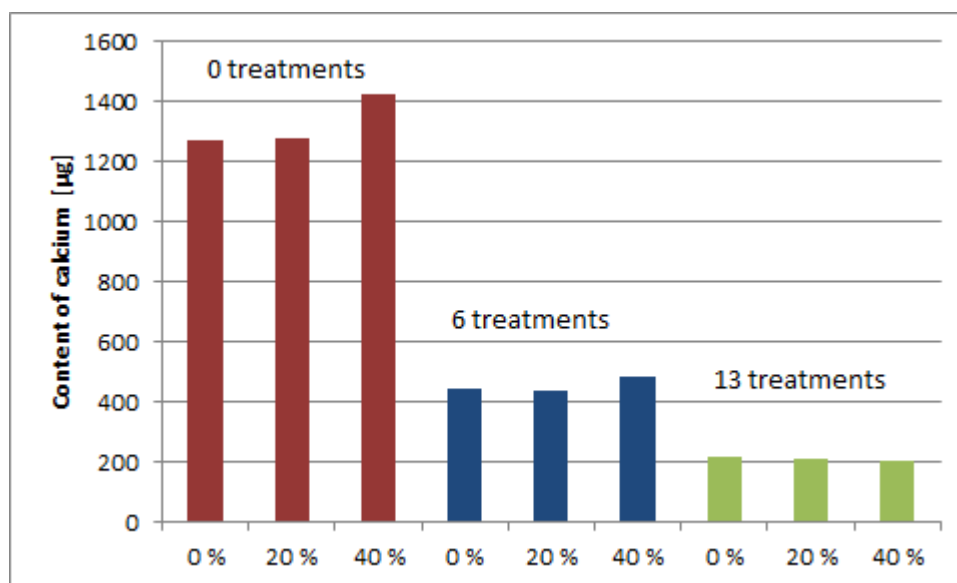


Figure 3.3.9: *The content of calcium in the 20 beads taken out from each of three alginate/alginate-sulfate samples after 0, 6 and 13 treatments with 0.9 % NaCl. The percentages given represent the percentage (w/w) of alginate-sulfate compared to total alginate content.*

The results from Figure 3.3.9 indicates that the sample containing 40 % alginate with DS 0.90 retained slightly more calcium than the beads containing a smaller proportion of sulfated alginate. This difference did however even out after 6 treatments. Figure 3.3.10 shows the content of sulfur in the 20 beads taken out from the samples after 0, 6 and 13 treatments with 0.9 % NaCl.

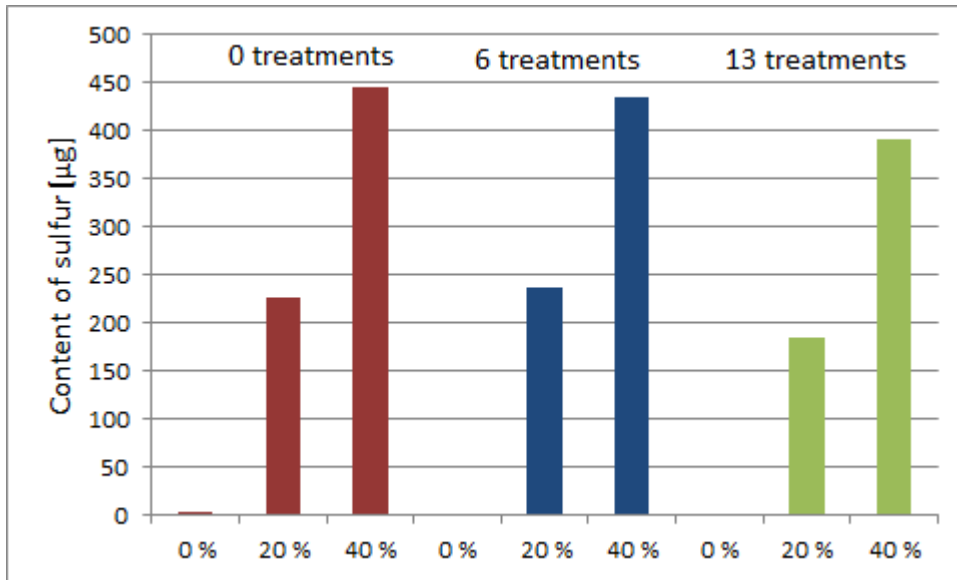


Figure 3.3.10: The content of sulfur in the 20 beads taken out from each of three alginate/alginate-sulfate samples after 0, 6 and 13 treatments with 0.9 % NaCl. The percentages given represent the percentage (w/w) of alginate-sulfate compared to total alginate content.

From Figure 3.3.10 it can be observed that the sulfur content in the beads is fairly constant throughout the first six saline treatments. There seems to be some decrease in the sulfur content between the 6th and 13th saline treatment.

3.4 The Young's Modulus

The Young's modulus of gels made from alginate DS 0.77/LF200S mixtures in different proportions were determined by use of a longitudinal compression test. The initial slope between 0.4 and 0.5 mm in the force- distance plot was used in the calculations of the Young's modulus of each sample, according to Equation 1.4.1.

The results of the calculations, together with the standard deviation between the six gel specimen for each sample and the coefficient of variation, is given in Table 3.4.1. An example calculation of the Young's modulus of one of the samples is given in Appendix G.

Table 3.4.1: The Young's modulus for gels from alginate DS 0.77/LF200S mixtures, along with the standard deviation between the six specimen of each sample, and the coefficient of variation (CoV). The % signifies the percentage (w/w) of alginate-sulfate compared to total alginate content.

Amount of Alginate-Sulfate [%]	The Young's Modulus E [kPa]	The Standard Deviation of E [kPa]	CoV
0	310	32	0.10
5	289	35	0.12
10	229	18	0.08
20	215	29	0.13
40	205	35	0.17
60	124	18	0.14
80	82	3	0.04
100	26	8	0.33

Because of the syneresis effects of alginate gels, the Young's modulus for each sample was corrected for syneresis according to Equation 1.4.2. The resulting corrected modulus, E_{corr} along with the average weight of each gel sample, the standard deviation and the coefficient of Variation, CoV, of E_{corr} are given in Table H.1 in Appendix H. Table H.2 in the same Appendix shows the calculated Young's modulus of three gel samples from mixtures of partially hydrolysed alginate ($M_w \approx 150$ kDa), both before and after correction for syneresis. It also contains the average gel weights, the standard deviation

between the six gel specimen for each sample and the coefficient of variation of E_{corr} . Figure 3.4.1 shows the graph for the corrected Young's modulus as a function of the content of alginate-sulfate, together with a plot of the corrected Young's modulus as a function of the content of partially hydrolysed alginate.

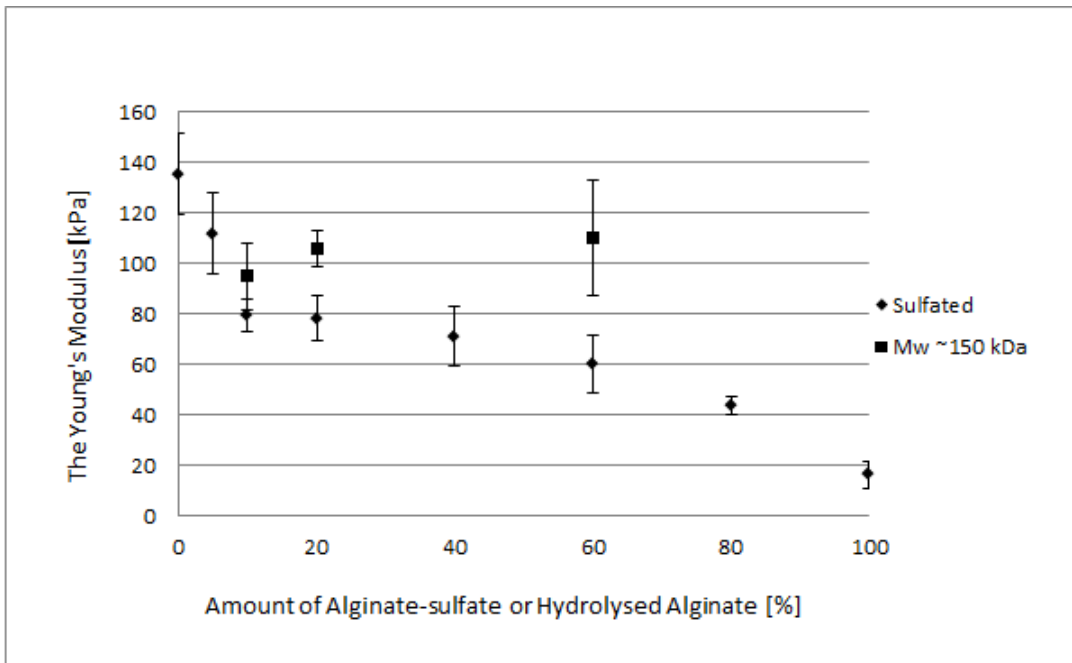


Figure 3.4.1: The Young's modulus of DS 0.77/LF200S mixtures corrected for syneresis, along with hydrolysed alginate/LF200S mixtures. The error bars correspond to one standard deviation in each direction.

The graphs in Figure 3.4.1 show that replacing small amounts of the unmodified LF200S alginate with either alginate-sulfate or partially hydrolysed alginate with approximately the same molecular weight as the sulfated sample, causes a drop in the Young's modulus. At larger proportions of alginate-sulfate or hydrolysed alginate in the gels, there is no or little change in the

Young's modulus of the gels containing hydrolysed alginate, while the drop in Young's modulus continues for larger proportions of alginate-sulfate.

The content of sulfate groups in the mixed gels was converted to an approximate value for degree of sulfation of the alginate sample as a whole, in order to be able to compare the results with earlier results of gels made from alginate-sulfate of various degrees of sulfation. The calculated approximate DS of the mixed gels are shown in Table 3.4.2.

Table 3.4.2: The approximated degree of sulfation for the mixtures of alginate-sulfate (DS 0.77) and LF200S. The calculations are based upon the total content of sulfate groups in the alginate sample as a whole.

% (w/w) sulfated alginate	DS _{app}
0	0.00
5	0.04
10	0.08
20	0.15
40	0.31
60	0.46
80	0.62
100	0.77

The Young's modulus corrected for syneresis for both the gels made from mixtures and gels made from pure sulfated alginate is plotted as a function of DS and DS_{app} in Figure 3.4.2.

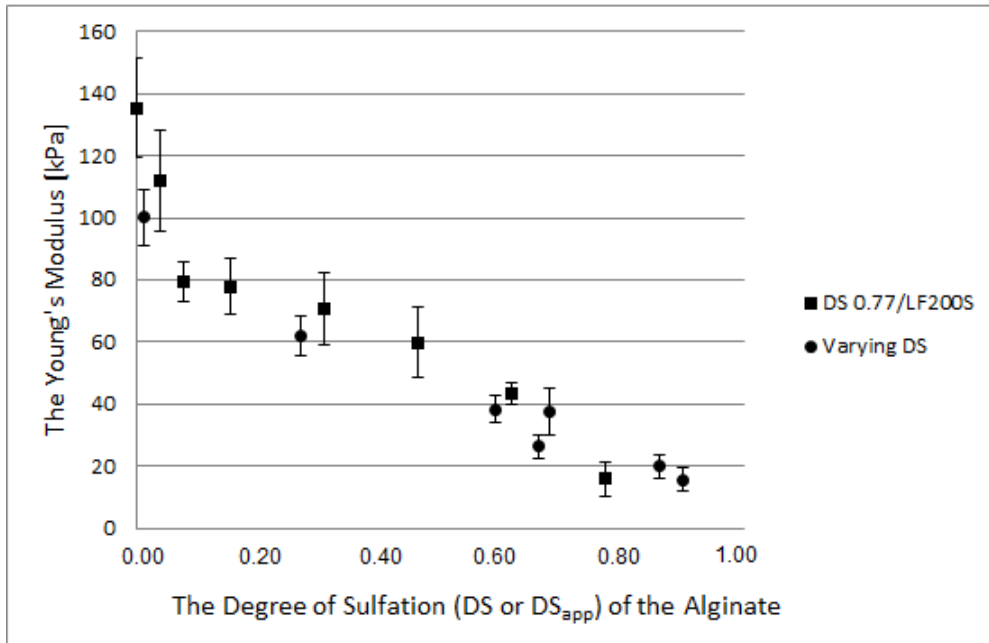


Figure 3.4.2: *The Young's modulus corrected for syneresis of DS 0.77/LF200S mixtures and gels made from pure sulfated alginate of various DS. The error bars correspond to one standard deviation in each direction.*

As shown in Figure 3.4.2 there is no apparent difference between the mechanical strength of alginate gels made from DS 0.77/LF200S mixtures and gels made from pure alginate-sulfate when the total sulfate content of the gels is approximately the same in both samples.

3.5 Distribution of Sulfated Alginate in Gel Beads

The distribution of fluorescence-labeled alginate-sulfate in gel beads was monitored weekly using LSCM over two weeks. The beads were made from mixtures of alginate Pronova UP LVG and fluorescence-labeled alginate-sulfate with a DS of 0.83. The alginate-sulfate made up 10 % of the total

alginate content in the beads.

Figure 3.5.2 shows the distribution of the alginate-sulfate in gel beads stored in a NaCl solution for two weeks (Solution 1 in Table 2.11.1). In Figure 3.5.2 the distribution of alginate-sulfate when the beads were kept in a solution containing CaCl₂ (Solution 2 in Table 2.11.1) is shown. Figure 3.5.3 shows the distribution in beads stored in a HEPES solution (Solution 3 in Table 2.11.1).

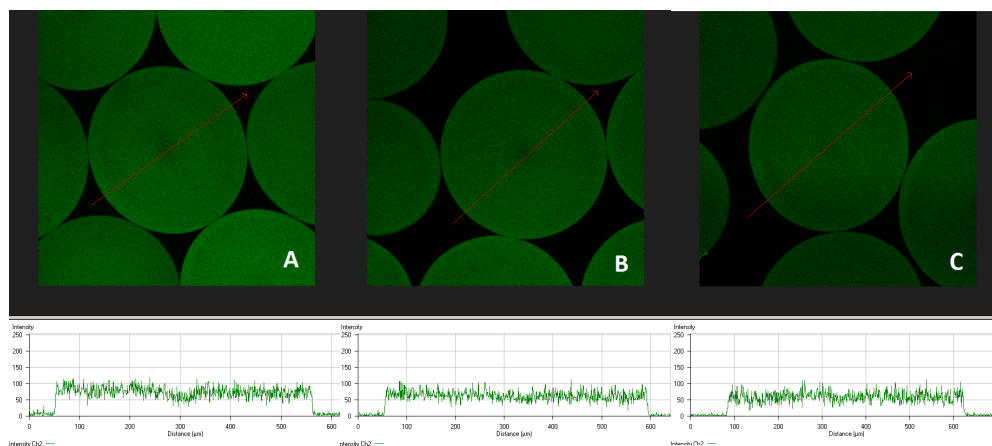


Figure 3.5.1: *The distribution of alginate-sulfate of low molecular weight in beads stored in a NaCl solution. The fluorescence intensity through the beads is shown below each picture. The distribution of alginate-sulfate in gel beads A) immediately after transfer to the NaCl solution; B) after one week storage; C) after two weeks storage.*

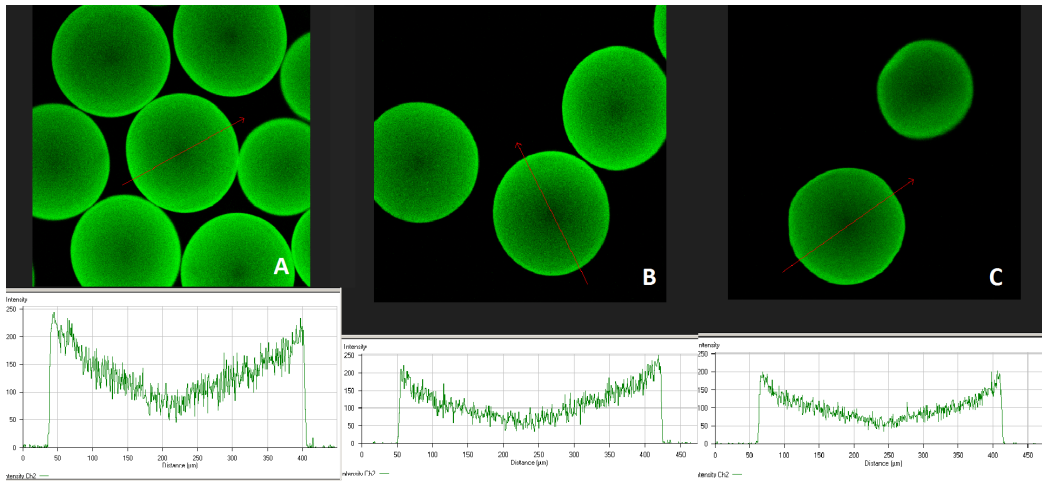


Figure 3.5.2: *The distribution of alginate-sulfate of low molecular weight in beads stored in a CaCl_2 solution. The fluorescence intensity through the beads is shown below each picture. The distribution of alginate-sulfate in gel beads A) immediately after transfer to the CaCl_2 solution; B) after one week storage; C) after two weeks storage.*

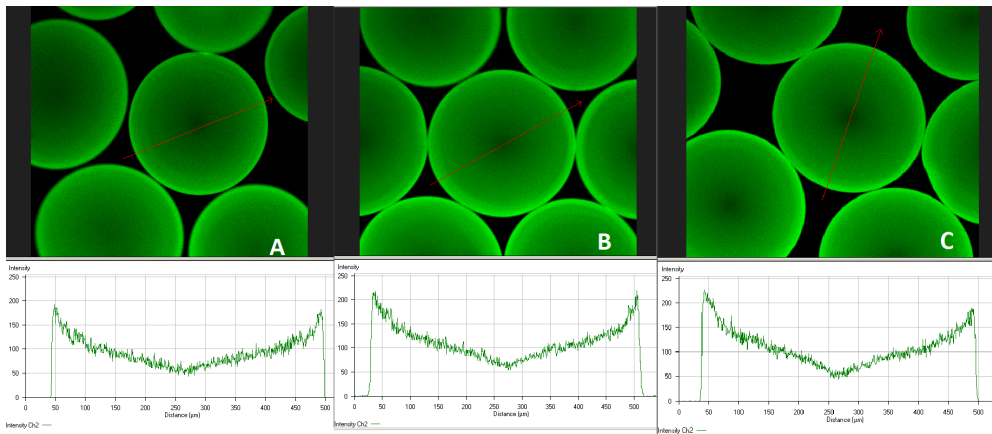


Figure 3.5.3: *The distribution of alginate-sulfate of low molecular weight in beads stored in a HEPES solution. The fluorescence intensity through the beads is shown below each picture. The distribution of alginate-sulfate in gel beads A) immediately after transfer to the HEPES solution; B) after one week storage; C) after two weeks storage.*

From Figure 3.5.1 it is clear that the beads stored in the NaCl solution obtained a homogeneous distribution of alginate-sulfate throughout the beads, with no apparent change taking place over the two weeks of storage. From Figure 3.5.2 and Figure 3.5.3 it can be seen that the storage in CaCl₂ and in HEPES both resulted in a distribution gradient of alginate-sulfate throughout the beads, with a gradual increase in the concentration of alginate-sulfate towards the surface of the beads. The beads stored in the CaCl₂ acquired uneven surfaces, and many of the beads ruptured during the storage time.

3.6 Interactions between FGF and Alginate/ Alginate-Sulfate

3.6.1 Alginate/Alginate-Sulfate in Solution

Alginate-sulfate of varying degrees of sulfation, as well as mixtures of alginate/ alginate-sulfate (DS 0.80) were used to inhibit binding of FGF to the surface of myeloma cells. FGF remaining on the cell surface was labelled with fluorescence and detected by use of flow cytometry. The mean fluorescence intensity of the cells was recorded and compared to the intensity of a sample not treated with alginate.

The median fluorescence intensity from the samples were all compared to the one obtained from cells not treated with alginate. The median fluorescence intensity was measured for cells with labelled FGF treated with alginates having different degrees of sulfation. The results are given in Figure 3.6.1. The resulting median fluorescence intensities of cells treated with alginate/alginate-sulfate (DS 0.80) mixtures are given in Figure 3.6.2.

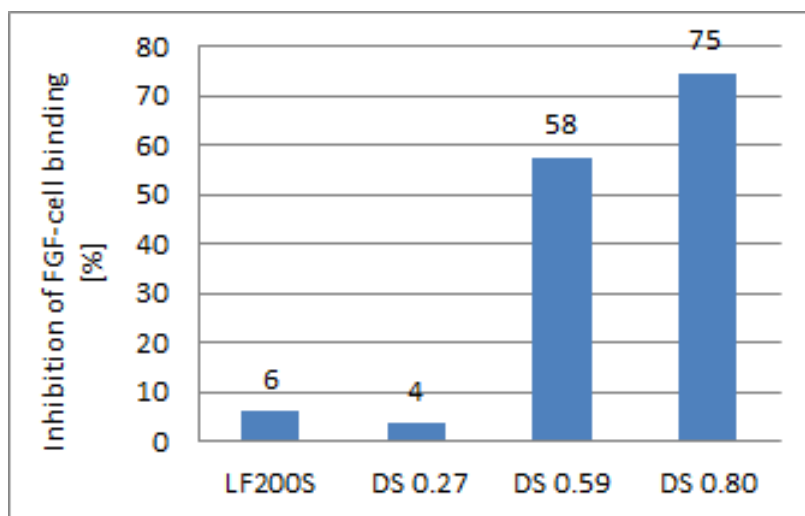


Figure 3.6.1: The median fluorescence intensity of cells with labelled FGF after treatment with alginates of different degrees of sulfation (DS). Results are given in percent inhibition of FGF-cell binding compared to the untreated sample.

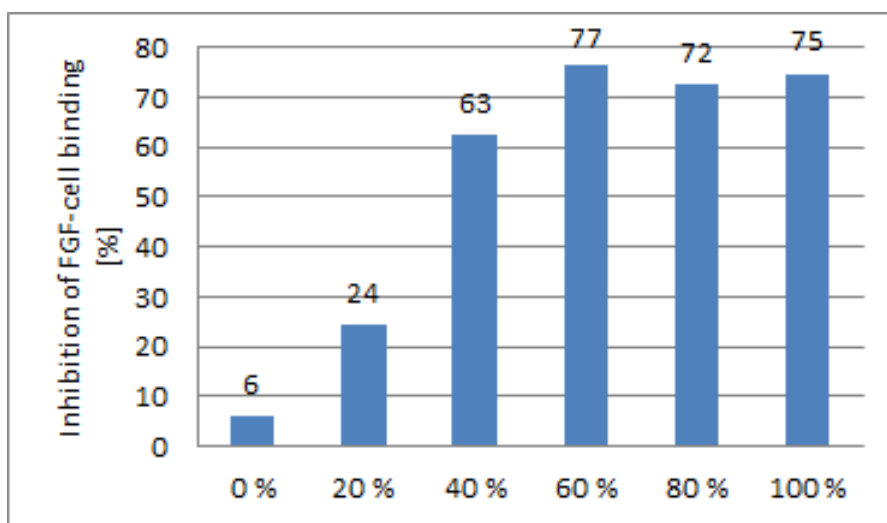


Figure 3.6.2: The median fluorescence intensity of cells with labelled FGF after treatment with alginate/alginate-sulfate (DS 0.80) mixtures. Results are given in percent inhibition of FGF-cell binding compared to the untreated sample.

The results from Figure 3.6.1 show that the sample containing alginate with a DS of 0.27 did not inhibit the interaction between FGF and cells, while the samples with DS 0.59 and 0.80 did show the ability to inhibit these interactions. In Figure 3.6.2 there is an increase in the ability to inhibit the interaction between cells and FGF with a higher content of alginate-sulfate in the solution. To compare the mixtures and the purely sulfated samples, an approximate DS (DS_{app}) was calculated for the mixtures. This value is based upon the total content of sulfate groups in the whole alginate sample. The values are given in Table 3.6.1.

Table 3.6.1: The approximated degree of sulfation for the mixtures of alginate-sulfate (DS 0.80) and LF200S. The calculations are based upon the total content of sulfate groups in the alginate sample as a whole.

% (w/w) sulfated alginate	DS_{app}
0	0.00
20	0.16
40	0.32
60	0.48
80	0.64
100	0.80

As shown in Table 3.6.1 the sample containing 20 % alginate-sulfate has an approximate DS of 0.16. Figure 3.6.2 shows that this sample has some ability to inhibit the FGF-cell interaction, in contrast to the pure sulfated sample with DS 0.27 shown in Figure 3.6.1. After the point where 60 % of the alginate in the mixed solution is sulfated, no further increase in the inhibition can be observed.

3.6.2 Release of FGF from Alginate/Alginate-Sulfate Gel Disks

The release of FGF from alginate/alginate-sulfate gel disks over a 12 day period was studied by use of ELISA. As the samples were not diluted prior

to the analysis, the samples fell outside the measured standard, and the measured absorbance for these samples are reported instead of concentrations. The remaining content of FGF in the gel disks was measured using ELISA after 12 days, and the absorbances converted to concentrations of FGF in the gel disks by use of a constructed standard curve.

The resulting absorbance measurements at 405 nm with 650 nm as a wavelength reference for the FGF release from gel disks are given in Figure 3.6.3.

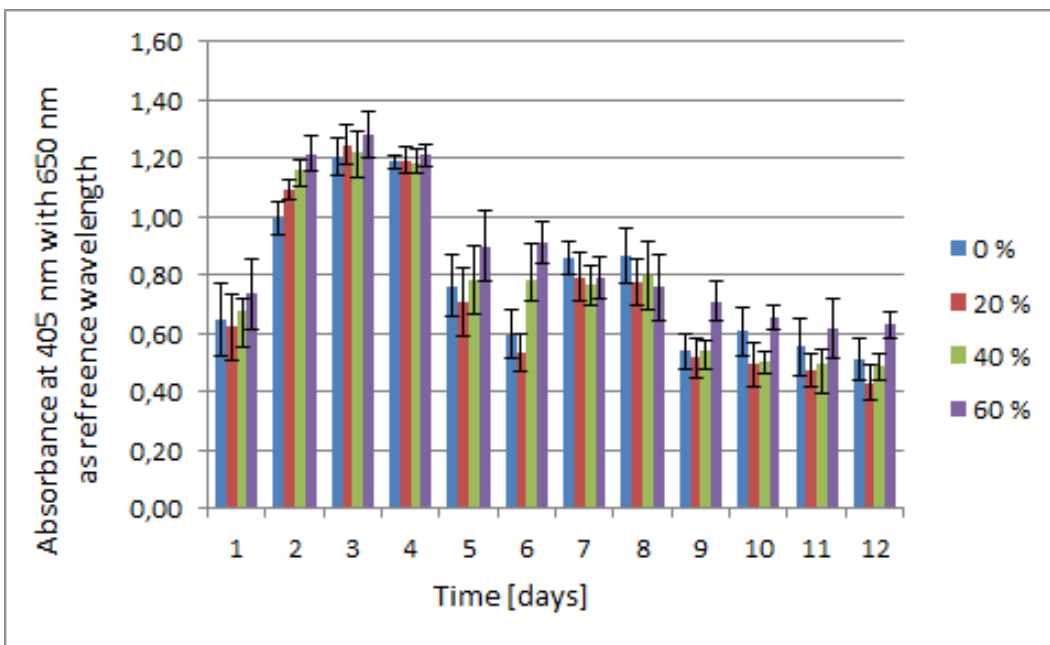


Figure 3.6.3: The measured absorbance at 405 nm for in an ELISA with samples from solutions over gel disks containing FGF. The samples were collected over a time range of 12 days. 650 nm was set as a reference wavelength, and the gel disks initially contained $2 \mu\text{g}/\text{ml}$ FGF. The percentage of the sample represents the content of alginate-sulfate compared to total alginate content. The error bars represents one standard deviation in each direction.

From Figure 3.6.3 it is clear that FGF is released from all the gel disks, and the release is observed to be largest the first four days of the experiment. The calculated FGF concentrations in the gel disks after 12 days are given in Figure 3.6.4. The values used in the calculations are all given in Table

I.1 in Appendix I. The standard curve used for these calculations is given in Figure I.1 in the same appendix.

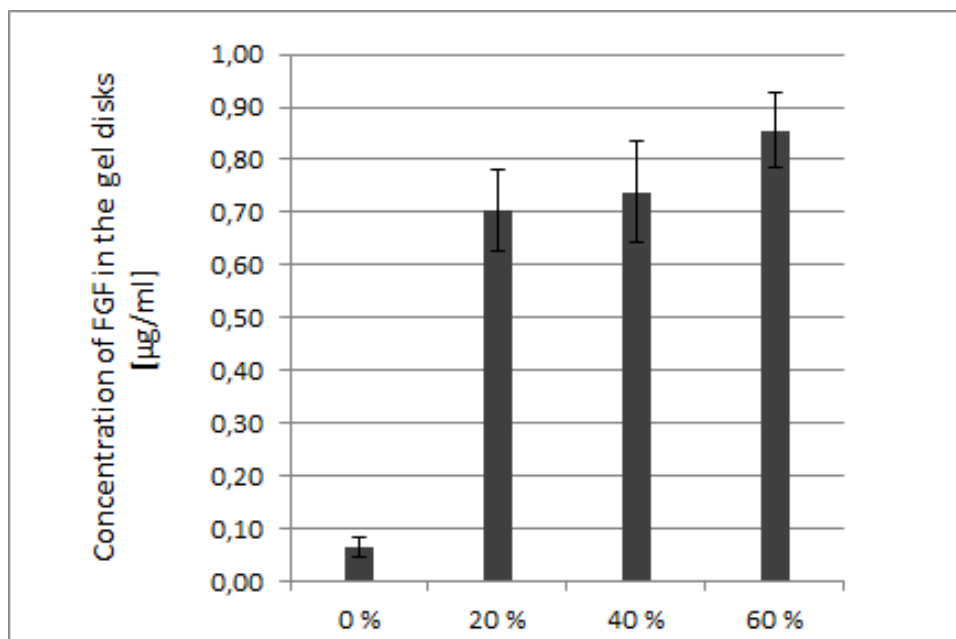


Figure 3.6.4: *The calculated concentration of FGF in gel disks after 12 days in a HEPES medium. The percentage of the sample represents the content of alginate-sulfate compared to total alginate content. The results are obtained from absorbance measurements of 1/10 diluted samples at 405 nm and a correction wavelength of 650 nm after ELISA.*

A series of higher diluted samples showed an overall higher concentration of FGF in the gels, suggesting some inaccuracy in the assay. However, the relative difference between the samples remained the same for all dilutions. The inaccuracies increased with higher dilutions, which is the reason why the 1/10 dilution was used even though the samples from the 60 % gel disks fall outside the standard curve.

4. Discussion

Alginate LF200S was successfully sulfated, with the resulting degree of sulfation (DS) depending mainly upon the concentration of chlorosulfonic acid in the sulfation mixture, although the solubility of the alginate and the reaction volume may also affect the DS of the sample. The effect of $HClSO_3$ concentration on the DS can be observed clearly in Table 3.1.1. The samples where 1.75 % to 2.75 % (v/v) $HClSO_3$ were used in the sulfation mixture show resulting DS varying between 0.27 for the lowest concentration of $HClSO_3$ and up to 0.79 for the highest concentration of acid. The effect of solubility of the alginate is clear from the various results obtained for the four batches of alginate-sulfate produced using 3.5 % $HClSO_3$ in the sulfation mixture, where the acid concentration was the same for all batches. The use of a freeze dried alginate in batch 2 and 3 gave a slowly dissolving alginate mixture where the slow mixing in the solution is probably the cause of lower degrees of sulfation (0.77 and 0.80) for these batches than the one observed for batch 1 (0.90), where alginate in powder form was used. Batch 2 even ended up with a lower DS than the sample where 2.75 % (v/v) $HClSO_3$ was used. However, the reaction volumes also differed between batch 1 and batch 2/3, and this may also have played a part in the resulting differences in the DS of the samples. The sulfation of the sample of a molecular weight 45 kDa ended up with only a slightly higher DS than batch 2 and 3, even though this sample seemed to dissolve rather quickly in the reaction mixture.

Acid hydrolysis revealed, as shown in Figure 3.2.1 and Table 3.2.2, a higher depolymerization rate for the sulfated samples compared to the unmodified alginate LF200S. The decrease in molecular weight of the two sulfated samples was similar, but as the sample of a higher DS has a higher molecular weight per monosaccharide, the drop in average chain length is more rapid for the highly sulfated sample. The calculated pseudo first order rate con-

stants increase with the DS, from 0.017 min^{-1} for LF200S, via 0.039 min^{-1} for DS 0.27, to 0.050 min^{-1} for DS 0.90. These results agree with the results found by Smidsrød *et al.* for dextran and dextran sulfate (Smidsrød *et al.*, 1966), and may be caused by a higher concentration of protons around the polysaccharides with many negatively charged sulfate groups compared to the bulk solution. It should be noted that the molecular weight of the sulfated samples may be underestimated, as the value of the refractive index, $\frac{dn}{dc}$ used in the analysis is that of unmodified alginate. If alginate follows the same trend as carrageenan from the experiments of Berth *et al.* (Berth *et al.*, 2008), the value of $\frac{dn}{dc}$ for sulfated samples should have been slightly lower when more sulfate groups are added to the polysaccharides. The sulfate groups in the sulfated samples may not be evenly distributed along the polysaccharide chain, as shown by Arlov *et al.* (Arlov *et al.*, 2014), and some parts of the chain may therefore be more susceptible to acid hydrolysis than other parts. As the heterogeneity observed by Arlov *et al.* was especially large for the less sulfated samples, this may especially be true for the sample with a DS of 0.27, and the local variations within the sample may be greater than for the highly sulfated sample.

Hydrolysis of LF200S was performed to produce a sample of similar average molecular weight as the sulfated sample used in the gel strength experiments, and a low molecular weight sample of 45 kDa for use in alginate microbeads, as shown in Table 3.2.3. Although differences in the solubility and reaction volume of alginate samples used to produce alginate of DS 0.90, DS 0.77 and DS 0.80 affected the final degree of sulfation, it did not affect the depolymerization of the samples during the sulfation process, as DS 0.90 and DS 0.77 have almost identical molecular weights. As the samples with DS 0.77 and 0.80 were produced under the same conditions, the difference in the molecular weight of these two are probably due to random variations during the sulfation process, or inaccurate measurements in the SEC-MALLS analysis.

Alginate-calcium gel beads made from alginate-sulfate were shown to have a much lower osmotic stability in a physiological saline solution compared to beads made of unmodified alginate, as observed in Figure 3.3.1 and Figure 3.3.2. The production of calcium-alginate beads using a sample with a DS of 0.79 failed, as the alginate solution only formed plaques on the surface of the gelling bath. The sample with a DS of 0.59 formed beads, but they were highly unstable, with all beads gone after only three treatments with 0.9

% NaCl, and a low tolerance for an increase in the volume of the beads. The beads with a DS of only 0.27 was somewhat more stable, but lasted for only 7 treatments, showing that alginate-sulfate on its own is not a stable material for use in physiological saline solutions. This is to be expected, as the charge of the alginate-sulfate increases the number of counter-ions held back in the beads, leading to a higher osmotic pressure inside the beads (Moe, 1993). In addition, the bulky sulfate groups are probably contributing to a weaker gel network as they disturb the ideal binding of ions described in the "egg-box" model (Grant et al., 1973).

Mixtures between alginate-sulfate (DS 0.90 or DS 0.68) and alginate LF200S showed a general decrease in stability with increasing proportions of alginate-sulfate. However, it appears that use of mixtures increase the stability of the beads with respect to total sulfate content, compared to beads made from only alginate-sulfate, as shown in Table 3.3.1. This is especially clear when comparing the sample with DS 0.27 and the sample made from 40 % alginate-sulfate with DS 0.68 and 60 % LF200S, where the total sulfate content of the beads corresponds to a DS of 0.27. Here, the beads made from only alginate-sulfate were all gone after 7 treatments and the last remaining beads tolerated an increase in volume of about 110 %, as shown in Figure 3.3.1 and Figure 3.3.2. In comparison, as showed in Figure 3.3.5 and Figure 3.3.6, the last beads made from the mixed solution did not rupture before after 13 treatments, and the increase in volume reached 200 %.

An exception to the general trend of decreasing stability with increasing content of alginate-sulfate is observed in beads containing low proportions of alginate-sulfate. Alginate/DS 0.90 beads containing 20 % DS 0.90, and alginate/DS 0.68 beads with 20 - 40 % DS 0.68 show a slightly higher stability than the beads made from only unsulfated alginate. Since the negative charges of the sulfate groups is likely to contribute to a higher osmotic pressure inside the beads, this stability is probably due to a strengthening of the elastic reaction of the gel network (Moe, 1993). It is unknown how the incorporation of few sulfate groups can give rise to more stable gel networks. Use of 50 mM BaCl₂ in the gelation bath of alginate/DS 0.90 beads to study whether the relationship between the stability of 0 % beads and 20 % beads was ion specific did not result in a clear answer of this question. As shown in Figure 3.3.7, stable beads were formed for mixtures containing less than 60 % DS 0.90 alginate, making it hard to judge whether the 20 % beads

were more stable than the 0 % beads for this ion. A lower concentration of BaCl_2 in the gelation bath should probably have been utilised in order to study the differences between the mixtures of low content of alginate-sulfate. Observing Figure 3.3.4 and Figure 3.3.8, the barium-alginate beads of a high alginate-sulfate content seem to tolerate a somewhat lower increase in the volume than the calcium-alginate beads.

The higher stability of the 20 % beads than the 0 % beads gelled in CaCl_2 was thought to be due to a higher ability to bind and retain calcium. However, this hypothesis was proved wrong by the results from the elemental analysis for calcium in the beads, as there was no observable difference in calcium content between the 0 % and 20 % beads neither after 0, 6 nor 13 measurements. The 40 % beads seemed to have a slightly higher calcium content before the first treatment with NaCl , but this difference was no longer observable after 6 treatments. The calcium content of the beads thereby show no sign of being the determining factor for the differences in bead stability between these three samples. The elemental analysis also revealed a sulfate content of the beads where the 40 % beads contained about double the amount of sulfur as the 20 % beads, indicating that the alginate/alginate-sulfate ratio in the solutions have been retained in the gels throughout the experiment. The method used for the studies of swelling of alginate beads does not provide very accurate measurements of diameters and hence volume of the beads, but does still provide the means to observe relative differences between samples. As long as many beads are present in the sample, the error associated with the measurement of the diameter of a single bead is kept quite small, as the error in the reading is distributed over a larger number of beads. The measurements of diameters for few beads have a larger error associated with them, and the values of maximum increase in volume of the beads may therefore not be very reliable.

The gel strength measurements showed a decrease in alginate gel strength as the proportion of alginate-sulfate in the gel increased. As shown in Figure 3.4.1, the gels cover a wide range of gel strengths from an average Young's modulus of 310 kPa (135 kPa when corrected for syneresis) for the gels containing only unsulfated alginate and down to only 26 kPa (16 kPa) for the gels containing only alginate-sulfate. These gels cover the range of several biological tissues, such as skeletal muscle and cardiac cells (Mathur et al., 2001). Partially depolymerized alginate LF200S of a molecular weight simi-

lar to the alginate-sulfate used in the mixtures was mixed with unmodified alginate for a control experiment on the effect of molecular weight on E. Comparisons of these mixtures with the alginate/alginate-sulfate mixtures show, in Figure 3.4.1, that the initial decrease, up to a content of alginate-sulfate or hydrolysed alginate of about 10 % seems to be caused at least partially by the lower molecular weight of the alginate-sulfate, which is at about 160 kDa, compared to about 280 kDa for unsulfated alginate. For a content of alginate-sulfate of 20 % and higher, it appears that the lower molecular weight is of less importance for the decrease in the Young's modulus than the content of sulfate groups in the gels. The drop caused by the addition of sulfate groups may be due to steric hindrance and by electrostatic repulsion between the negatively charged sulfate groups, interfering with the junction formation in the gel. All the gels experienced some syneresis effects during gelation, and the Young's modulus was corrected for this effect according to the new weight and concentration of the gels.

In contrast to the gel stability, Figure 3.4.2 reveals that strength of the gels does not show any apparent improvement by mixing of alginate and alginate-sulfate. This is showed by comparison between gels made from alginate-sulfate and gels made from alginate/alginate-sulfate mixtures, where the total sulfate content of the mixed gels is translated into an approximate DS with respect to all the alginate in the gel. This may imply that the gel strength is affected mostly by the total sulfate content of the gels rather than by the distribution of these sulfate groups.

The calcium-alginate gel beads produced from mixtures of alginate and fluorescence-labelled alginate-sulfate showed, as can be observed in Figure 3.5.2 and Figure 3.5.3, a clear gradient in the distribution of alginate-sulfate when the beads were stored in the gelation solution or in a HEPES solution. This is the same behaviour as observed for calcium-alginate beads produced by other groups, with a higher alginate concentration at the bead surface than in the core of the bead (Skjåk-Bræk et al., 1989). The gradient kept constant throughout the two weeks of observation for the two samples. The beads stored in CaCl_2 experienced a dramatic drop in mechanical stability over the two week period, observed by a drop in the number of beads in the solution, as well as by more uneven surfaces for the remaining beads. It has been shown by other groups that washing with NaCl leads to less heterogeneity in microcapsules (Strand et al., 2003a). This effect also holds true for beads

containing alginate-sulfate, as the alginate-sulfate, as shown in Figure 3.5.1, is distributed evenly throughout the beads subjected to washing with, as well as storage in, NaCl. These beads also kept their profiles through the two weeks of observations. In order to observe whether the distribution of alginate-sulfate differs in any way from the distribution of unsulfated alginate in the beads, both the alginates should have been labelled with fluorescence in two separate parts of the emission spectra. The molecular weight of the two alginate would also have to be equal, as the heterogeneity in the beads increases with lower molecular weights (Skjåk-Bræk et al., 1989).

Alginate-sulfate samples at 10 $\mu\text{g}/\text{ml}$ in solution with DS 0.59 and DS 0.80 showed the ability to bind to FGF and inhibit its interaction with the surface of RPMI-8226 cells compared to a control sample without alginate. As shown in Figure 3.6.1, unsulfated alginate LF200S and alginate-sulfate with a DS of 0.27 did not show the same ability. The highest sulfated sample showed the highest degree of inhibition of FGF-cell surface interaction. For mixtures consisting of alginate-sulfate (DS 0.80) and unsulfated LF200S, a trend of increased binding to FGF with a higher content of alginate-sulfate can be observed in Figure 3.6.2. For mixtures where 60 % or more of the alginate was sulfated, an increase in the content of alginate-sulfate did not affect the ability to inhibit cell-FGF interaction. Even the mixture with only 20 % alginate-sulfate showed some ability to bind to FGF, in contrast to the sample consisting of only alginate-sulfate with a DS of 0.27. This may indicate that a certain density of sulfate groups can promote binding to FGF, and that this density is not reached for the DS 0.27 sample.

FGF was, as shown in Figure 3.6.3, released from all the gel disks made from alginate/alginate-sulfate mixtures, with a seemingly greater release from the gels during the first four days of the experiment. As the samples were not diluted before the ELISA and the measured absorbances were all outside the range of the standard, the concentrations of the solutions are not accurately known. Hence the release profile from the gels could not be calculated, and no exact comparisons between the gel disks can be made. From the solutions of dissolved gel disks the results, given in Figure 3.6.4, show that almost no FGF was left in the pure LF200S gel disks after 14 days, while there was still FGF left in all the gel disks containing alginate-sulfate. Both the interaction shown between FGF and alginate-sulfate in solution, and the pore size of the gels, can affect the diffusion of FGF from the gel disks. Larger average pore

size is correlated to weaker gel strength (Shoichet et al., 1996), and the gels containing alginate-sulfate could thus be expected to have a larger average pore size than the gels made from pure LF200S alginate. The interaction between FGF and alginate-sulfate is expected to delay the outward diffusion of FGF from the gel disks. The results showing that there was still some FGF remaining in the gels containing alginate-sulfate, and not in pure alginate gels, indicate that the interaction with FGF is the dominating factor for diffusion rate in this system. These results correspond well to the results found by Freeman *et al.* for release of FGF from gel beads containing alginate/alginate-sulfate mixtures (Freeman et al., 2008). As FGF is released from all the gel disks initially, it might be that the initial average pore size of all the gels are large enough to accommodate diffusion of FGF out of the gels, and that a further increase in pore size is of no significant effect.

As gels from alginate/alginate-sulfate mixtures can obtain a higher stability in physiological solutions as well as better ability to interact with FGF than alginate-sulfate alone, mixtures are probably better suited for tissue engineering applications than alginate-sulfate alone. The gels also have mechanical stabilities covering the range of several tissues, which is an advantage for tissue engineering. Microcapsules made from mixtures are able to retain the polymer gradient that is often desirable for microcapsules (Strand et al., 2003a). In addition to varying the G/M ratio, molecular weight and degree of sulfation on the alginate, use of different proportions of alginate and alginate-sulfate in the gels can be used to tune the strength, stability and biological activity of the gels, making the mixtures interesting candidates for future use within tissue engineering applications.



5. Future Directions

The FGF release studies should be repeated with dilution series in order to acquire release profiles for the gel disks made from different alginate/alginate-sulfate mixtures. When incorporating growth factors in hydrogel scaffolds, the release rate should be controllable. If it turns out that the release profile varies between different mixtures of alginate and alginate-sulfate, the proportions in the mixture can be tuned to achieve the desired release rate or profile from the hydrogel. The role of pore size on the diffusion rate from the gels could be further investigated by diffusion studies using a macromolecule of about the same hydrodynamic volume as FGF, but without the ability to interact with the alginate-sulfate of the gels. The difference in pore sizes between gels made from different mixtures could be investigated by use of electron microscopy or packing columns using macromolecular standards (Gombotz and Wee, 2012b).

The stability of the gels made from mixtures should also be further investigated. Especially the gels from mixtures of a low alginate-sulfate content are interesting for further studies, as these have shown surprisingly high stability. Use of alginate-sulfates with a wide range of DS could be used in the mixtures to study the effect of the sulfate distribution on the osmotic stability. Subtoxic amounts of BaCl_2 in the gelation bath, such as the 1 mM BaCl_2 , 50 mM CaCl_2 solutions used by Mørch *et al.* (Mørch *et al.*, 2012), may be used to investigate whether these beads are still more stable than the pure LF200S alginate beads when other ions than only calcium are involved in the crosslinking. This could also contribute to a smaller increase in volume of the beads, helping to maintain the original shape of beads or scaffolds. The bead stability could also be studied in a medium with even higher resemblance to a biological system.

As the possibility of cell anchorage is a desired property of tissue engineering scaffolds, cell adhesion and differentiation on hydrogels made from alginate/alginate-sulfate mixtures should be studied. This could be done by the method described by Rowley *et al.* for their investigation of peptide-coupled hydrogels (Rowley et al., 1999a). This method involves seeding of cells onto the hydrogels and the included controls, with cell counts and observations being carried out over time.

6. Conclusions

Alginate was successfully sulfated using chlorosulfonic acid and formamide. The degree of sulfation depended on the concentration of HClSO_3 and the solubility of the alginate. The sulfation process caused some depolymerization of the alginate and led to a higher susceptibility to acid hydrolysis. Beads made from alginate/alginate-sulfate mixtures had a higher osmotic stability with respect to total sulfate content than beads made from pure alginate-sulfate. A general decrease in stability for increasing sulfate content was observed. However, beads containing small amounts of alginate-sulfate obtained a higher stability than the beads made from unmodified alginate. There was no observable difference in calcium content of the pure LF200S beads and the beads containing small amounts of alginate-sulfate. The gel strength of alginate/alginate-sulfate mixtures decreased with an increasing proportion of alginate-sulfate in the gel, where the initial drop was probably caused by the lower molecular weight of the alginate-sulfate. The distribution of alginate-sulfate in microbeads made of alginate/alginate-sulfate was similar to the distribution in gels made from pure alginate. Alginate-sulfate showed interactions with FGF in solution, and FGF was released gradually from alginate/alginate-sulfate gel disks.

Use of mixtures between alginate and alginate-sulfate improves osmotic stability and FGF interactions, with no apparent effect on gel strength and distribution in microbeads, and may be a better suited material for use in tissue engineering than pure alginate-sulfate. The mixtures have gel strengths covering the range of several tissues, can interact with FGF, and have tunable stability, making them interesting materials for future research on tissue engineering scaffolds.



Bibliography

- Andresen, I.-L., Painter, T., and Smidsrød, O. (1977). Concerning the effect of periodate oxidation upon the intrinsic viscosity of alginate. *Carbohydrate Research*, 59(2):563–566.
- Arlov, Ø., Aachmann, F. L., Sundan, A., Espevik, T., and Skjåk-Bræk, G. (2014). Heparin-like properties of sulfated alginates with defined sequences and sulfation degrees. *Biomacromolecules*.
- Ashman, R., Cowin, S., Van Buskirk, W., and Rice, J. (1984). A continuous wave technique for the measurement of the elastic properties of cortical bone. *Journal of Biomechanics*, 17(5):349–361.
- Augst, A. D., Kong, H. J., and Mooney, D. J. (2006). Alginate hydrogels as biomaterials. *Macromolecular bioscience*, 6(8):623–633.
- Barth, H. G., Boyes, B. E., and Jackson, C. (1996). Size exclusion chromatography. *Analytical Chemistry*, 68(12):445–466.
- Berth, G., Vukovic, J., and Lechner, M. D. (2008). Physicochemical characterization of carrageenans - a critical reinvestigation. *Journal of Applied Polymer Science*, 110:3508–3524.
- Boontheekul, T., Kong, H.-J., and Mooney, D. J. (2005). Controlling alginate gel degradation utilizing partial oxidation and bimodal molecular weight distribution. *Biomaterials*, 26(15):2455–2465.
- Bose, S., Roy, M., and Bandyopadhyay, A. (2012). Recent advances in bone tissue engineering scaffolds. *Trends in biotechnology*, 30(10):546–554.
- Butler, J. E. (2000). Enzyme-linked immunosorbent assay. *Journal of Immunoassay*, 21(2-3):165–209.

-
- Casu, B. (1985). Structure and biological activity of heparin. *Advances in carbohydrate chemistry and biochemistry*, 43:51–134.
- Chen, E. J., Novakofski, J., Jenkins, W. K., and O'Brien Jr, W. D. (1996). Young's modulus measurements of soft tissues with application to elasticity imaging. *Ultrasonics, Ferroelectrics and Frequency Control, IEEE Transactions on*, 43(1):191–194.
- Christensen, B. E. (2013). *Compendium TBT4135 Biopolymers*. Akademika Forlag.
- Dart, R. C. (2004). *Medical toxicology*. Lippincott Williams & Wilkins.
- de Prost, D. (1986). Heparin fractions and analogues: a new therapeutic possibility for thrombosis. *Trends in Pharmacological Sciences*, 7(0):496 – 500.
- Draget, K., Simensen, M., Onsøyen, E., and Smidsrød, O. (1993). Gel strength of ca-limited alginate gels made in situ. *Hydrobiologia*, 260(1):563–565.
- Draget, K., Skjåk Bræk, G., and Smidsrød, O. (1994). Alginic acid gels: the effect of alginate chemical composition and molecular weight. *Carbohydrate Polymers*, 25(1):31–38.
- Draget, K. I., Østgaard, K., and Smidsrød, O. (1989). Alginate-based solid media for plant tissue culture. *Applied microbiology and biotechnology*, 31(1):79–83.
- Draget, K. I., Østgaard, K., and Smidsrød, O. (1990). Homogeneous alginate gels: a technical approach. *Carbohydrate Polymers*, 14(2):159–178.
- Draget, K. I., Skjåk-Bræk, G., and Smidsrød, O. (1997). Alginate based new materials. *International journal of biological macromolecules*, 21(1):47–55.
- Drury, J. L. and Mooney, D. J. (2003). Hydrogels for tissue engineering: scaffold design variables and applications. *Biomaterials*, 24(24):4337–4351.
- Engelmayr, G. C., Cheng, M., Bettinger, C. J., Borenstein, J. T., Langer, R., and Freed, L. E. (2008). Accordion-like honeycombs for tissue engineering of cardiac anisotropy. *Nature materials*, 7(12):1003–1010.

-
- Engvall, E. and Perlmann, P. (1971). Enzyme-linked immunosorbent assay (elisa) quantitative assay of immunoglobulin g. *Immunochemistry*, 8(9):871–874.
- Fischer, F. G. and Dörfel, H. (1955). Die polyuronsÄduren der braunalgen (kohlenhydrate der algen i). *Hoppe-SeylerÄts Zeitschrift fÄijr physiologische Chemie*, 302:186–203.
- Flaumenhaft, R., Moscatelli, D., and Rifkin, D. B. (1990). Heparin and heparan sulfate increase the radius of diffusion and action of basic fibroblast growth factor. *The Journal of cell biology*, 111(4):1651–1659.
- Freeman, I., Kedem, A., and Cohen, S. (2008). The effect of sulfation of alginate hydrogels on the specific binding and controlled release of heparin-binding proteins. *Biomaterials*, 29(22):3260–3268.
- Gacesa, P. (1998). Bacterial alginate biosynthesis-recent progress and future prospects. *Microbiology*, 144(5):1133–1143.
- Gießmann, U. and Greb, U. (1994). High resolution icp-msÄÄa new concept for elemental mass spectrometry. *Fresenius’ journal of analytical chemistry*, 350(4-5):186–193.
- Gombotz, W. R. and Wee, S. F. (2012a). Protein release from alginate matrices. *Advanced drug delivery reviews*, 64:194–205.
- Gombotz, W. R. and Wee, S. F. (2012b). Protein release from alginate matrices. *Advanced drug delivery reviews*, 64:194–205.
- Gospodarowicz, D. (1975). Purification of a fibroblast growth factor from bovine pituitary. *Journal of Biological Chemistry*, 250(7):2515–2520.
- Gospodarowicz, D. and Cheng, J. (1986). Heparin protects basic and acidic fgf from inactivation. *Journal of cellular physiology*, 128(3):475–484.
- Grant, G. T., Morris, E. R., Rees, D. A., Smith, P. J., and Thom, D. (1973). Biological interactions between polysaccharides and divalent cations: The egg-box model. *FEBS Letters*, 32(1):195 – 198.
- Gronthos, S., Franklin, D. M., Leddy, H. A., Robey, P. G., Storms, R. W., and Gimble, J. M. (2001). Surface protein characterization of human adipose tissue-derived stromal cells. *Journal of cellular physiology*, 189(1):54–63.

-
- Guillemette, M. D., Park, H., Hsiao, J. C., Jain, S. R., Larson, B. L., Langer, R., and Freed, L. E. (2010). Combined technologies for microfabricating elastomeric cardiac tissue engineering scaffolds. *Macromolecular bio-science*, 10(11):1330–1337.
- Haug, A. (1964). *Composition and Properties of Alginates*. PhD thesis, Norwegian Institute of Seaweed Research, NTH.
- Haug, A., Larsen, B., and Smidsrød, O. (1966). A study of the constitution of alginic acid by partial hydrolysis. *Acta Chem. Scand.*, 20:183–190.
- Haug, A., Larsen, B., and Smidsrød, O. (1967a). Studies on the sequence of uronic acid residues in alginic acid. *Acta Chem Scand*, 21:691–704.
- Haug, A., Larsen, B., and Smidsrød, O. (1974). Uronic acid sequence in alginate from different sources. *Carbohydrate Research*, 32(2):217 – 225.
- Haug, A., Myklestad, S., Larsen, B., and Smidsrød, O. (1967b). Correlation between chemical structure and physical properties of alginates. *Acta Chem Scand*, 21(3):768–78.
- Haug, A. and Smidsrød, O. (1965). The effect of divalent metals on the properties of alginate solutions. *Acta Chem. Scand*, 19(2).
- Holme, H. K., Davidsen, L., Kristiansen, A., and Smidsrød, O. (2008). Kinetics and mechanisms of depolymerization of alginate and chitosan in aqueous solution. *Carbohydrate Polymers*, 73(4):656 – 664.
- Ingber, D. E. and Folkman, J. (1989). Mechanochemical switching between growth and differentiation during fibroblast growth factor-stimulated angiogenesis in vitro: role of extracellular matrix. *The Journal of cell biology*, 109(1):317–330.
- Jeon, O., Bouhadir, K. H., Mansour, J. M., and Alsberg, E. (2009). Photocrosslinked alginate hydrogels with tunable biodegradation rates and mechanical properties. *Biomaterials*, 30(14):2724–2734.
- Johnson, D. E., Lee, P. L., Lu, J., and Williams, L. T. (1990). Diverse forms of a receptor for acidic and basic fibroblast growth factors. *Molecular and cellular biology*, 10(9):4728–4736.

-
- Kong, H. J., Kaigler, D., Kim, K., and Mooney, D. J. (2004). Controlling rigidity and degradation of alginate hydrogels via molecular weight distribution. *Biomacromolecules*, 5(5):1720–1727.
- Kuo, C. K. and Ma, P. X. (2001). Ionically crosslinked alginate hydrogels as scaffolds for tissue engineering: part 1. structure, gelation rate and mechanical properties. *Biomaterials*, 22(6):511–521.
- Lanza, R., Langer, R., and Vacanti, J. P. (2011). *Principles of tissue engineering*. Academic press.
- Leach, M., Drummond, M., and Doig, A. (2013). *Practical Flow Cytometry in Haematology Diagnosis*. John Wiley & Sons.
- Lee, K. Y. and Mooney, D. J. (2001). Hydrogels for tissue engineering. *Chemical reviews*, 101(7):1869–1880.
- LeRoux, M. A., Guilak, F., Setton, L. A., et al. (1999). Compressive and shear properties of alginate gel: effects of sodium ions and alginate concentration. *Journal of biomedical materials research*, 47(1):46–53.
- Levenberg, S., Rouwkema, J., Macdonald, M., Garfein, E. S., Kohane, D. S., Darland, D. C., Marini, R., van Blitterswijk, C. A., Mulligan, R. C., D’Amore, P. A., et al. (2005). Engineering vascularized skeletal muscle tissue. *Nature biotechnology*, 23(7):879–884.
- Lindahl, U., Bäckström, G., Höök, M., Thunberg, L., Fransson, L.-A., and Linker, A. (1979). Structure of the antithrombin-binding site in heparin. *Proceedings of the National Academy of Sciences*, 76(7):3198–3202.
- Linhardt, R. J. (2003). 2003 claudie s. hudson award address in carbohydrate chemistry. heparin: structure and activity. *Journal of medicinal chemistry*, 46(13):2551–2564.
- Linker, A. and Jones, R. S. (1966). A new polysaccharide resembling alginic acid isolated from pseudomonads. *Journal of Biological Chemistry*, 241(16):3845–3851.
- Mackie, W., Noy, R., and Sellen, D. (1980). Solution properties of sodium alginate. *Biopolymers*, 19(10):1839–1860.

-
- Martinsen, A., Skjåk-Bræk, G., and Smidsrød, O. (1989). Alginate as immobilization material: I. correlation between chemical and physical properties of alginate gel beads. *Biotechnology and bioengineering*, 33(1):79–89.
- Mathur, A. B., Collinsworth, A. M., Reichert, W. M., Kraus, W. E., and Truskey, G. A. (2001). Endothelial, cardiac muscle and skeletal muscle exhibit different viscous and elastic properties as determined by atomic force microscopy. *Journal of Biomechanics*, 34(12):1545 – 1553.
- Melchels, F. P., Barradas, A., Van Blitterswijk, C. A., De Boer, J., Feijen, J., and Grijpma, D. W. (2010). Effects of the architecture of tissue engineering scaffolds on cell seeding and culturing. *Acta Biomaterialia*, 6(11):4208–4217.
- Moe, S. T. (1993). *Superswelling Alginate Gels – Preparation and Some Physical Properties*. PhD thesis, Department of Biotechnology, NTH.
- Moe, S. T., Skjåk-Bræk, G., Elgsæter, A., and Smidsrød, O. (1993). Swelling of covalently crosslinked alginate gels: influence of ionic solutes and non-polar solvents. *Macromolecules*, 26(14):3589–3597.
- Mørch, Y. A. (2008). *Novel Alginate Microcapsules for Cell Therapy—A study of the structure-function relationships in native and structurally engineered alginates*. PhD thesis, Fakultet for naturvitenskap og teknologi, NTNU.
- Mørch, Y. A., Donati, I., Strand, B. L., and Skjåk-Bræk, G. (2006). Effect of Ca^{2+} , Ba^{2+} , and Sr^{2+} on alginate microbeads. *Biomacromolecules*, 7(5):1471–1480.
- Mørch, Y. A., Qi, M., Gundersen, P. O. M., Formo, K., Lacik, I., Skjåk-Bræk, G., Oberholzer, J., and Strand, B. L. (2012). Binding and leakage of barium in alginate microbeads. *Journal of Biomedical Materials Research Part A*, 100(11):2939–2947.
- Mori, S. and Barth, H. G. (1999). *Size exclusion chromatography*. Springer.
- Murphy, D. B. and Davidson, M. W. (2013). Chapter 13: Confocal laser scanning microscopy. In *Fundamentals of Light Microscopy and Electronic Imaging, (2nd ed.)*, pages 265–305. John Wiley and Sons, Inc., Hoboken, NJ USA.

-
- Nelson, W. L. and Cretcher, L. H. (1930). The isolation and identification of d-mannuronic acid lactone from the macrocystis pyriferia. *Journal of the American Chemical Society*, 52(5):2130–2132.
- Olivier, T. and Moine, B. (2013). Confocal laser scanning microscopy. In *Optics in Instruments: Applications in Biology and Medicine*, pages 1–77. John Wiley and Sons, Inc., Hoboken, NJ USA.
- Orive, G., Tam, S. K., Pedraz, J. L., and Hallé, J.-P. (2006). Biocompatibility of alginate–poly-l-lysine microcapsules for cell therapy. *Biomaterials*, 27(20):3691–3700.
- Ornitz, D. M. and Itoh, N. (2001). Fibroblast growth factors. *Genome Biol*, 2(3):1–12.
- Paddock, S. W. (2000). Principles and practices of laser scanning confocal microscopy. *Molecular biotechnology*, 16(2):127–149.
- Peppas, N., Bures, P., Leobandung, W., and Ichikawa, H. (2000). Hydrogels in pharmaceutical formulations. *European journal of pharmaceuticals and biopharmaceutics*, 50(1):27–46.
- Podzimek, S. (2003). The use of gpc coupled with a multiangle laser light scattering photometer for the characterization of polymers. on the determination of molecular weight, size and branching. *Journal of applied polymer science*, 54(1):91–103.
- Podzimek, S. (2011). *Light scattering, size exclusion chromatography and asymmetric flow field flow fractionation: powerful tools for the characterization of polymers, proteins and nanoparticles*. John Wiley & Sons.
- Polyak, B., Geresh, S., and Marks, R. S. (2004). Synthesis and characterization of a biotin-alginate conjugate and its application in a biosensor construction. *Biomacromolecules*, 5(2):389–396.
- Rastello De Boisseson, M., Leonard, M., Hubert, P., Marchal, P., Stequert, A., Castel, C., Favre, E., and Dellacherie, E. (2004). Physical alginate hydrogels based on hydrophobic or dual hydrophobic/ionic interactions: Bead formation, structure, and stability. *Journal of colloid and interface science*, 273(1):131–139.

-
- Rokstad, A. M., Brekke, O.-L., Steinkjer, B., Ryan, L., Kolláriková, G., Strand, B. L., Skjåk-Bræk, G., Lacík, I., Espevik, T., and Mollnes, T. E. (2011). Alginate microbeads are complement compatible, in contrast to polycation containing microcapsules, as revealed in a human whole blood model. *Acta biomaterialia*, 7(6):2566–2578.
- Ronghua, H., Yumin, D., and Jianhong, Y. (2003). Preparation and in vitro anticoagulant activities of alginate sulfate and its quaterized derivatives. *Carbohydrate polymers*, 52(1):19–24.
- Rowley, J. A., Madlambayan, G., and Mooney, D. J. (1999a). Alginate hydrogels as synthetic extracellular matrix materials. *Biomaterials*, 20(1):45–53.
- Rowley, J. A., Madlambayan, G., and Mooney, D. J. (1999b). Alginate hydrogels as synthetic extracellular matrix materials. *Biomaterials*, 20(1):45–53.
- Sandford, P. A., Cottrell, I. W., and Pettitt, D. J. (1984). Microbial polysaccharides: New products and their commercial applications. *Pure and Appl. Chem.*, 56(7):879–892.
- Schlessinger, J., Plotnikov, A. N., Ibrahimi, O. A., Eliseenkova, A. V., Yeh, B. K., Yayon, A., Linhardt, R. J., and Mohammadi, M. (2000). Crystal structure of a ternary fgf-fgfr-heparin complex reveals a dual role for heparin in fgfr binding and dimerization. *Molecular cell*, 6(3):743–750.
- Shapiro, H. M. (2005). *Practical flow cytometry*. John Wiley & Sons.
- Sherbrock-Cox, V., Russell, N. J., and Gacesa, P. (1984). The purification and chemical characterisation of the alginate present in extracellular material produced by mucoid strains of pseudomonas aeruginosa. *Carbohydrate Research*, 135(1):147 – 154.
- Shoichet, M. S., Li, R. H., White, M. L., and Winn, S. R. (1996). Stability of hydrogels used in cell encapsulation: An in vitro comparison of alginate and agarose. *Biotechnology and bioengineering*, 50(4):374–381.
- Shriver, Z., Capila, I., Venkataraman, G., and Sasisekharan, R. (2012). Heparin and heparan sulfate: analyzing structure and microheterogeneity. In *Heparin-A Century of Progress*, pages 159–176. Springer.

-
- Skjåk-Bræk, G., Grasdalen, H., and Smidsrød, O. (1989). Inhomogeneous polysaccharide ionic gels. *Carbohydrate polymers*, 10(1):31–54.
- Skjåk-Bræk, G., Smidsrød, O., and Larsen, B. (1986). Tailoring of alginates by enzymatic modification; *in vitro*. *International Journal of Biological Macromolecules*, 8(6):330–336.
- Smetana Jr, K. (1993). Cell biology of hydrogels. *Biomaterials*, 14(14):1046–1050.
- Smidsrød, O. (1974). Molecular basis for some physical properties of alginates in the gel state. *Faraday discussions of the Chemical Society*, 57:263–274.
- Smidsrød, O., Haug, A., and Larsen, B. (1966). The influence of pH on the rate of hydrolysis of acidic polysaccharides. *Acta Chem. Scand*, 20(4).
- Smidsrød, O., Haug, A., and Lian, B. (1972). Properties of poly (1, 4-hexuronates) in the gel state. i. evaluation of a method for the determination of stiffness. *Acta Chemica Scandinavica*, 26(1):71–78.
- Smidsrød, O. and Moe, S. T. (2008). *Biopolymer Chemistry*. Akademika Publishing.
- Smidsrød, O. and Skjåk-Bræk, G. (1990). Alginate as immobilization matrix for cells. *Trends in Biotechnology*, 8(0):71 – 78.
- Strand, B. L., Mørch, Y. A., Espevik, T., and Skjåk-Bræk, G. (2003a). Visualization of alginate–poly-l-lysine–alginate microcapsules by confocal laser scanning microscopy. *Biotechnology and bioengineering*, 82(4):386–394.
- Strand, B. L., Mørch, Y. A., Syvertsen, K. R., Espevik, T., and Skjåk-Bræk, G. (2003b). Microcapsules made by enzymatically tailored alginate. *Journal of Biomedical Materials Research Part A*, 64(3):540–550.
- Thomas, R. (2013). *Practical guide to ICP-MS: a tutorial for beginners (3rd ed.)*. CRC press.
- Thu, B., Bruheim, P., Espevik, T., Smidsrød, O., Soon-Shiong, P., and Skjåk-Bræk, G. (1996). Alginate polycation microcapsules: ii. some functional properties. *Biomaterials*, 17(11):1069–1079.

-
- Türk, H., Haag, R., and Alban, S. (2004). Dendritic polyglycerol sulfates as new heparin analogues and potent inhibitors of the complement system. *Bioconjugate chemistry*, 15(1):162–167.
- Vold, I. M. N., Kristiansen, K. A., and Christensen, B. E. (2006). A study of the chain stiffness and extension of alginates, in vitro epimerized alginates, and periodate-oxidized alginates using size-exclusion chromatography combined with light scattering and viscosity detectors. *Biomacromolecules*, 7(7):2136–2146.
- Wang, W., Huang, X.-J., Cao, J.-D., Lan, P., and Wu, W. (2014). Immobilization of sodium alginate sulfates on polysulfone ultrafiltration membranes for selective adsorption of low-density lipoprotein. *Acta biomaterialia*, 10(1):234–243.
- Yang, J.-S., Xie, Y.-J., and He, W. (2011). Research progress on chemical modification of alginate: A review. *Carbohydrate polymers*, 84(1):33–39.
- Yoon, H. S. and Katz, J. L. (1976). Ultrasonic wave propagation in human cortical bone—ii. measurements of elastic properties and microhardness. *Journal of Biomechanics*, 9(7):459 – 464.
- Zhao, X., Yu, G., Guan, H., Yue, N., Zhang, Z., and Li, H. (2007). Preparation of low-molecular-weight polyguluronate sulfate and its anticoagulant and anti-inflammatory activities. *Carbohydrate polymers*, 69(2):272–279.



Appendices

A. Risk Assessment

A risk assessment was conducted prior to the master project, to identify potential hazards associated with the work in the biopolymer laboratory.

The risk assessment consists of two parts, the first being a list identifying activities that should be assessed, along with already existing measures to prevent damage, existing documentation on the matter and important additional information.

The second part is the actual risk assessment of the previous listed activities, including possible hazards, the probability for them to happen, the severity and consequences of such an event, and measures that should be taken to avoid such an episode. The combined values from the evaluation of probability and consequences of an unwanted event, make up a risk value, where different values come with different requirements for measures to be taken.



NU	Hazardous activity identification process				Prepared by HSE section	Number HMSRV-26/01	Date 01.12.2006
					Approved by The Rector	Page 1 out of 2	Replaces 15.12.2003
HSE							

Unit: IBT Biopolymer chemistry
 Participants in the identification process (including their function): Ann-Sissel Uiset (Senior engineer), Marit Syversveen, PhD, Wenche Iren Strand (Senior engineer), Marianne Dalheim (PhD student), Berit L. Strand (researcher), Øystein Arlov (PhD student)

Date: 06/01 2014

Short description of the main activity/main process: Specialization Project – Sulfation of alginate and study of chemical and physical properties

ID nr	Activity/process	Responsible person	Existing documentation	Existing safety measures	Laws, regulations etc.	Comment
1	Freeze drying		Manual + procedure	Safety goggles Nitrile-gloves when handling vacuum-oil Disposal of waste oil		Training required
2	Concentrated acids/bases		Material Safety data sheet	Safety goggles, nitrile gloves, fume hood.	NTNU HSE guidelines regarding working with chemicals	New procedure regarding chemical spills will come soon.
3	Chemical modification of alginate: Sulfation with formamide and chlorosulfonic acid		Material Safety data sheet	Safety goggles, nitrile gloves, lab coat, fume hood or fume point.. Waste/solutions are collected for disposal. Chemicals are kept in a ventilated chemical cabinet The door to the lab is locked.	NTNU HSE guidelines regarding working with chemicals	Students are given material and safety data sheets regarding the chemicals that will be used, and are given a thorough review of the experiment before startup. Training in how to work the valve is recommended.
4	Gas flasks/tanks			Secured by chains to prevent tilting.		

	<h3>Hazardous activity identification process</h3>				<table border="1"> <tr> <td>Prepared by</td> <td>Number</td> <td>Date</td> </tr> <tr> <td>HSE section</td> <td>HMSRV-26/01</td> <td>01.12.2006</td> </tr> <tr> <td>Approved by</td> <td>Page</td> <td>Replaces</td> </tr> <tr> <td>The Rector</td> <td>2 out of 2</td> <td>15.12.2003</td> </tr> </table>	Prepared by	Number	Date	HSE section	HMSRV-26/01	01.12.2006	Approved by	Page	Replaces	The Rector	2 out of 2	15.12.2003	
Prepared by	Number	Date																
HSE section	HMSRV-26/01	01.12.2006																
Approved by	Page	Replaces																
The Rector	2 out of 2	15.12.2003																
5	Work with liquid N ₂		Regulation for filling and transportation of liquid nitrogen	<p>Safety goggles, thick gloves (thermo resistant), Footwear must be easy to remove, avoid boots with wide openings to avoid N₂ accumulation inside the boot. Use specified containers for transportation.</p>	<p>NTNU HSE guidelines regarding working with chemicals and gasses.</p>	<p>Training required See separate risk assessment for transportation of N₂ in K1...</p>												

NTNU	Risk assessment		Prepared by	Number	Date
			HSE section	HMSRV/2603E	04.02.2011
HSE/KS			Approved by	Page	Replaces
			The Rector	3 out of 3	01.12.2006



Unit: IBT -Biopolymer chemistry

Date: 27.08.2013

Line manager: Kjetil Rasmussen

Updated 24.10.2012 and 06.09.2013

Participants in the risk assessment (including their function): Ann-Sissel Uiset (Senior engineer), Marit Syversveen (PhD og Wenche Iren Strand (Senior engineer)

ID nr	Activity from the identification process form	Potential undesirable incident/strain	Likelihood: (1-5)	Consequence:		Risk value	Comments/status
				Human (A-E)	Environment (A-E)		
1	Freeze-drying	Cuts/injuries as a result of imploding flasks	2	A	A	B2	Use gloves when handling vacuum-oil
		Exposure to harmful oil vapor	4	A	A	B4	Avoid vapor in room?
2	Concentrated acids/bases	Chemical burns	2	A	A	B2	
3	Chemical modification of alginate	Inhalation of carcinogenic or toxic substances, or exposure to chemicals that can cause fetal damage.	1	D	B	D1	The largest risk is during weighing the substances, therefore point ventilation and protective masks have to be used. Sulfation involves exothermic reactions, so reagents have to be mixed carefully, and inside a fume hood.

NTNU	Risk assessment		Prepared by	Number	Date
 HSE/KS			HSE section	HMSRV/2603E	04.02.2011
			Approved by	Page	Replaces
			The Rector	4 out of 3	01.12.2006



			1	B	A	A	A	B1	
4	Gas flasks/tanks	Exposure to concentrated acid. Personal injury due to tilting gas-flasks/tanks. (also explosion)	1	B	A	B	A	B1	
5	Working with liquid N2	Frostbite	2	C	A	A	B	C2	Follow rules for filling bottles and transportation.
		Suffocation	1	E	A	A	E	E1	Oxygen measurements/ gas alarm?

Likelihood, e.g.:

1. Minimal
2. Low
3. Medium
4. High
5. Very high

Consequence, e.g.:

- A. Safe
- B. Relatively safe
- C. Dangerous
- D. Critical
- E. Very critical

Risk value (each one to be estimated separately):

- Human = Likelihood x Human Consequence
 Environmental = Likelihood x Environmental consequence
 Financial/material = Likelihood x Consequence for Economy/material

NTNU		Risk assessment		Prepared by	Number	Date
				HSE section	HMSRV/2603E	04.02.2011
HSE/KS				Approved by	Page	Replaces
				The Rector	5 out of 3	01.12.2006



Potential undesirable incident/strain

Identify possible incidents and conditions that may lead to situations that pose a hazard to people, the environment and any material/equipment involved.

Criteria for the assessment of likelihood and consequence in relation to fieldwork

Each activity is assessed according to a worst-case scenario. Likelihood and consequence are to be assessed separately for each potential undesirable incident. Before starting on the quantification, the participants should agree what they understand by the assessment criteria:

Likelihood

Minimal 1	Low 2	Medium 3	High 4	Very high 5
Once every 50 years or less	Once every 10 years or less	Once a year or less	Once a month or less	Once a week

Consequence

Grading	Human	Environment	Financial/material
E Very critical	May produce fatality/ies	Very prolonged, non-reversible damage	Shutdown of work > 1 year.
D Critical	Permanent injury, may produce serious health damage/sickness	Prolonged damage. Long recovery time.	Shutdown of work 0.5-1 year.
C Dangerous	Serious personal injury	Minor damage. Long recovery time	Shutdown of work < 1 month
B Relatively safe	Injury that requires medical treatment	Minor damage. Short recovery time	Shutdown of work < 1week
A Safe	Injury that requires first aid	Insignificant damage. Short recovery time	Shutdown of work < 1day


The unit makes its own decision as to whether opting to fill in or not consequences for economy/material, for example if the unit is going to use particularly valuable equipment. It is up to the individual unit to choose the assessment criteria for this column.

Risk = Likelihood x Consequence

Please calculate the risk value for "Human", "Environment" and, if chosen, "Economy/material", separately.

About the column "Comments/status, suggested preventative and corrective measures":

Measures can impact on both likelihood and consequences. Prioritize measures that can prevent the incident from occurring; in other words, likelihood-reducing measures are to be prioritized above greater emergency preparedness, i.e. consequence-reducing measures.

NTNU		Risk assessment matrix		Dato	
				08.03.2010	
HMS/IKS				Erstatter	
		utarbeidet av		Nummer	
		HMS-avd.		HMSRV/2604	
		godkjent av		side	
		Rektor		6 av 1	
				09.02.2010	



Risk assessment matrix NTNU

		CONSEQUENCE									
Very serious	E1	E2	E3	E4	E5						
Serious	D1	D2	D3	D4	D5						
Moderate	C1	C2	C3	C4	C5						
Small	B1	B2	B3	B4	B5						
Very small	A1	A2	A3	A4	A5						
	Very small	Small	Moderate	High	Very high						
						PROBABILITY					

Color-coding in the risk assessment matrix

Color	Description
Red	Unacceptable risk. Measures must be implemented to reduce risk.
Yellow	Evaluation area. Evaluate whether measures need to be implemented.
Grønn	Acceptable risk. Measures may be considered based on other factors.

B. Calculation of the Degree of Sulfation from Elemental Analysis Data

The data from the elemental analysis using HR-ICP-MS are given as $\frac{\mu\text{g sulfur}}{\text{g sample}}$, which can easily be converted to the weight fraction of sulfur (% S) in the sample. To calculate the degree of sulfation (DS), the average number of sulfate groups attached to each alginate monosaccharide, a standard curve was constructed to give the relationship between % S and DS.

The standard curve was constructed by calculating % S for a range of theoretical values of DS. The maximum theoretical value for DS is 2, corresponding to the replacement of both the free hydroxyl groups of a monosaccharide in the polymer chain with sulfur groups. An example calculation for DS = 1 is given in Equation B.1 to B.6. For calculations of average molecular weight of a monosaccharide it was assumed that one water molecule is associated with each monosaccharide, and that a sodium ion is associated with each carboxylgroup and sulfate group.

$$M_w = C_6O_6H_5 + H_2O + (1 + DS) \times Na^+ + DS \times SO_3^- \quad (\text{B.1})$$

$$M_w = 173 \text{ g/mol} + 18 \text{ g/mol} + (1 + 1) \times 23 \text{ g/mol} + 1 \times 80 \text{ g/mol} \quad (\text{B.2})$$

$$M_w = 317 \text{ g/mol} \quad (\text{B.3})$$

$$\%S = \frac{DS \times M_S}{M_w} \times 100\% \quad (\text{B.4})$$

$$\%S = \frac{1 \times 32 \text{ g/mol}}{317 \text{ g/mol}} \times 100\% \quad (\text{B.5})$$

$$\%S = 10.1\% \quad (\text{B.6})$$

The calculated values for the standard curve are all given in Table B.1.

Table B.1: The calculated values of % S for theoretical DS values in the range 0 to 2, used in the standard curve.

DS	M_w	% S
2.00	420.0	15.2
1.75	394.3	14.2
1.50	368.5	13.0
1.25	342.8	11.7
1.00	317.0	10.1
0.75	291.3	8.2
0.50	265.5	6.0
0.25	239.8	3.3
0.00	214.0	0.0

Using the values from Table B.1, the standard curve was constructed by plotting % S as a function of DS. A second degree polynomial was fitted to the curve, as shown in Figure B.1. The second degree polynomial allows for the calculation of an approximate value of DS when the % S is known.

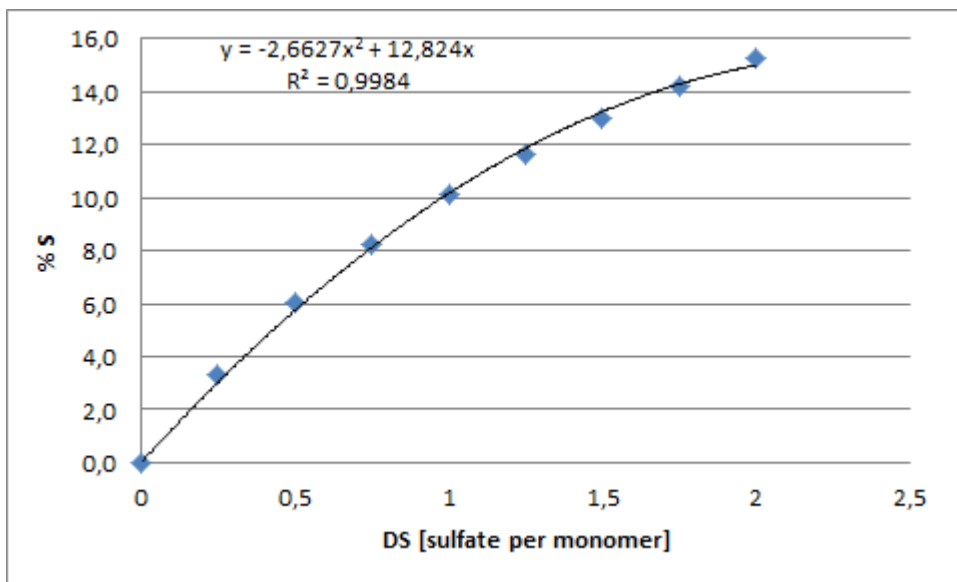


Figure B.1: *The standard curve for the relationship between % S and the degree of sulfation (DS), constructed from the values in Table B.1. A second order polynomial is fitted to the curve, with the formula shown in the figure.*

The DS can thus be calculated from the % S values from the elemental analysis by use of the formula given in Equation B.7.

$$DS = \frac{-12.824 + \sqrt{12.824^2 - 4 \times 2.6627 \times \%S}}{-2 \times 2.6627} \quad (\text{B.7})$$



C. The Young's Modulus of Gels Made from Sulfated Alginate of Varying DS

From earlier work on my specialization project at the Department of Biotechnology, NTNU, the Young's moduli of samples containing only sulfated alginate with different degrees of sulfation have been calculated. These results were used to compare the effect of using mixtures instead of homogeneous samples on the gel strength.

This Appendix contains the calculated Young's modulus for each sample of a different DS, both before and after correction for syneresis, along with the standard deviation and the coefficient of variation for the corrected Young's modulus, all given in Table C.1.

Table C.1: The calculated Young's modulus for samples of alginate-sulfate with varying DS, both before and after correction for syneresis (E and E_{corr} respectively), along with the standard deviation (std) and the coefficient of variation (CoV) for the corrected Young's modulus. All results are from the specialization project.

DS	E [kPa]	E_{corr} [kPa]	$std_{E_{corr}}$ [kPa]	CoV
0.01	232	100	9	0.09
0.27	135	62	6	0.10
0.59	72	38	4	0.11
0.66	44	26	4	0.14
0.68	64	38	7	0.20
0.86	35	20	4	0.19
0.90	25	16	4	0.24

D. Calculating the Pseudo First Order Rate Constant of Acid Hydrolysis

Sulfated alginate samples of DS 0.27 and DS 0.90 were together with an unmodified sample of alginate LF200S subjected to acid hydrolysis in a time series. The calculated weight average molecular weights of the samples from analysis using SEC-MALLS were used to find the pseudo first order rate constant.

For the calculations, the molecular weights of the single monosaccharides, M_0 in each sample were required. They were calculated as shown in Equation D.1 and Equation D.2, assuming one sodium ion associated with each monomer, and an extra ion for each sulfate group on the monomer.

$$M_0 = C_6O_6H_7 + SO_3 \times DS + Na^+ \times (1 + DS) \quad (D.1)$$

$$175 \frac{g}{mol} + 80 \frac{g}{mol} \times DS + 23 \frac{g}{mol} \times (1 + DS) \quad (D.2)$$

The calculated values of M_0 for each sample are given in Section 3.2.1.

Table D.1 shows the calculated values of $\frac{1}{M_w}$ and the degree of polymerisation, DP_w for the sample of unmodified alginate. The same results for the sulfated samples are shown in Table D.2 and Table D.3.

Table D.1: The weight average molecular weights of the unmodified alginate sample after acid hydrolysis for a time series, along with the calculated value of $\frac{1}{M_w}$ and the degree of polymerisation, DP_w .

LF200S			
Time [min]	M_w [kDa]	$\frac{1}{M_w}$	DP_w
0	284	3.5E-03	1326
10	229	4.4E-03	1072
20	204	4.9E-03	953
30	196	5.1E-03	917
50	157	6.4E-03	735
100	114	8.7E-03	534
150	93	1.1E-02	434
200	81	1.2E-02	380

Table D.2: The weight average molecular weights of the sulfated alginate sample with DS 0.27 after acid hydrolysis for a time series, along with the calculated value of $\frac{1}{M_w}$ and the degree of polymerisation, DP_w .

DS 0.27			
Time [min]	M_w [kDa]	$\frac{1}{M_w}$	DP_w
0	159	6.3E-03	658
10	152	6.6E-03	629
20	135	7.4E-03	558
30	127	7.9E-03	525
50	95	1.1E-02	393
100	68	1.5E-02	281
150	53	1.9E-02	219
200	44	2.3E-02	182

Table D.3: The weight average molecular weights of the sulfated alginate sample with DS 0.90 after acid hydrolysis for a time series, along with the calculated value of $\frac{1}{M_w}$ and the degree of polymerisation, DP_w .

DS 0.90			
Time [min]	M_w [kDa]	$\frac{1}{M_w}$	DP_w
0	161	6.2E-03	525
10	139	7.2E-03	453
20	131	7.6E-03	427
30	109	9.2E-03	355
50	92	1.1E-02	300
100	67	1.5E-02	218
150	50	2.0E-02	163
200	44	2.3E-02	143

The plot of $\frac{1}{M_w}$ against time is shown in Figure 3.2.1 in Section 3.2.1.

E. Data From the Swelling of Alginate Beads in NaCl

E.1 Sulfated Alginate Samples

Alginate gel beads were made by use of external gelation with 50 mM CaCl_2 for sulfated alginate samples of DS 0.27, DS 0.59, DS 0.79 and unmodified alginate LF200S. The beads were submitted to treatments with 18 ml 0.9 % (w/v) NaCl every hour. The number of beads and the average diameter for the beads of each sample were measured between every treatment. This Appendix contains the measured number of beads, average diameter and average increase in volume for the beads between every treatment with 0.9 % (w/v) NaCl.

The number of beads made from different alginate samples at every measurement point is shown in Table E.1.1. The average diameter of the beads can be found in Table E.1.2, while the average increase in volume over time is found in Table E.1.3.

Table E.1.1: The number of beads made from samples of alginate of different DS after subsequent 1 hour treatments with 0.9 % NaCl.

Number of Treatments	Number of Alginate Beads		
	LF200S	DS 0.27	DS 0.59
0	53	53	53
1	53	53	49
2	53	53	20
3	53	53	0
4	52	44	0
5	52	24	0
6	52	9	0
7	50	0	0

Table E.1.2: The average diameter of beads made from samples of alginate of different DS after subsequent 1 hour treatments with 0.9 % NaCl.

Number of Treatments	Average Diameter of Alginate Beads [mm]		
	LF200S	DS 0.27	DS 0.59
0	3.49	3.55	3.21
1	3.51	3.57	3.20
2	3.57	3.71	3.70
3	3.74	3.92	
4	3.92	4.09	
5	4.06	4.42	
6	4.10	4.56	
7	4.64		

Table E.1.3: The average increase in volume of beads made from samples of alginate of different DS after subsequent 1 hour treatments with 0.9 % NaCl.

Number of treatments	Relative Increase in Volume [%]		
	LF200S	DS 0.27	DS 0.59
0	0	0	0
1	2	2	-1
2	7	14	53
3	23	35	
4	42	53	
5	57	93	
6	62	112	
7	135		

A graphical representation of the number and the average increase in volume as a function of the number of treatments can be found in Figure 3.3.1 and Figure 3.3.2 in Section 3.3.1.

E.2 Alginate/Alginate-Sulfate Mixtures, CaCl_2

Alginate gel beads were made by use of external gelation with 50 mM CaCl_2 for mixtures of sulfated alginate of DS 0.68 or DS 0.90 with unmodified alginate LF200S. The beads were submitted to treatments with 18 ml 0.9 % (w/v) NaCl every hour. The number of beads and the average diameter for the beads of each sample were measured between every treatment. This Appendix contains the measured number of beads, average diameter and average increase in volume for the beads between every treatment with 0.9 % (w/v) NaCl.

Alginate/Alginate-Sulfate Mixtures using a DS 0.90 Alginate

The number of Ca-alginate beads made from DS 0.90/LF200S mixtures at different proportions, at every measurement point is shown in Table E.2.1. The average diameter of the beads can be found in Table E.2.2, while the average increase in volume over time is found in Table E.2.3.

Table E.2.1: The number of Ca-alginate beads made from alginate DS 0.90/LF200S mixtures after each treatment with 0.9 % NaCl.

Number of Measurements	Number of Alginate Beads				
	0 %	20 %	40 %	60 %	80 %
0	50	50	50	50	50
1	50	50	50	50	50
2	50	50	50	50	42
3	50	50	50	49	28
4	50	50	49	46	8
5	50	50	47	33	1
6	50	50	47	28	0
7	50	50	39	17	
8	48	50	31	6	
9	40	49	14	0	
10	27	49	7		
11	10	45	1		
12	5	42	0		
13	0	37			
14		7			
15		3			
16		0			

Table E.2.2: The average diameter of Ca-alginate beads made from alginate DS 0.90/LF200S mixtures after each treatment with 0.9 % NaCl.

Number of Treatments	Average Diameter of Alginate Beads [mm]				
	0 %	20 %	40 %	60 %	80 %
0	3.82	3.94	3.38	3.60	3.26
1	3.76	3.84	3.42	3.56	3.40
2	3.84	3.90	3.58	3.72	3.62
3	4.04	4.04	3.72	4.00	3.93
4	4.22	4.18	3.88	4.15	4.25
5	4.32	4.34	4.00	4.45	
6	4.56	4.36	4.15	4.43	
7	4.60	4.52	4.26	5.35	
8	4.73	4.60	4.42	5.33	
9	5.13	4.80	4.64		
10	5.11	4.90	5.29		
11	5.30	4.93	5.50		
12	5.40	4.95			
13		5.05			
14		5.57			
15		5.67			

Table E.2.3: The average increase in volume of Ca-alginate beads made from alginate DS 0.90/LF200S mixtures after each treatment with 0.9 % NaCl.

Number of Treatments	Relative Increase in Volume of Alginate Beads [%]				
	0 %	20 %	40 %	60 %	80 %
0	0	0	0	0	0
1	-5	-7	4	-3	13
2	2	-3	19	10	37
3	18	8	33	37	75
4	35	19	51	53	122
5	45	34	66	89	261
6	70	36	85	86	
7	75	51	100	229	
8	90	59	124	225	
9	141	80	159		
10	140	92	282		
11	167	96	331		
12	182	99			
13		111			
14		183			
15		198			

A graphical representation of the number and the average increase in volume as a function of the number of treatments can be found in Figure 3.3.3 and Figure 3.3.4 in Section 3.3.2.

Alginate/Alginate-Sulfate Mixtures using a DS 0.68 Alginate

The number of beads made from DS 0.68/LF200S mixtures at different proportions, at every measurement point is shown in Table E.2.4. The average diameter of the beads can be found in Table E.2.5, while the average increase in volume over time is found in Table E.2.6.

Table E.2.4: The number of Ca-alginate beads made from alginate DS 0.68/LF200S mixtures after each treatment with 0.9 % NaCl.

Number of Treatments	Number of Alginate Beads					
	0 %	20 %	40 %	60 %	80 %	100 %
0	50	50	50	50	50	50
1	50	50	50	50	50	42
2	50	50	50	50	50	9
3	50	50	50	50	50	0
4	50	50	50	50	40	0
5	50	50	50	50	15	0
6	50	50	50	50	3	0
7	46	50	50	50	0	0
8	45	50	50	45	0	0
9	42	50	49	30	0	0
10	31	47	47	16	0	0
11	8	45	40	5	0	0
12	0	33	20	0	0	0
13	0	8	0	0	0	0
14	0	4	0	0	0	0
15	0	0	0	0	0	0

Table E.2.5: The average diameter of Ca-alginate beads made from alginate DS 0.68/LF200S mixtures after each treatment with 0.9 % NaCl.

Number of Treatments	Average Diameter of Alginate Beads [mm]					
	0 %	20 %	40 %	60 %	80 %	100 %
0	3.64	3.48	3.54	3.64	3.52	2.96
1	3.64	3.5	3.54	3.68	3.58	3.29
2	3.74	3.58	3.64	3.76	3.84	3.67
3	3.86	3.74	3.78	3.96	4.06	
4	4.02	3.88	3.92	4.14	4.30	
5	4.12	4.02	4.06	4.28	4.93	
6	4.30	4.06	4.2	4.52	5.33	
7	4.48	4.22	4.34	4.56		
8	4.56	4.30	4.50	4.69		
9	4.64	4.40	4.45	4.73		
10	4.71	4.45	4.57	5.19		
11	5.13	4.56	4.65	5.20		
12		4.85	5.1			
13		5.13				
14		5.75				

Table E.2.6: The average increase in volume of Ca-alginate beads made from alginate DS 0.68/LF200S mixtures after each treatment with 0.9 % NaCl.

Treatment number	Relative Increase in Volume of Alginate Beads [%]					
	0 %	20 %	40 %	60 %	80 %	100 %
0	0	0	0	0	0	0
1	0	2	0	3	5	37
2	8	9	9	10	30	90
3	19	24	22	29	53	
4	35	39	36	47	82	
5	45	54	51	63	175	
6	65	59	67	91	248	
7	86	78	84	97		
8	96	89	105	114		
9	108	102	99	120		
10	117	109	116	189		
11	179	124	127			
12		170	199			
13		219				
14		351				

A graphical representation of the number and the average increase in volume as a function of the number of treatments can be found in Figure 3.3.5 and Figure 3.3.6 in Section 3.3.2.

E.3 Beads from Alginate/Alginate-Sulfate Mixtures Gelled with BaCl₂

To investigate whether gelation with BaCl₂ would give the same results with respect to the 0 % sample and the 20 % sample for the DS 0.90/LF200S beads as gelation with CaCl₂, the experiment was repeated using 50 mM BaCl₂ in the gelation bath. The data from this experiment are given below.

The number of beads from each sample of DS 0.90/LF200S mixtures, counted between every measurement is shown in Table E.3.1. The measured average diameter of the beads and the average increase in volume of the beads are given in Table E.3.2 and Table E.3.3.

Table E.3.1: The number of Ba-alginate beads made from alginate DS 0.90/LF200S mixtures after each treatment with 0.9 % NaCl.

Treatment Number	Average Increase in Diameter of Ba-Alginate Beads [%]					
	0 %	20 %	40 %	60 %	80 %	100 %
0	50	50	50	50	50	50
1	50	50	50	50	50	50
2	50	50	50	50	50	50
3	50	50	50	50	50	48
4	50	50	50	50	50	48
5	50	50	50	50	50	48
6	50	50	50	50	49	47
7	50	50	50	50	49	47
8	50	50	50	50	49	45
9	50	50	50	50	49	44
10	50	50	50	50	49	44
11	50	50	50	50	49	40
12	50	50	50	50	49	28
13	50	50	50	50	49	21
14	50	50	50	50	49	2
15	50	50	50	50	49	1

Continued on next page

Table E.3.1 – continued from previous page

Treatment Number	Relative Increase in Volume of Ba-Alginate Beads [%]					
	0 %	20 %	40 %	60 %	80 %	100 %
16	50	50	50	50	49	0
17	50	50	50	50	42	0
18	50	50	50	50	33	0
19	50	50	50	50	28	0
20	50	50	50	50	13	0
21	50	50	50	50	8	0
22	50	50	50	50	6	0
23	50	50	50	50	5	0
24	50	50	50	50	1	0
25	50	50	50	50	0	0
26	50	50	50	47	0	0
27	50	50	50	46	0	0
28	50	50	50	45	0	0
29	50	50	50	45	0	0
30	50	50	50	40	0	0
31	50	50	50	38	0	0
32	50	50	50	38	0	0
33	50	50	50	37	0	0
34	50	50	50	32	0	0
35	50	50	50	30	0	0
36	50	50	50	28	0	0
37	50	50	50	25	0	0
38	50	50	50	21	0	0
39	50	50	50	19	0	0
40	50	50	50	11	0	0
41	50	50	50	11	0	0
42	50	50	50	4	0	0
43	50	50	50	2	0	0
44	50	50	50	1	0	0
45	50	50	50	0	0	0
46	50	50	50	0	0	0

Continued on next page

Table E.3.1 – continued from previous page

Treatment Number	Relative Increase in Volume of Ba-Alginate Beads [%]					
	0 %	20 %	40 %	60 %	80 %	100 %
47	50	50	50	0	0	0
48	50	50	49	0	0	0
49	50	50	49	0	0	0
50	50	49	48	0	0	0
51	50	49	47	0	0	0
52	50	49	47	0	0	0
53	50	49	47	0	0	0
54	50	49	47	0	0	0
55	50	48	47	0	0	0
56	50	48	47	0	0	0
57	50	48	47	0	0	0
58	50	48	47	0	0	0
59	50	48	47	0	0	0
60	50	48	47	0	0	0
61	50	48	47	0	0	0
62	50	48	47	0	0	0
63	50	48	47	0	0	0
64	50	48	47	0	0	0
65	50	48	47	0	0	0

Table E.3.2: The average diameter of Ba-alginate beads made from DS 0.90/LF200S mixtures after each treatment with 0.9 % NaCl.

Treatment Number	Average Increase in Diameter of Ba-Alginate Beads [%]					
	0 %	20 %	40 %	60 %	80 %	100 %
0	3.74	3.74	3.88	3.76	3.72	3.92
1	3.74	3.70	3.80	3.76	3.70	3.92
2	3.68	3.70	3.80	3.76	3.66	3.86

Continued on next page

Table E.3.2 – continued from previous page

Treatment Number	Relative Increase in Volume of Ba-Alginate Beads [%]					
	0 %	20 %	40 %	60 %	80 %	100 %
3	3.68	3.70	3.78	3.78	3.62	3.83
4	3.68	3.68	3.76	3.74	3.66	3.86
5	3.70	3.70	3.76	3.84	3.70	3.83
6	3.76	3.76	3.84	3.84	3.73	3.85
7	3.78	3.80	3.88	3.86	3.78	3.87
8	3.80	3.80	3.86	3.86	3.78	3.93
9	3.88	3.80	3.86	3.92	3.88	3.95
10	3.90	3.84	3.92	3.92	3.88	4.09
11	3.90	3.86	3.92	3.94	3.88	4.13
12	3.90	3.86	3.92	3.94	3.98	4.14
13	3.90	3.86	3.92	3.94	3.98	4.33
14	3.92	3.86	3.96	3.96	3.98	4.50
15	3.92	3.88	3.98	3.98	4.00	5.00
16	3.94	3.90	4.00	4.02	4.08	
17	3.96	3.90	4.00	4.02	4.12	
18	3.96	3.92	4.00	4.12	4.09	
19	3.96	3.92	4.02	4.12	4.14	
20	3.98	3.94	4.04	4.12	4.38	
21	4.00	3.96	4.08	4.18	4.50	
22	4.02	3.96	4.08	4.20	4.67	
23	4.06	4.02	4.10	4.32	4.80	
24	4.08	4.04	4.14	4.30	5.00	
25	4.10	4.04	4.14	4.32		
26	4.10	4.06	4.16	4.32		
27	4.12	4.08	4.26	4.37		
28	4.14	4.12	4.26	4.42		
29	4.14	4.12	4.26	4.42		
30	4.14	4.12	4.26	4.40		
31	4.14	4.12	4.26	4.42		
32	4.14	4.12	4.26	4.42		
33	4.14	4.12	4.26	4.43		

Continued on next page

Table E.3.2 – continued from previous page

Treatment Number	Relative Increase in Volume of Ba-Alginate Beads [%]					
	0 %	20 %	40 %	60 %	80 %	100 %
34	4.14	4.12	4.26	4.41		
35	4.14	4.12	4.32	4.43		
36	4.14	4.12	4.28	4.46		
37	4.14	4.08	4.32	4.52		
38	4.14	4.12	4.32	4.48		
39	4.12	4.1	4.32	4.63		
40	4.12	4.10	4.32	4.64		
41	4.12	4.12	4.32	4.64		
42	4.14	4.10	4.32	4.75		
43	4.14	4.12	4.36	5.00		
44	4.14	4.12	4.36	5.00		
45	4.12	4.10	4.40			
46	4.12	4.12	4.40			
47	4.14	4.12	4.40			
48	4.14	4.12	4.41			
49	4.16	4.14	4.41			
50	4.16	4.16	4.42			
51	4.16	4.18	4.43			
52	4.14	4.16	4.43			
53	4.14	4.16	4.43			
54	4.14	4.10	4.43			
55	4.14	4.19	4.43			
56	4.16	4.21	4.43			
57	4.18	4.21	4.43			
58	4.16	4.19	4.43			
59	4.16	4.21	4.43			
60	4.16	4.21	4.43			
61	4.16	4.19	4.43			
62	4.16	4.21	4.43			
63	4.18	4.19	4.45			
64	4.18	4.19	4.43			

Continued on next page

Table E.3.2 – continued from previous page

Treatment Number	Relative Increase in Volume of Ba-Alginate Beads [%]					
	0 %	20 %	40 %	60 %	80 %	100 %
65	4.16	4.19	4.43			

Table E.3.3: The average increase in volume of Ba-alginate beads made from DS 0.90/LF200S mixtures after each treatment with 0.9 % NaCl.

Treatment Number	Relative Increase in Volume of Ba-Alginate Beads [%]					
	0 %	20 %	40 %	60 %	80 %	100 %
0	0	0	0	0	0	0
1	0	-3	-6	0	-2	0
2	-5	-3	-6	0	-5	-5
3	-5	-3	-8	2	-8	-6
4	-5	-5	-9	-2	-5	-5
5	-3	-3	-9	7	-2	-6
6	2	2	-3	7	1	-5
7	3	5	0	8	5	-4
8	5	5	-2	8	5	1
9	12	5	-2	13	13	3
10	13	8	3	13	13	14
11	13	10	3	15	13	17
12	13	10	3	15	22	18
13	13	10	3	15	22	35
14	15	10	6	17	22	51
15	15	12	8	19	24	108
16	17	13	10	22	32	
17	19	13	10	22	36	
18	19	15	10	32	33	
19	19	15	11	32	38	

Continued on next page

Table E.3.3 – continued from previous page

Treatment Number	Relative Increase in Volume of Ba-Alginate Beads [%]					
	0 %	20 %	40 %	60 %	80 %	100 %
20	21	17	13	32	64	
21	22	19	16	37	77	
22	24	19	16	39	97	
23	28	24	18	52	115	
24	30	26	21	50	143	
25	32	26	21	52		
26	32	28	23	52		
27	34	30	32	57		
28	36	34	32	63		
29	36	34	32	63		
30	36	34	32	60		
31	36	34	32	63		
32	36	34	32	63		
33	36	34	32	64		
34	36	34	32	61		
35	36	34	38	64		
36	36	34	34	67		
37	36	30	38	74		
38	36	34	38	69		
39	34	32	38	87		
40	34	32	38	87		
41	34	34	38	87		
42	36	32	38	102		
43	36	34	42	135		
44	36	34	42	135		
45	34	32	46			
46	34	34	46			
47	36	34	46			
48	36	34	47			
49	38	36	47			
50	38	38	47			

Continued on next page

Table E.3.3 – continued from previous page

Treatment Number	Relative Increase in Volume of Ba-Alginate Beads [%]					
	0 %	20 %	40 %	60 %	80 %	100 %
51	38	40	48			
52	36	38	48			
53	36	38	48			
54	36	32	48			
55	36	40	48			
56	38	42	48			
57	40	42	48			
58	38	40	48			
59	38	42	48			
60	38	42	48			
61	38	40	48			
62	38	42	48			
63	40	40	51			
64	40	40	48			
65	38	40	48			

Graphical representations of the number of beads and the relative increase in volume is given in Figure 3.3.7 and Figure 3.3.8 in Section 3.3.3.



F. Data from the Longitudinal Compression Test of Gels

This Appendix contains the data acquired from the longitudinal compression test conducted on alginate gels made from different mixtures of sulfated or partially hydrolysed alginate with unmodified alginate LF200S. The data includes the initial slope obtained from the area of the force-distance plot between 0.4 and 0.5 mm of compression, the measured diameter, height and weight of the gels, and the calculated cross-sectional surface area of the gels.

The force-distance plots for the six gels from the 10 % DS 0.77/LF200S sample are shown in Figure F.1. The two red vertical lines mark the distance between 0.4 and 0.5 mm, used to find the initial slope of each curve. The linear regression lines from this area of the graph are shown in red.

The data for the mixtures between sulfated alginate with a DS of 0.77 and unmodified alginate LF200S in different proportions to each other, are given in Table F.1 to Table F.8. Table F.9, Table F.10 and Table F.11 contain the data for gels made from mixtures between partially hydrolysed alginate and unmodified alginate LF200S.

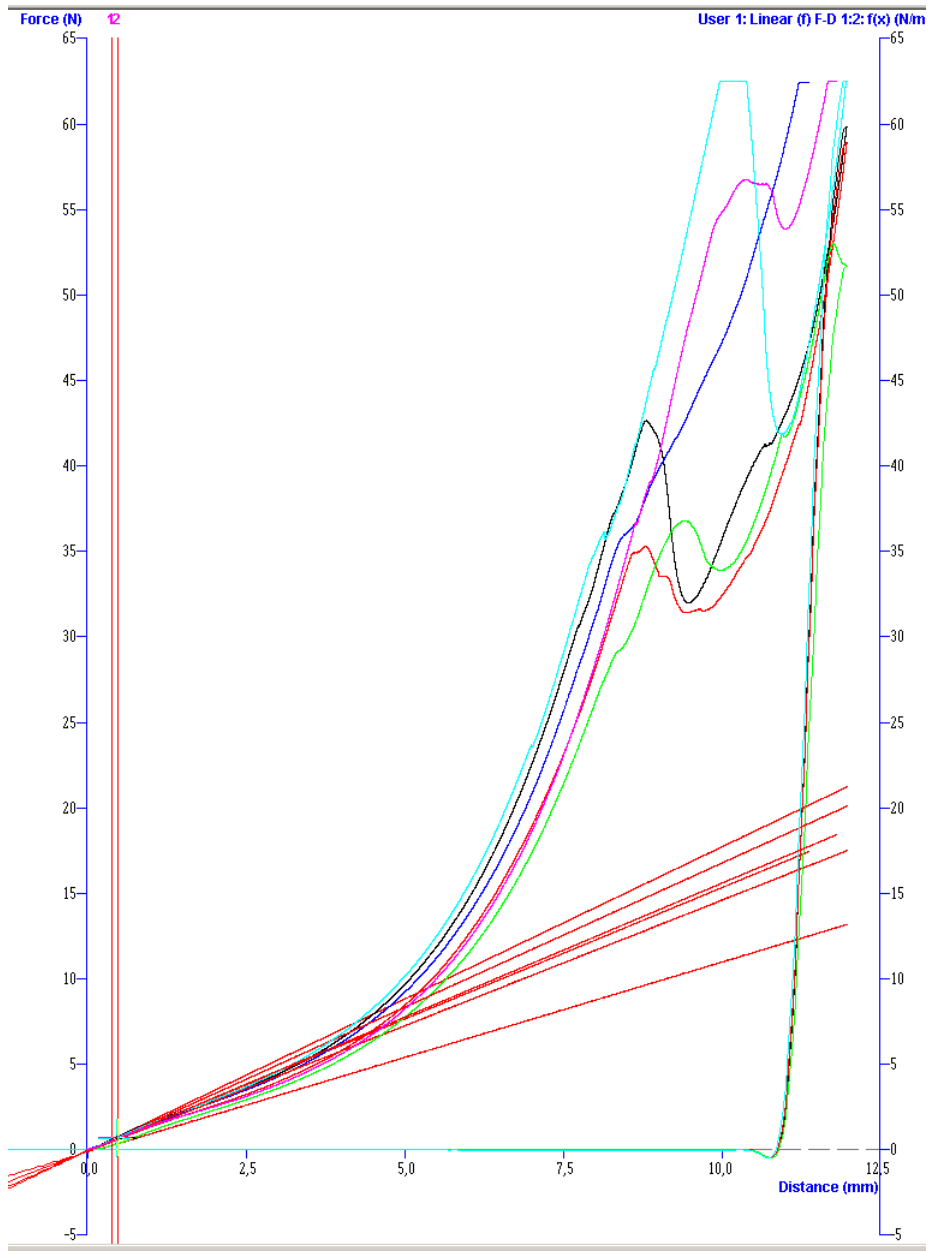


Figure F.1: The force-distance plots for the six gels from the 10 % DS 0.77/LF200S sample, where the red lines are the regression lines fitted to the graphs in the area marked by the two red vertical lines.

Table F.1: The weight of the gels from the 0 % sample of DS 0.77/LF200S before and after syneresis, the measured slope of the initial force-distance plot in the longitudinal compression test, the measured diameter and height of the gels, and the calculated cross-sectional surface area of the gels.

Gel Number	Slope [N/mm]	d [mm]	h[mm]	a [mm ²]	Weight of Gel [g]	
					Before Synere-sis	After Synere-sis
1	2.04	11.41	14.40	102	2.31	1.50
2	2.40	11.27	14.20	100	2.31	1.52
3	2.13	11.23	14.86	99	2.31	1.49
4	2.12	12.12	14.90	115	2.31	1.56
5	2.08	11.49	14.30	104	2.31	1.52
6	2.47	11.54	14.80	105	2.31	1.57
Average	2.21	11.51	14.58	104	2.31	1.53
St.dev	0.18	0.32	0.31	6	0	0.03

Table F.2: The weight of the gels from the 5 % sample of DS 0.77/LF200S before and after syneresis, the measured slope of the initial force-distance plot in the longitudinal compression test, the measured diameter and height of the gels, and the calculated cross-sectional surface area of the gels.

Gel Number	Slope [N/mm]	d [mm]	h[mm]	a [mm ²]	Weight of Gel [g]	
					Before Synere-sis	After Synere-sis
1	2.34	11.40	14.88	102	2.31	1.46
2	1.60	11.00	14.42	95	2.31	1.42
3	2.01	11.09	14.20	97	2.31	1.45
4	2.12	11.20	14.21	99	2.31	1.43
5	1.98	11.24	14.72	99	2.31	1.44
6	1.83	11.30	14.00	100	2.31	1.41
Average	1.98	11.21	14.41	99	2.31	1.44
St.dev	0.25	0.14	0.34	3	0.00	0.02

Table F.3: The weight of the gels from the 10 % sample of DS 0.77/LF200S before and after syneresis, the measured slope of the initial force-distance plot in the longitudinal compression test, the measured diameter and height of the gels, and the calculated cross-sectional surface area of the gels. One of the specimens of the sample was omitted from the calculations as the slope was not linear in the area between 0.4 and 0.5 mm of compression.

Gel Number	Slope [N/mm]	d [mm]	h[mm]	a [mm ²]	Weight of Gel [g]	
					Before Synere-sis	After Synere-sis
1	1.54	11.75	14.42	108	2.31	1.38
2	1.47	11.12	14.32	97	2.31	1.34
3	1.69	11.25	14.22	99	2.31	1.35
4	1.57	11.13	14.74	97	2.31	1.36
5	1.78	11.34	13.99	101	2.31	1.37
Average	1.61	11.32	14.34	101	2.31	1.36
St.dev	0.12	0.26	0.28	5	0.00	0.02

Table F.4: The weight of the gels from the 20 % sample of DS 0.77/LF200S before and after syneresis, the measured slope of the initial force-distance plot in the longitudinal compression test, the measured diameter and height of the gels, and the calculated cross-sectional surface area of the gels.

Gel Number	Slope [N/mm]	d [mm]	h[mm]	a [mm ²]	Weight of Gel [g]	
					Before Synere-sis	After Synere-sis
1	1.78	11.05	13.91	96	2.31	1.39
2	1.33	11.66	14.20	107	2.31	1.42
3	1.44	11.02	14.51	95	2.31	1.39
4	1.32	11.15	14.18	98	2.31	1.42
5	1.51	11.14	14.07	97	2.31	1.37
6	1.49	10.84	14.22	92	2.31	1.36
Average	1.48	11.14	14.18	98	2.31	1.39
St.dev	0.17	0.28	0.20	5	0.00	0.02

Table F.5: The weight of the gels from the 40 % sample of DS 0.77/LF200S before and after syneresis, the measured slope of the initial force-distance plot in the longitudinal compression test, the measured diameter and height of the gels, and the calculated cross-sectional surface area of the gels.

Gel Number	Slope [N/mm]	d [mm]	h[mm]	a [mm ²]	Weight of Gel [g]	
					Before Synere-sis	After Synere-sis
1	1.48	11.39	14.86	102	2.31	1.43
2	1.00	11.05	14.32	96	2.31	1.36
3	1.71	11.74	14.26	108	2.31	1.34
4	1.68	11.93	13.98	94	2.31	1.30
5	1.27	11.32	14.40	101	2.31	1.35
6	1.39	11.01	14.27	95	2.31	1.37
Average	1.42	11.24	14.35	99	2.31	1.36
St.dev	0.27	0.30	0.29	5	0	0.04

Table F.6: The weight of the gels from the 60 % sample of DS 0.77/LF200S before and after syneresis, the measured slope of the initial force-distance plot in the longitudinal compression test, the measured diameter and height of the gels, and the calculated cross-sectional surface area of the gels. One of the specimens of the sample was omitted from the calculations as the slope was not linear in the area between 0.4 and 0.5 mm of compression.

Gel Number	Slope [N/mm]	d [mm]	h[mm]	a [mm ²]	Weight of Gel [g]	
					Before Synere-sis	After Synere-sis
1	1.14	11.39	14.30	102	2.31	1.51
2	1.19	11.50	14.35	104	2.31	1.47
3	0.88	11.51	14.26	104	2.31	1.43
4	1.15	11.55	14.40	105	2.31	1.54
5	0.98	11.23	14.28	99	2.31	1.35
Average	1.07	11.44	14.35	103	2.31	1.46
St.dev	0.13	0.13	0.29	2	0	0.07

Table F.7: The weight of the gels from the 80 % sample of DS 0.77/LF200S before and after syneresis, the measured slope of the initial force-distance plot in the longitudinal compression test, the measured diameter and height of the gels, and the calculated cross-sectional surface area of the gels. One of the specimens of the sample was omitted from the calculations as the slope was not linear in the area between 0.4 and 0.5 mm of compression.

Gel Number	Slope [N/mm]	d [mm]	h[mm]	a [mm ²]	Weight of Gel [g]	
					Before Synere-sis	After Synere-sis
1	0.61	11.59	14.17	106	2.31	1.65
2	0.56	11.59	14.54	106	2.31	1.63
3	0.67	12.03	14.62	114	2.31	1.72
4	0.66	11.80	14.07	109	2.31	1.70
5	0.62	11.87	14.29	111	0	1.68
Average	0.62	11.78	14.34	109	2.31	1.68
St.dev	0.04	0.19	0.24	4	0	0.04

Table F.8: The weight of the gels from the 100 % sample of DS 0.77/LF200S before and after syneresis, the measured slope of the initial force-distance plot in the longitudinal compression test, the measured diameter and height of the gels, and the calculated cross-sectional surface area of the gels.

Gel Number	Slope [N/mm]	d [mm]	h[mm]	a [mm ²]	Weight of Gel [g]	
					Before Synere-sis	After Synere-sis
1	0.25	12.62	14.36	125	2.31	1.87
2	0.11	12.28	14.65	118	2.31	1.82
3	0.21	12.01	13.99	113	2.31	1.70
4	0.16	12.70	14.56	127	2.31	1.81
5	0.27	12.37	14.36	120	2.31	1.86
6	0.28	12.25	14.76	118	2.31	1.82
Average	0.21	12.37	14.45	120	2.31	1.81
St.dev	0.07	0.25	0.27	5	0	0.06

Table F.9: The weight of the gels from the 10 % sample of partially hydrolysed alginate/LF200S before and after syneresis, the measured slope of the initial force-distance plot in the longitudinal compression test, the measured diameter and height of the gels, and the calculated cross-sectional surface area of the gels.

Gel Number	Slope [N/mm]	d [mm]	h[mm]	a [mm ²]	Weight of Gel [g]	
					Before Synere-sis	After Synere-sis
1	1.63	11.37	13.65	102	2.31	1.44
2	1.62	11.40	14.76	102	2.31	1.52
3	1.85	11.09	14.22	97	2.31	1.51
4	1.25	11.09	14.85	97	2.31	1.47
5	1.49	11.03	14.83	96	2.31	1.49
6	1.40	10.96	14.83	94	2.31	1.50
Average	1.54	11.16	14.52	98	2.31	1.49
St.dev	0.21	0.18	0.49	3	0	0.03

Table F.10: The weight of the gels from the 20 % sample of partially hydrolysed alginate/LF200S before and after syneresis, the measured slope of the initial force-distance plot in the longitudinal compression test, the measured diameter and height, and the calculated cross-sectional surface area of the gels. One of the specimens of the sample was omitted from the calculations as the slope was not linear in the area between 0.4 and 0.5 mm of compression.

Gel Number	Slope [N/mm]	d [mm]	h[mm]	a [mm ²]	Weight of Gel [g]	
					Before Synere-sis	After Synere-sis
1	1.71	11.06	14.38	96	2.31	1.48
2	1.72	10.68	14.00	90	2.31	1.48
3	1.96	11.13	13.52	97	2.31	1.47
4	1.70	11.05	14.36	96	2.31	1.52
5	1.62	11.06	14.12	96	2.31	1.45
Average	1.74	11.00	14.08	95	2.31	1.48
St.dev	0.13	0.18	0.35	3	0	0.03

Table F.11: The weight of the gels from the 60 % sample of partially hydrolysed alginate/LF200S before and after syneresis, the measured slope of the initial force-distance plot in the longitudinal compression test, the measured diameter and height of the gels, and the calculated cross-sectional surface area of the gels.

Gel Number	Slope [N/mm]	d [mm]	h[mm]	a [mm ²]	Weight of Gel [g]	
					Before Syneresis	After Syneresis
1	1.98	11.28	14.35	100	2.31	1.51
2	2.09	11.32	14.40	101	2.31	1.61
3	1.81	11.74	14.84	108	2.31	1.60
4	1.77	11.32	14.32	101	2.31	1.42
5	1.29	11.40	14.92	102	2.31	1.52
6	1.66	11.57	14.74	105	2.31	1.50
Average	1.77	11.44	14.60	103	2.31	1.53
St.dev	0.28	0.18	0.27	3	0	0.07

G. Calculations of the Young's Modulus

Gels made from DS 0.77/LF200S mixtures were subjected to a longitudinal compression test, and the Young's modulus calculated from the initial slope of the force-distance plot obtained from this test. This Appendix contains the calculation of the Young's modulus of the first gel from the sample 5 %, where 5 % (w/w) of the total alginate content is alginate with a DS of 0.77, along with the correction for syneresis of the gel.

The slope from the initial force-distance plot from the compression test, along with the diameter, height and weight of each of the gels from the 5 % sample can be found in Table F.2 in Appendix F, with a summary of the values of the first gel given in Table G.1.

Table G.1: The values of weight, slope of the initial force-distance plot in the longitudinal compression test, diameter, height and cross-sectional surface area of the first gel from the 5 % sample of DS 0.77/LF200S.

Slope [N/mm]	d [mm]	h[mm]	a [mm ²]	Weight of Gel [g]	
				Before Syneresis	After Syneresis
2.34	11.40	14.88	102	2.31	1.46

The Young's modulus can be calculated according to Equation 1.4.1 in Section 1.4 when the slope of the initial force-deformation curve, the cross-sectional area of the gel, and the initial length or height of the gel is known.

For the 5 % sample of DS 0.77/LF200S mixtures, this gives the Young's modulus shown in Equation G.1.

$$E = \frac{F}{\Delta l} \times \frac{l}{A} = 2.34 \frac{N}{mm} \times \frac{14.88 mm}{102 mm^2} \times 10^6 \frac{mm^2}{m^2} \approx 341 kPa \quad (G.1)$$

As the weight of the gel has decreased from the gel was made and until the gel measurements were conducted 24 h later, the Young's modulus can be corrected for syneresis according to Equation 1.4.2 in Section 1.4. For the first of the 5 % gels this gives the result shown in Equation G.2.

$$E_{corrected} = E_{measured} \times \left(\frac{w_t}{w_0}\right)^2 = 341 kPa \times \left(\frac{1.45}{2.31}\right)^2 = 136 kPa \quad (G.2)$$

The average of the calculated Young's modulus of all the 6 gels in the sample with 5 % (w/w) sulfated alginate is given in Table 3.4.1 in Section 3.4, while the average value for the corrected Young's modulus is found in Table H.1 in Appendix H.

H. The Young's Modulus of Alginate/Alginate-Sulfate Gels

The Young's modulus of gels made from alginate DS 0.77/LF200S mixtures in different proportions were determined by use of a longitudinal compression test. The initial slope between 0.4 and 0.5 mm in the force- distance plot was used in the calculations of the Young's modulus of each sample, according to Equation 1.4.1.

Because of the syneresis effects of alginate gels, the Young's modulus for each sample was corrected for syneresis according to Equation 1.4.2. The resulting corrected modulus, E_{corr} along with the average weight of each gel sample, the standard deviation and the coefficient of Variation, CoV, of E_{corr} are given in Table H.1, calculated from the initial Young's modulus given in Table 3.4.1 in Section 3.4.

As a control for the effect of molecular weight of alginate on gel strength, gels from three mixtures of hydrolysed alginate ($M_w \approx 150$ kDa) and LF200S were subjected to the same compression test. The resulting weights of the gels, the calculated Young's modulus, the Young's modulus after correction for syneresis, and the standard deviation and coefficient of variation of the corrected E, is given in Table H.2.

Table H.1: The average weight of the gels from each sample of DS 0.77/LF200S mixtures after syneresis, the corrected Young's modulus, E_{corr} , the standard deviation and the coefficient of variation, CoV, for the corrected Young's modulus.

Amount of the Alginate that is Sulfated [%]	Average Weight of Gels Before Syneresis [g]	Average Weight of Gels After Syneresis [g]	E_{corr} [kPa]	The Standard Deviation of E_{corr} [kPa]	CoV
0	2.31	1.53	135	16	0.12
5	2.31	1.44	119	16	0.15
10	2.31	1.36	794	62	0.08
20	2.31	1.39	779	89	0.11
40	2.31	1.36	708	12	0.17
60	2.31	1.46	599	11	0.19
80	2.31	1.68	43	4	0.08
100	2.31	1.81	16	6	0.35

Table H.2: The average weight of the gels from each sample of hydrolysed alginate/LF200S mixtures before and after syneresis, the Young's modulus, before and after correction for syneresis (E and E_{corr} respectively) the standard deviation and the coefficient of variation, CoV, for the corrected Young's modulus.

Amount Hydrolysed Alginate [%]	Average weight before syneresis [g]	Average Weight After Syneresis [g]	The Young's Modulus, E [kPa]	E_{corr} [kPa]	The Standard Deviation of E_{corr} [kPa]	CoV
10	2.31	1.49	228	95	13	0.14
20	2.31	1.49	258	106	7	0.07
60	2.31	1.53	251	110	23	0.21

I. Standard for FGF Using ELISA and Results from Gel Disk Measurements

The release of FGF from alginate/alginate-sulfate gel disks, as well as the remaining concentration of FGF in the gel disks after 12 days, were studied by use of ELISA. A standard curve for FGF concentrations was constructed using concentrations ranging from 0 to 4000 pg/ml, with the resulting standard curve and the results for the gel disk measurements given in this appendix.

The standard curve was constructed using the procedure described by the manufacturer for the ELISA kit, with samples in triplicate. A plate reader set at 405 nm with 650 nm as the correction wavelength was used to read the absorbance of the samples. The absorbance read at 650 nm was subtracted from the one read at 405 nm, giving a net absorbance for all samples. A second degree polynomial regression line was fitted to the data, with the constructed standard curve given in Figure I.1.

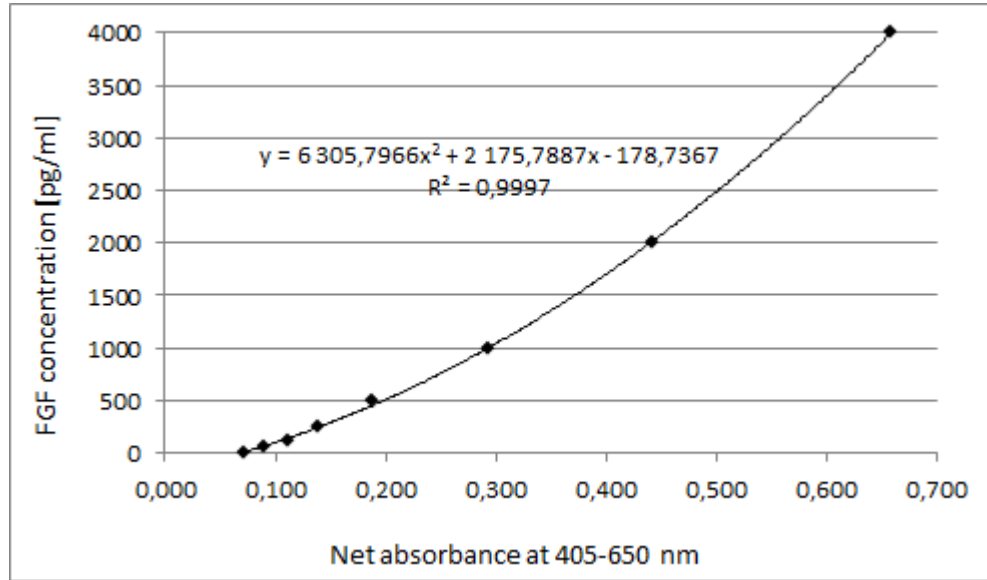


Figure I.1: *The constructed standard curve for FGF using a sandwich ELISA. The plate was read with a plate reader set at 405 nm with 650 nm as the reference wavelength. The net absorbance was found by subtracting the absorbance read at 650 nm from the one read at 405 nm. A second degree polynomial regression line was fitted to the data points, and is shown in the figure.*

The remaining concentration of FGF in each gel disks was found using the procedure described by the manufacturer for the ELISA kit, with samples in duplicate. A plate reader set at 405 nm with 650 nm as the correction wavelength was used to read the absorbance of the samples. The absorbance read at 650 nm was subtracted from the one read at 405 nm, giving a net absorbance for all samples. The diameter and height of each gel disk were measured in order to calculate the volume. From the volume, the dilution factor of each gel disk solution was found using Equation I.1.

$$Dilution\ Factor = 10 \times \frac{V_{gel} + 10.5\ ml}{V_{gel}} \quad (I.1)$$

where V_{gel} is the volume of the gel disk, 10.5 is the volume the gel disk was dissolved in, and 10 is the dilution factor for this solution before the ELISA.

The concentration of FGF in each sample was found by using the average of the measured absorbances, and the standard curve from Figure I.1. The concentration of FGF in each gel disk was calculated as the product of the concentration in the sample and the dilution factor. The measured absorbances, volumes, dilution factor and FGF concentration of each gel disk are all given in Table I.1.

Table I.1: The measured absorbances of samples made from dissolved gel disks containing FGF after 12 days in a HEPES solution. A sandwich ELISA was used, and the plates were read using a plate reader set at 405 nm with 605 nm as a reference wavelength. The gel diameter and height of each gel disk after 12 days were measured before the disks were dissolved, and used to calculate the volume and dilution factor of each gel disk, with results shown in the table. The concentration of FGF in the samples was calculated using the average absorbance and the standard curve from Figure I.1. The concentration in the gel disks were found from these results and the dilution factor of the gel disks, and can be found in the table.

Sample	1	2	Average	Volume of Gel Disk [ml]	Dilution Factor	Concentration in Plate Well [pg/ml]	Concentration in Sample [$\mu\text{g}/\text{ml}$]
0, 1	0.132	0.133	0.132	0.54	204	219	0.04
0, 2	0.214	0.186	0.200	0.69	162	510	0.08
0, 3	0.177	0.178	0.178	0.72	155	406	0.06
20, 1	0.611	0.635	0.623	0.60	185	3623	0.67
20, 2	0.711	0.662	0.686	0.60	185	4286	0.79
20, 3	0.675	0.698	0.686	0.74	151	4285	0.65
40, 1	0.674	0.725	0.699	0.60	186	4428	0.82
40, 2	0.629	0.773	0.701	0.65	170	4447	0.76
40, 3	0.661	0.623	0.642	0.67	166	3817	0.63
60, 1	0.871	0.805	0.838	0.75	150	6077	0.91
60, 2	0.799	0.818	0.809	0.73	154	5707	0.88
60, 3	0.727	0.826	0.777	0.77	146	5315	0.78